

**Politecnico of Milan**

School of Industrial and Information Engineering  
Master of Science in Mathematical Engineering

MASTER THESIS

# **The DRPM Strikes Back: Improvements on a Bayesian Spatio-Temporal Clustering Model**

Advisor

**Prof. Alessandra Guglielmi**

Coadvisor

**Prof. Alessandro Carminati**

Candidate

**Federico Angelo Mor**

**Matr. 221429**



*to my cats Otto  
and La Micia*



# Abstract

Clustering is a key technique for identifying patterns and structures in complex datasets, whose relevance is intensified in spatio-temporal contexts where observations are simultaneously influenced by multiple factors such as space, time, and covariates. To this end, the Dependent Random Partition Model (DRPM) is one of the most relevant bayesian models due to its explicit consideration of temporal dependence in the partitions. However, the current implementation lacks of the inclusion of covariates, the handling of missing data, and the efficiency in execution times. Therefore, in this work we improve the original DRPM model by addressing those issues trough updates on the model formulation and a brand new implementation in Julia. These advancements are then tested on synthetic and real-world datasets, including air quality data from the AgrImOnIA project in Lombardy, Italy.

KEYWORDS: bayesian modelling, clustering, spatio-temporal data, computational statistics



# Sommario

Il clustering è una tecnica fondamentale per identificare strutture e pattern in dataset complessi, la cui importanza è intensificata nei contesti spazio-temporali in cui le osservazioni sono influenzate simultaneamente da molteplici fattori come spazio, tempo e covariate. In tal senso, il modello DRPM (Dependent Random Partition Model, modello per partizioni aleatorie dipendenti) è uno dei modelli bayesiani più rilevanti in quanto tiene conto in modo esplicito della dipendenza temporale delle partizioni. Tuttavia, l'attuale implementazione manca dell'inclusione di covariate, della gestione dei dati mancanti, e di efficienza nei tempi di esecuzione. In questo lavoro abbiamo quindi migliorato l'originale modello DRPM affrontando tali problemi tramite aggiornamenti sulla formulazione del modello e una fiammante implementazione in Julia. Questi sviluppi sono stati poi testati su dataset sintetici e reali, compresi i dati sulla qualità dell'aria in Lombardia del progetto AgrImOnIA.

PAROLE CHIAVE: modello bayesiano, clustering, dati spazio-temporali, statistica computazionale





# Contents

<b>1</b>	<b>Introduction</b>	<b>1</b>
<b>2</b>	<b>Description of the model</b>	<b>3</b>
2.1	Update rules derivation . . . . .	7
2.2	Spatial cohesions analysis . . . . .	10
2.3	Covariates similarities analysis . . . . .	14
<b>3</b>	<b>Implementation and optimizations</b>	<b>19</b>
3.1	Optimizations . . . . .	19
3.1.1	Optimizing spatial cohesions . . . . .	21
3.1.2	Optimizing covariates similarities . . . . .	24
<b>4</b>	<b>Testing</b>	<b>27</b>
4.1	Assessing the equivalence of the models . . . . .	27
4.1.1	Target variable only . . . . .	28
4.1.2	Target variable plus space . . . . .	29
4.2	Performance with missing values . . . . .	33
4.2.1	Target variable only (NA case) . . . . .	36
4.2.2	Target variable plus space (NA case) . . . . .	37
4.3	Effects of the covariates . . . . .	39
4.3.1	Covariates in the likelihood . . . . .	39
4.3.2	Covariates in the clustering . . . . .	42
4.4	Scaling performances . . . . .	44
<b>5</b>	<b>Conclusion</b>	<b>49</b>
<b>A</b>	<b>Theoretical details</b>	<b>51</b>
A.1	Extended computations of the full conditionals . . . . .	51

<b>B Computational details</b>	<b>61</b>
B.1 Fitting algorithm code . . . . .	61
B.2 Interface . . . . .	76
<b>C Further plots</b>	<b>79</b>
<b>Bibliography</b>	<b>81</b>

# List of Figures

2.1	Updated DRPM model graph . . . . .	6
2.2	Partition considered for the cohesion analysis . . . . .	11
2.3	Cohesions 1, 2, and 3 illustration . . . . .	12
2.4	Cohesions 4, 5, and 6 illustration . . . . .	13
2.5	Partition considered for the similarity analysis . . . . .	15
2.6	Similarities 1, 2 and 3 illustration . . . . .	16
2.7	Similarity 4 illustration . . . . .	17
3.1	Flame graph of a test fit . . . . .	21
3.2	Cohesions 3 and 4 implementation comparison . . . . .	23
3.3	Similarity 4 annotations comparison . . . . .	25
4.1	Lagged ARI values of CDRPM and JDRPM fits, target values only	28
4.2	Clusters produced by JDRPM and CDRPM fits, target values only	29
4.3	Visual representation of the clusters of JDRPM and CDRPM fits, target values only . . . . .	30
4.4	Generated and fitted values of JDRPM and CDRPM fits, target values only . . . . .	31
4.5	Comparison of the two possible mean centering methods on the target variable . . . . .	32
4.6	Lagged ARI values of CDRPM and JDRPM fits, target plus space values . . . . .	33
4.7	Target and fitted values of JDRPM and CDRPM fits, target plus space values . . . . .	34
4.8	Clusters generated by CDRPM and JDRPM fits, target plus space values . . . . .	35
4.9	Fitted values of JDRPM fit, target values only, NA dataset . . . . .	36
4.10	Clusters produced by JDRPM fits, target values only, full vs NA dataset . . . . .	37

4.11 Lagged ARI values of JDRPM fits, target values only, full vs NA dataset . . . . .	37
4.12 Visual representation of the clusters of JDRPM fit, target values only, NA dataset . . . . .	38
4.13 Lagged ARI values of JDRPM fits, target plus space values, full vs NA dataset . . . . .	38
4.14 Comparison of the two possible mean centering methods on a covariate	40
4.15 Regression vector of the fit with multiple covariates in the likelihood, full dataset . . . . .	41
4.16 Regression vector of the fit with multiple covariates in the likelihood, NA dataset . . . . .	42
4.17 Target and fitted values of JDRPM fits, target plus space values, NA dataset, with covariates in the likelihood . . . . .	43
4.18 Lagged ARI values of JDRPM fit, target plus space values, full vs NA dataset, with covariates in the likelihood . . . . .	44
4.19 Clusters generated by JDRPM fits, target plus space values, full vs NA dataset, with covariates in the likelihood . . . . .	45
4.20 Execution times of JDRPM and CDRPM fits, target values only . .	46
4.21 Execution times of JDRPM and CDRPM fits, target plus space values	47
4.22 Execution times of JDRPM fits, target plus space plus covariates .	47
4.23 Visual representation of all fitting performances . . . . .	48

# List of Tables

4.1	Accuracy metrics of CDRPM and JDRPM fits, target values only .	28
4.2	Accuracy metrics of CDRPM and JDRPM fits, target plus space values	33
4.3	Accuracy metrics of JDRPM fits, target values only, full vs NA dataset	37
4.4	Accuracy metrics of JDRPM fits, target plus space values, full vs NA dataset . . . . .	38
4.5	Accuracy metrics of JDRPM fits, target plus space values, full vs NA dataset, with vs without covariates in the likelihood . . . . .	39



# Chapter 1

## Introduction

Clustering has always been a powerful tool to identify structures and patterns in data, especially in contexts where relationships between the observations are complex such as when the target variable is affected by many factors simultaneously. For this reason, clustering techniques saw an increase in popularity in a variety of scientific fields, including social sciences, climate and environmental analysis, economics, and healthcare. The importance of clustering becomes even more noticeable when working with spatio-temporal data, where observations are collected over time and across different spatial locations, possibly concealing trends behind both information levels. This type of data, in fact, is inherently complex due to this dependence and interaction between spatial and temporal dimensions; a complexity increased if also covariates are available. For that reason, effective analyses of such data demand models that could account for this dependence and maintaining reasonable computational loads to be applied also on large scale datasets, which in this context are frequently available.

In recent years, the use of bayesian methods to perform clustering has gained some attention, particularly in this field of spatio-temporal analysis. Bayesian clustering allows in fact to incorporate prior information into the model, enhancing the flexibility and interpretability of the results. Throughout the years, several models have been developed, but one of the most relevant and recent in this context is the Dependent Random Partition Model (DRPM), which stands out for being able to handle explicitly the temporal dependence of partitions into the model formulation, while also possibly accounting for the spatial information. However, the current DRPM implementation, written in C and available trough a R interface, lacks of some relevant utilities such as the inclusion of covariates, which could further enhance the generation of the clusters, the handling of missing data, and an efficient implementation, which would speed up the model fitting to e.g. run multiple chains in parallel of be more easily applied on large number of units and time horizons.

In this work, we aim to address these three issues by broadening the original model, i.e. preserving the original idea of the formulation but making it richer, improved. We will show how this updated model can perform better than the original one, under the same test conditions, and improve the clustering accuracy

and interpretation through the inclusion of covariates. All this with also providing faster execution times. In fact, deploying the model using the Julia language, rather than the original implementation in C, we took advantage of its high-performance capabilities and well well-equipped statistical ecosystem.

Our comparison will focus on both synthetic datasets and real-world applications, with the latter involving air quality measurements from the AgrImOnIA dataset, a comprehensive record of air pollutant levels and other environmental variables across the Lombardy region in Italy.

Chapter 2 will briefly review the literature about bayesian clustering models to then dive deeply into the analysis and description of the DRPM, and of our updated version, about their core aspects of sampling algorithm, spatial cohesions, and covariates similarities.

Chapter 3 will provide some insights about the computational aspects of the model implementation, motivating the choice of the Julia language and reporting the optimizations possibilities emerged when developing the algorithm.

Chapter 4 will be devoted to test and compare the original DRPM model to our updated version, to check if they perform similarly at a common testing level, and to assess the performances of the fits of the new version when we employ the new updates, i.e. the handling of missing data and the insertion of covariates at clustering and/or likelihood levels.

Finally, in Chapter 5, we will briefly review the benefits and drawbacks that these analysis revealed and suggest possible further improvements or development paths.



# Chapter 2

## Description of the model

*“Come on, gentlemen, why shouldn’t we get rid of all this calm reasonableness with one good kick, just so as to send all these logarithms to the devil and be able to live our own lives at our own sweet will?”*  
— Fëdor Dostoevskij, *Notes from the Underground*

In the bayesian framework, clustering is possible by employing a random probability measure of discrete type that induces a distribution over random partitions. This discreteness is obtained through the Dirichlet Process (DP), which several clustering models implement either through the stick-breaking representation [Bar+12] [AW15] [GMR16] [Jo+16] [KG18] [DK18] [De +19] or through the Pólya urn scheme [Car+17]. However, when dealing with dependence in the random partitions, these traditional bayesian methods rely on modeling such dependencies by modeling the dependence inside the random probability measures, i.e. on the parameters which underlie those DP representations, rather than to the clusters themselves. This approach is therefore kind of a “step back” from the main object of interest, the clusters, which are then only *induced* by the random partition model. In this way there is no guarantee that the correlation that appears in the parameters would subsequently reflect into correlation among the partitions, often producing counterintuitive behaviours in the results. The Dependent Random Partition Model (DRPM) [PQD22], instead, models *directly* the sequence of partitions, improving the temporal relation among the clusters and providing a more reasonable and interpretable temporal evolution.

Before diving into the model description, we provide some reference notations. We setup in a spatio-temporal context with  $i = 1, \dots, n$  and  $t = 1, \dots, T$  being the indexes for units and time instants. We will denote with  $\rho_t = \{S_{1t}, \dots, S_{k_t t}\}$  the partition at time  $t$  of the  $n$  experimental units, composed by  $k_t$  cluster, with of course  $k_t$  that could be varying with respect time, i.e. is not fixed a priori, thanks to the bayesian framework in which we are. Another possible representation of the partition could be through cluster labels  $\mathbf{c}_t = \{c_{1t}, \dots, c_{nt}\}$  where  $c_{it} = h$  is unit  $i$  belongs to cluster  $S_{jt}$ . Finally, we will denote with a  $\star$  superscript all the variables or quantities which are cluster-specific.

To implement the random dependence in the partition, the authors proposed a joint probability model for  $(\rho_1, \dots, \rho_T)$ , denoted as  $P(\rho_1, \dots, \rho_T)$ , and letting each  $\rho_t$  being possibly affected by all the other partitions. This principle, however, would have required even more complexity in the model, therefore the authors limited this temporal connection to a first-order Markov-chain structure, where the conditional distribution of  $\rho_t$  given all the predecessor  $\rho_{t-1}, \rho_{t-2}, \dots, \rho_1$  actually depends only on  $\rho_{t-1}$ , bringing the random partition model to the form

$$P(\rho_1, \dots, \rho_T) = P(\rho_T | \rho_{T-1}) \cdots P(\rho_2 | \rho_1) P(\rho_1)$$

To explicitly manage the relation between  $\rho_t$  and  $\rho_{t-1}$  some auxiliary variables are introduced. The idea is that if two partitions are highly time-dependent, few changes will occur between them. In turn, partitions which are quite independent will possibly exhibit very different configurations. To express this fixity or flexibility concept, for each unit  $i = 1, \dots, n$  the following variable is introduced <sup>1</sup>

$$\gamma_{it} = \begin{cases} 1 & \text{if unit } i \text{ is } \textit{not} \text{ reallocated when moving from time } t-1 \text{ to } t \\ 0 & \text{otherwise (i.e. unit } i \text{ is reallocated)} \end{cases}$$

By construction, we set  $\gamma_{i1} = 0$  for all  $i$ , meaning that at the first time instant all units get reallocated, since they have no partition to be possibly fixed at. Regarding their modeling, the authors proposed  $\gamma_{it} \stackrel{\text{ind}}{\sim} \text{Ber}(\alpha_t)$ , with  $\alpha_t \in [0, 1]$  behaving as a temporal parameter. At the two extremes,  $\alpha_t = 1$  will denote perfect temporal dependence, with  $\rho_t = \rho_{t-1}$ , while  $\alpha_t = 0$  will imply full independence of  $\rho_t$  from  $\rho_{t-1}$ . For the sake of clarity, the vector  $\gamma_t = (\gamma_{1t}, \dots, \gamma_{nt})$  is created, and the augmented joint model now becomes in the form

$$P(\gamma_1, \rho_1, \dots, \gamma_T, \rho_T) = P(\rho_T | \gamma_T, \rho_{T-1}) P(\gamma_T) \cdots P(\rho_2 | \gamma_2, \rho_1) P(\gamma_2) P(\rho_1)$$

The insertion of this additional variables make the model powerful in describing the temporal relationship of the partitions, but hinders a bit the design of the sampling algorithm. To outline it, we firstly need a

**Definition 2.1** (compatibility). Two partitions  $\rho_t$  and  $\rho_{t-1}$  are *compatible* with respect to  $\gamma_t$  if  $\rho_t$  may be obtained from  $\rho_{t-1}$  by reallocating items as indicated by  $\gamma_t$ ; i.e. only moving the units with  $\gamma_{it} = 0$  for  $i = 1, \dots, n$ .

To perform this check, it is enough to ensure that the reduced partitions from  $\rho_t$  and  $\rho_{t-1}$  are the same, with reduced meaning their restriction to the units which *can't* move. Indicating the set of fixed units as  $\mathfrak{R}_t = \{i : \gamma_{it} = 1\}$ , this check translates into asking that  $\rho_t^{\mathfrak{R}_t} = \rho_{t-1}^{\mathfrak{R}_t}$ .

The sampling algorithm then requires that when we are drawing the new sample for the  $\gamma_{it}$  parameters, or also for the cluster labels  $c_{it}$ , we firstly need to check if these draws can be performed, i.e. would keep compatible all the partitions and parameters involved. For example, during each iteration  $d$  of the algorithm,

---

<sup>1</sup>a quick way to remind this convention is thinking that  $\gamma_{it}$  answers to the question “do I stay fixed?” asked from unit’s  $i$  perspective.

when updating  $\gamma_{it}$ , the only case which can raise problems is when we pass from  $\gamma_{it}^{(d-1)} = 0$  to  $\gamma_{it}^{(d)} = 1$ . This step corresponds to the case where a unit  $i$  that was initially (i.e. according to the previous iteration values) free to be reassigned is now instead deemed to stay fixed in her cluster. However, this change may not align to the current sampled values of the partitions  $\rho_{t-1}$  and  $\rho_t$ . Therefore compatibility between their reductions to all the units inside  $\mathfrak{R}_t \cup \{i\}$  needs to be checked, otherwise we block the tentative update  $\gamma_{it}^{(d-1)} = 0 \rightarrow \gamma_{it}^{(d)} = 1$  and we leave  $\gamma_{it}^{(d)} = 0$ . Similar checks are conducted when  $\rho_t$  is updated. In this step, only the units that can actually move, i.e. that have  $\gamma_{it} = 0$ , are updated and therefore there are no compatibility problems between  $\rho_{t-1}$  and  $\rho_t$ . However, since the update of  $\gamma_{it}$  occurs before the one of the partition, compatibility needs to be checked between  $\rho_t$  and  $\rho_{t+1}$ .

In any case, once the partition model is specified, there is a great flexibility in how to setup the rest of the hierarchical model. To also allow temporal dependence to propagate through the model, an autoregressive AR(1) component is added (but only optionally in the software implementation) to the formulation of the model. All this led the authors to this complete model design

$$\begin{aligned}
Y_{it}|Y_{it-1}, \boldsymbol{\mu}_t^*, \boldsymbol{\sigma}_t^{2*}, \boldsymbol{\eta}, \mathbf{c}_t &\stackrel{\text{ind}}{\sim} \mathcal{N}(\mu_{c_{it}}^* + \eta_{1i}Y_{it-1}, \sigma_{c_{it}}^{2*}(1 - \eta_{1i}^2)) \\
Y_{i1} &\stackrel{\text{ind}}{\sim} \mathcal{N}(\mu_{c_{i1}}^*, \sigma_{c_{i1}}^{2*}) \\
\xi_i = \text{Logit}(\tfrac{1}{2}(\eta_{1i} + 1)) &\stackrel{\text{ind}}{\sim} \text{Laplace}(a, b) \\
(\mu_{jt}^*, \sigma_{jt}^{2*}) &\stackrel{\text{ind}}{\sim} \mathcal{N}(\vartheta_t, \tau_t^2) \times \mathcal{U}(0, A_\sigma) \\
\vartheta_t|\vartheta_{t-1} &\stackrel{\text{ind}}{\sim} \mathcal{N}((1 - \varphi_1)\varphi_0 + \varphi_1\vartheta_{t-1}, \lambda^2(1 - \varphi_1^2)) \\
(\vartheta_1, \tau_t) &\stackrel{\text{iid}}{\sim} \mathcal{N}(\varphi_0, \lambda^2) \times \mathcal{U}(0, A_\tau) \\
(\varphi_0, \varphi_1, \lambda) &\sim \mathcal{N}(m_0, s_0^2) \times \mathcal{U}(-1, 1) \times \mathcal{U}(0, A_\lambda) \\
\{\mathbf{c}_t, \dots, \mathbf{c}_T\} &\sim \text{tRPM}(\boldsymbol{\alpha}, M) \text{ with } \alpha_t \stackrel{\text{iid}}{\sim} \text{Beta}(a_\alpha, b_\alpha) \quad (2.1)
\end{aligned}$$

Moving on towards our updates, we decided to refine some parts of it. Regarding the variances, we chose to model them through invGamma distribution, rather than the  $\mathcal{U}$  employed originally. This is indeed a more sophisticated choice, since the tuning of the parameters of the new distribution are a bit more difficult than simply setting the bounds of a uniform law, but should guarantee a better mixing in the chain. In fact, the invGamma recover conjugacy in the model, since are related to gaussian parameters, allowing the update step to be performed through the analytically exact Gibbs sampler rather than the acceptance-rejection method of Metropolis algorithm. To improve the accuracy in fitting the target values, we also added a regression parameter  $\beta_t$  in the likelihood. We chose to make it only time-dependent and not unit-dependent to lighten the already quite-heavy model formulation.

The final updated model design is now proposed, with highlighted in dark red the changes and insertions that we made.

$$\begin{aligned}
Y_{it}|Y_{it-1}, \boldsymbol{\mu}_t^*, \boldsymbol{\sigma}_t^{2*}, \boldsymbol{\eta}, \mathbf{c}_t &\stackrel{\text{ind}}{\sim} \mathcal{N}(\mu_{c_{it}}^* + \eta_{1i}Y_{it-1} + \mathbf{x}_{it}^T \boldsymbol{\beta}_t, \sigma_{c_{it}}^{2*}(1 - \eta_{1i}^2)) \\
Y_{i1} &\stackrel{\text{ind}}{\sim} \mathcal{N}(\mu_{c_{i1}}^* + \mathbf{x}_{i1}^T \boldsymbol{\beta}_1, \sigma_{c_{i1}}^{2*}) \\
\boldsymbol{\beta}_t &\stackrel{\text{ind}}{\sim} \mathcal{N}_p(\mathbf{b}, s^2 I) \\
\xi_i = \text{Logit}(\tfrac{1}{2}(\eta_{1i} + 1)) &\stackrel{\text{ind}}{\sim} \text{Laplace}(a, b) \\
(\mu_{jt}^*, \sigma_{jt}^{2*}) &\stackrel{\text{ind}}{\sim} \mathcal{N}(\vartheta_t, \tau_t^2) \times \text{invGamma}(a_\sigma, b_\sigma) \\
\vartheta_t|\vartheta_{t-1} &\stackrel{\text{ind}}{\sim} \mathcal{N}((1 - \varphi_1)\varphi_0 + \varphi_1\vartheta_{t-1}, \lambda^2(1 - \varphi_1^2)) \\
(\vartheta_1, \tau_t^2) &\stackrel{\text{iid}}{\sim} \mathcal{N}(\varphi_0, \lambda^2) \times \text{invGamma}(a_\tau, b_\tau) \\
(\varphi_0, \varphi_1, \lambda^2) &\sim \mathcal{N}(m_0, s_0^2) \times \mathcal{U}(-1, 1) \times \text{invGamma}(a_\lambda, b_\lambda) \\
\{\mathbf{c}_t, \dots, \mathbf{c}_T\} &\sim \text{tRPM}(\boldsymbol{\alpha}, M) \text{ with } \alpha_t \stackrel{\text{iid}}{\sim} \text{Beta}(a_\alpha, b_\alpha) \quad (2.2)
\end{aligned}$$

A visual representation of this new version of the DRPM model is also present in Figure 2.1, to more clearly appreciate the hierarchical structure and the relations among the parameters.

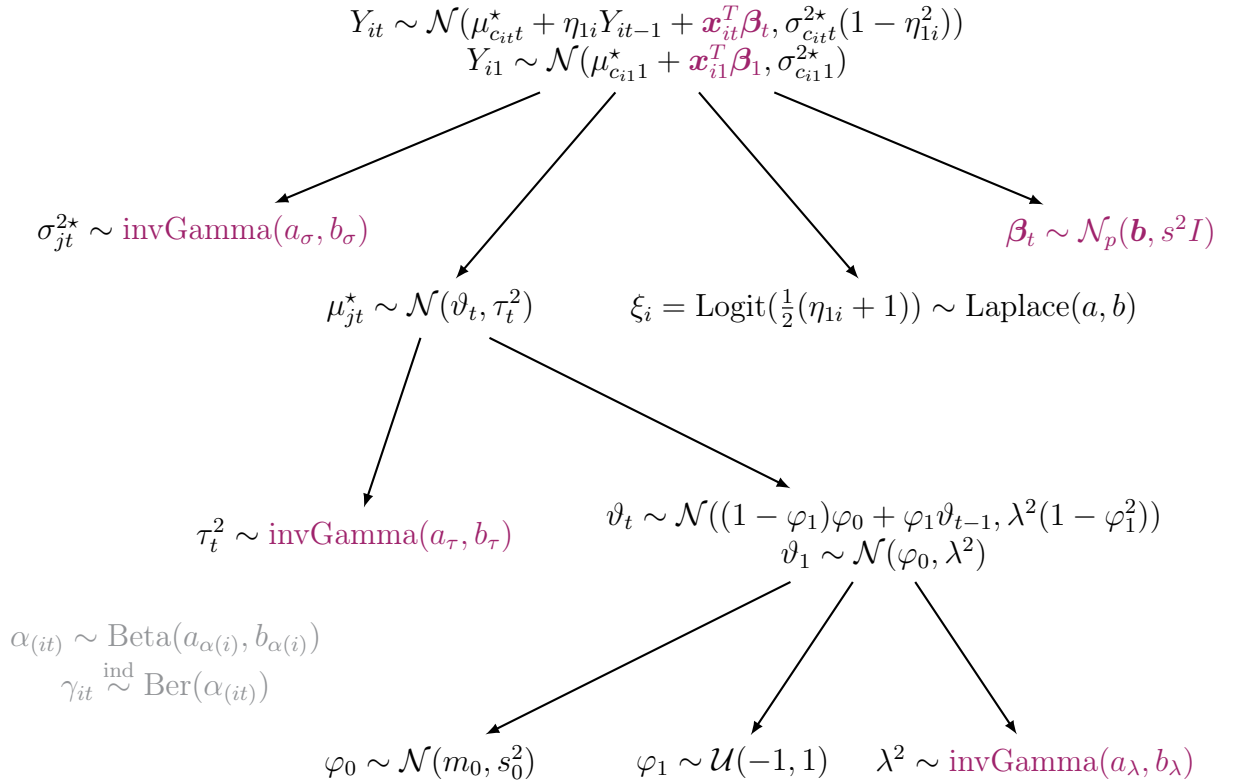


**Figure 2.1:** Graph visualization of the DRPM model, with highlighted in dark red the changes that we made to the original formulation and in gray the internal variables of the model.

We will now dive more deeply into the characteristics of the models, deriving the update rules for the parameters which will be used to implement the MCMC fitting algorithm, and then inspecting the behaviours of the spatial cohesions and covariates similarities.

## 2.1 Update rules derivation

We now report the full conditionals derivation for the parameters which had a conjugacy in the model (for the full computations see Appendix A). The other variables not included here, namely  $\eta_{1i}$  and  $\varphi_1$ , involved instead the classical Metropolis update.

- update  $\sigma_{jt}^{2\star}$

for  $t = 1$ :  $f(\sigma_{jt}^{2\star}|-) \propto$  kernel of a  $\text{invGamma}(a_{\sigma(\text{post})}, b_{\sigma(\text{post})})$  with

$$a_{\tau(\text{post})} = a_{\sigma} + \frac{|S_{jt}|}{2} \quad b_{\tau(\text{post})} = b_{\sigma} + \frac{1}{2} \sum_{i \in S_{jt}} (Y_{it} - \mu_{jt}^* - \mathbf{x}_{it}^T \boldsymbol{\beta}_t)^2$$

for  $t > 1$ :  $f(\sigma_{jt}^{2\star}|-) \propto$  kernel of a  $\text{invGamma}(a_{\sigma(\text{post})}, b_{\sigma(\text{post})})$  with

$$a_{\tau(\text{post})} = a_{\sigma} + \frac{|S_{jt}|}{2} \quad b_{\tau(\text{post})} = b_{\sigma} + \frac{1}{2} \sum_{i \in S_{jt}} (Y_{it} - \mu_{jt}^* - \eta_{1i} Y_{it-1} - \mathbf{x}_{it}^T \boldsymbol{\beta}_t)^2$$

(2.3)

- update  $\mu_{jt}^*$

for  $t = 1$ :  $f(\mu_{jt}^*|-) \propto$  kernel of a  $\mathcal{N}(\mu_{\mu_{jt}^*}(\text{post}), \sigma_{\mu_{jt}^*}^2(\text{post}))$  with

$$\sigma_{\mu_{jt}^*}^2(\text{post}) = \frac{1}{\frac{1}{\tau_t^2} + \frac{|S_{jt}|}{\sigma_{jt}^{2\star}}} \quad \mu_{\mu_{jt}^*}(\text{post}) = \sigma_{\mu_{jt}^*}^2(\text{post}) \left( \frac{\vartheta_t}{\tau_t^2} + \frac{\sum_{i \in S_{jt}} (Y_{it} - \mathbf{x}_{it}^T \boldsymbol{\beta}_t)}{\sigma_{jt}^{2\star}} \right)$$

for  $t > 1$ :  $f(\mu_{jt}^*|-) \propto$  kernel of a  $\mathcal{N}(\mu_{\mu_{jt}^*}(\text{post}), \sigma_{\mu_{jt}^*}^2(\text{post}))$  with

$$\sigma_{\mu_{jt}^*}^2(\text{post}) = \frac{1}{\frac{1}{\tau_t^2} + \frac{\sum_{i \in S_{jt}} \frac{1}{1 - \eta_{1i}^2}}{\sigma_{jt}^{2\star}}} \quad \mu_{\mu_{jt}^*}(\text{post}) = \sigma_{\mu_{jt}^*}^2(\text{post}) \left( \frac{\vartheta_t}{\tau_t^2} + \frac{\sum_{i \in S_{jt}} \frac{Y_{it} - \eta_{1i} Y_{it-1} - \mathbf{x}_{it}^T \boldsymbol{\beta}_t}{1 - \eta_{1i}^2}}{\sigma_{jt}^{2\star}} \right)$$

(2.4)

- update  $\boldsymbol{\beta}_t$

for  $t = 1$ :  $f(\boldsymbol{\beta}_t|-) \propto$  kernel of a  $\mathcal{N}(\mathbf{b}_{(\text{post})}, A_{(\text{post})})$  with

$$A_{(\text{post})} = \left( \frac{1}{s^2} I + \sum_{i=1}^n \frac{\mathbf{x}_{it} \mathbf{x}_{it}^T}{\sigma_{c_{it}}^{2\star}} \right)^{-1} \quad \mathbf{b}_{(\text{post})} = A_{(\text{post})} \left( \frac{\mathbf{b}}{s^2} + \sum_{i=1}^n \frac{(Y_{it} - \mu_{c_{it}}^*) \mathbf{x}_{it}}{\sigma_{c_{it}}^{2\star}} \right)$$

i.e.  $f(\boldsymbol{\beta}_t|-) \propto$  kernel of a  $\mathcal{N}\text{Canon}(\mathbf{h}_{(\text{post})}, J_{(\text{post})})$  with

$$\mathbf{h}_{(\text{post})} = \left( \frac{\mathbf{b}}{s^2} + \sum_{i=1}^n \frac{(Y_{it} - \mu_{c_{it}}^*) \mathbf{x}_{it}}{\sigma_{c_{it}}^{2\star}} \right) \quad J_{(\text{post})} = \left( \frac{1}{s^2} I + \sum_{i=1}^n \frac{\mathbf{x}_{it} \mathbf{x}_{it}^T}{\sigma_{c_{it}}^{2\star}} \right)$$

for  $t > 1$ :  $f(\boldsymbol{\beta}_t|-) \propto$  kernel of a  $\mathcal{N}(\mathbf{b}_{(\text{post})}, A_{(\text{post})})$  with

$$A_{(\text{post})} = \left( \frac{1}{s^2} I + \sum_{i=1}^n \frac{\mathbf{x}_{it} \mathbf{x}_{it}^T}{\sigma_{c_{it}}^{2\star}} \right)^{-1} \quad \mathbf{b}_{(\text{post})} = A_{(\text{post})} \left( \frac{\mathbf{b}}{s^2} + \sum_{i=1}^n \frac{(Y_{it} - \mu_{c_{it}}^* - \eta_{1i} Y_{it-1}) \mathbf{x}_{it}}{\sigma_{c_{it}}^{2\star}} \right)$$

i.e.  $f(\boldsymbol{\beta}_t|-) \propto$  kernel of a  $\mathcal{N}\text{Canon}(\mathbf{h}_{(\text{post})}, J_{(\text{post})})$  with

$$\mathbf{h}_{(\text{post})} = \left( \frac{\mathbf{b}}{s^2} + \sum_{i=1}^n \frac{(Y_{it} - \mu_{c_{it}t}^* - \eta_{1i}Y_{it-1})\mathbf{x}_{it}}{\sigma_{c_{it}t}^{2*}} \right) \quad J_{(\text{post})} = \left( \frac{1}{s^2}I + \sum_{i=1}^n \frac{\mathbf{x}_{it}\mathbf{x}_{it}^T}{\sigma_{c_{it}t}^{2*}} \right) \quad (2.5)$$

Here  $\mathcal{N}\text{Canon}(\mathbf{h}, J)$  is the canonical formulation of the  $\mathcal{N}(\boldsymbol{\mu}, \Sigma)$ , with  $\mathbf{h} = \Sigma^{-1}\boldsymbol{\mu}$  and  $J = \Sigma^{-1}$ . This other distribution facilitates the sampling, since these full conditional computations allow to derive directly the parameters of the canonical one, e.g. the inverse of the variance matrix, rather than the variance matrix itself; and therefore sampling through it does not require any inversion of matrices which would produce more computational load, numerical instabilities, and loss of accuracy. So in Julia we can write `rand(MvNormalCanon(h_star, J_star))`, rather than the riskier one `rand(MvNormal(inv(J_star)*h_star, inv(J_star)))`; which apart from the previously mentioned disadvantages would be a statistically equivalent form.

- update  $\tau_t^2$

$$f(\tau_t^2 | -) \propto \text{kernel of a invGamma}(a_{\tau(\text{post})}, b_{\tau(\text{post})}) \text{ with} \\ a_{\tau(\text{post})} = \frac{k_t}{2} + a_{\tau} \quad b_{\tau(\text{post})} = \frac{\sum_{j=1}^{k_t} (\mu_{jt}^* - \vartheta_t)^2}{2} + b_{\tau} \quad (2.6)$$

- update  $\vartheta_t$

for  $t = T$ :  $f(\vartheta_t | -) \propto \text{kernel of a } \mathcal{N}(\mu_{\vartheta_t(\text{post})}, \sigma_{\vartheta_t(\text{post})}^2)$  with

$$\sigma_{\vartheta_t(\text{post})}^2 = \frac{1}{\frac{1}{\lambda^2(1-\varphi_1^2)} + \frac{k_t}{\tau_t^2}} \\ \mu_{\vartheta_t(\text{post})} = \sigma_{\vartheta_t(\text{post})}^2 \left( \frac{\sum_{j=1}^{k_t} \mu_{jt}^*}{\tau_t^2} + \frac{(1-\varphi_1)\varphi_0 + \varphi_1\vartheta_{t-1}}{\lambda^2(1-\varphi_1^2)} \right)$$

for  $1 < t < T$ :  $f(\vartheta_t | -) \propto \text{kernel of a } \mathcal{N}(\mu_{\vartheta_t(\text{post})}, \sigma_{\vartheta_t(\text{post})}^2)$  with

$$\sigma_{\vartheta_t(\text{post})}^2 = \frac{1}{\frac{1+\varphi_1^2}{\lambda^2(1-\varphi_1^2)} + \frac{k_t}{\tau_t^2}} \\ \mu_{\vartheta_t(\text{post})} = \sigma_{\vartheta_t(\text{post})}^2 \left( \frac{\sum_{j=1}^{k_t} \mu_{jt}^*}{\tau_t^2} + \frac{\varphi_1(\vartheta_{t-1} + \vartheta_{t+1}) + \varphi_0(1-\varphi_1)^2}{\lambda^2(1-\varphi_1^2)} \right)$$

for  $t = 1$ :  $f(\vartheta_t | -) \propto \text{kernel of a } \mathcal{N}(\mu_{\vartheta_t(\text{post})}, \sigma_{\vartheta_t(\text{post})}^2)$  with

$$\sigma_{\vartheta_t(\text{post})}^2 = \frac{1}{\frac{1}{\lambda^2} + \frac{\varphi_1^2}{\lambda^2(1-\varphi_1^2)} + \frac{k_t}{\tau_t^2}} \\ \mu_{\vartheta_t(\text{post})} = \sigma_{\vartheta_t(\text{post})}^2 \left( \frac{\varphi_0}{\lambda^2} + \frac{\varphi_1(\vartheta_{t+1} - (1-\varphi_1)\varphi_0)}{\lambda^2(1-\varphi_1^2)} + \frac{\sum_{j=1}^{k_t} \mu_{jt}^*}{\tau_t^2} \right) \quad (2.7)$$

- update  $\varphi_0$

$f(\varphi_0 | -) \propto \text{kernel of a } \mathcal{N}(\mu_{\varphi_0(\text{post})}, \sigma_{\varphi_0(\text{post})}^2)$  with

$$\sigma_{\varphi_0(\text{post})}^2 = \frac{1}{\frac{1}{s_0^2} + \frac{1}{\lambda^2} + \frac{(T-1)(1-\varphi_1)^2}{\lambda^2(1-\varphi_1^2)}}$$

$$\mu_{\varphi_0(\text{post})} = \sigma_{\varphi_0(\text{post})}^2 \left( \frac{m_0}{s_0^2} + \frac{\vartheta_1}{\lambda^2} + \frac{1-\varphi_1}{\lambda^2(1-\varphi_1^2)} \sum_{t=2}^T (\vartheta_t - \varphi_1 \vartheta_{t-1}) \right) \quad (2.8)$$

- update  $\lambda^2$

$$f(\lambda^2|-) \propto \text{kernel of a invGamma}(a_{\lambda(\text{post})}, b_{\lambda(\text{post})}) \text{ with}$$

$$a_{\lambda(\text{post})} = \frac{T}{2} + a_{\lambda}$$

$$b_{\lambda(\text{post})} = \frac{(\vartheta_1 - \varphi_0)^2}{2} + \sum_{t=2}^T \frac{(\vartheta_t - (1-\varphi_1)\varphi_0 - \varphi_1 \vartheta_{t-1})^2}{2} + b_{\lambda} \quad (2.9)$$

- update  $\alpha$

if global  $\alpha$ :  $f(\alpha|-) \propto \text{kernel of a Beta}(a_{\alpha(\text{post})}, b_{\alpha(\text{post})})$  with

$$a_{\alpha(\text{post})} = a_{\alpha} + \sum_{i=1}^n \sum_{t=1}^T \gamma_{it} \quad b_{\alpha(\text{post})} = b_{\alpha} + nT - \sum_{i=1}^n \sum_{t=1}^T \gamma_{it}$$

if time specific  $\alpha$ :  $f(\alpha_t|-) \propto \text{kernel of a Beta}(a_{\alpha(\text{post})}, b_{\alpha(\text{post})})$  with

$$a_{\alpha(\text{post})} = a_{\alpha} + \sum_{i=1}^n \gamma_{it} \quad b_{\alpha(\text{post})} = b_{\alpha} + n - \sum_{i=1}^n \gamma_{it}$$

if unit specific  $\alpha$ :  $f(\alpha_i|-) \propto \text{kernel of a Beta}(a_{\alpha(\text{post})}, b_{\alpha(\text{post})})$  with

$$a_{\alpha(\text{post})} = a_{\alpha i} + \sum_{t=1}^T \gamma_{it} \quad b_{\alpha(\text{post})} = b_{\alpha i} + T - \sum_{t=1}^T \gamma_{it}$$

if time and unit specific  $\alpha$ :  $f(\alpha_{it}|-) \propto \text{kernel of a Beta}(a_{\alpha(\text{post})}, b_{\alpha(\text{post})})$  with

$$a_{\alpha(\text{post})} = a_{\alpha i} + \gamma_{it} \quad b_{\alpha(\text{post})} = b_{\alpha i} + 1 - \gamma_{it} \quad (2.10)$$

- update a missing observation  $Y_{it}$

for  $t = 1$ :  $f(Y_{it}|-) \propto \text{kernel of a } \mathcal{N}(\mu_{Y_{it}(\text{post})}, \sigma_{Y_{it}(\text{post})}^2)$  with

$$\sigma_{Y_{it}(\text{post})}^2 = \frac{1}{\frac{1}{\sigma_{c_{it}t}^{2*}} + \frac{\eta_{1i}^2}{2\sigma_{c_{it+1}t+1}^{2*}(1-\eta_{1i}^2)}}$$

$$\mu_{Y_{it}(\text{post})} = \sigma_{Y_{it}(\text{post})}^2 \left( \frac{\mu_{c_{it}t}^* + \mathbf{x}_{it}^T \boldsymbol{\beta}_t}{\sigma_{c_{it}t}^{2*}} + \frac{\eta_{1i}(Y_{it+1} - \mu_{c_{it+1}t+1}^* - \mathbf{x}_{it+1}^T \boldsymbol{\beta}_{t+1})}{\sigma_{c_{it+1}t+1}^{2*}(1-\eta_{1i}^2)} \right)$$

for  $1 < t < T$ :  $f(Y_{it}|-) \propto \text{kernel of a } \mathcal{N}(\mu_{Y_{it}(\text{post})}, \sigma_{Y_{it}(\text{post})}^2)$  with

$$\sigma_{Y_{it}(\text{post})}^2 = \frac{1 - \eta_{1i}^2}{\frac{1}{\sigma_{c_{it}t}^{2*}} + \frac{\eta_{1i}^2}{\sigma_{c_{it+1}t+1}^{2*}}}$$

$$\mu_{Y_{it}(\text{post})} = \sigma_{Y_{it}(\text{post})}^2 \left( \frac{\mu_{c_{it}t}^* + \eta_{1i}Y_{it-1} + \mathbf{x}_{it}^T \boldsymbol{\beta}_t}{\sigma_{c_{it}t}^{2*}(1-\eta_{1i}^2)} + \frac{\eta_{1i}(Y_{it+1} - \mu_{c_{it+1}t+1}^* - \mathbf{x}_{it+1}^T \boldsymbol{\beta}_{t+1})}{\sigma_{c_{it+1}t+1}^{2*}(1-\eta_{1i}^2)} \right)$$

for  $t = T$ :  $f(Y_{it}|-) \propto \text{kernel of a } \mathcal{N}(\mu_{Y_{it}(\text{post})}, \sigma_{Y_{it}(\text{post})}^2)$  with

$$(2.11)$$

## 2.2 Spatial cohesions analysis

To include spatial information into the clustering process, the idea is to extend the PPM from being a function of just  $C(S_{jt})$  to the more informed one  $C(S_{jt}, \mathbf{s}_{jt}^*)$ , where  $S_{jt}$  is the  $j$ -th cluster at time instant  $t$  and  $\mathbf{s}_{jt}^*$  is the subset of spatial coordinates of the units inside  $S_{jt}$ . For the sake of clarity, in this section where we are just interested in analysing the cohesions we employ the  $S_h$  notation to indicate a general  $h$ -th cluster, rather than the more pedantic  $S_{jt}$ .

Regarding the computation of spatial cohesion, several choices are available [PQ15]. The main common idea of the following formulas is to favour few spatially connected clusters rather than a lot of singleton ones, to derive more interpretable and meaningful results. For this reason, most of the cohesions employ the  $M \cdot \Gamma(|S_h|)$  term, which resembles the DP partitioning method that helps in reaching that goal.

We will now describe briefly all the cohesions which are implemented in the JDRPM model, and were implemented as well in the CDRPM model, and conduct tests on each of them, to see how the tuning of their parameters reflects on the computed values.

All the tests of Figures 2.3 and 2.4 refer to the partition of Figure 2.2, taken as test case here from a general fit on the same spatio-temporal dataset of Chapter 4. The following results, as well as the ones of the next section, are presented with the logarithm applied to better highlight the differences among them, otherwise for example all values could be really close together and make the analysis less understandable, and moreover because this is the actual perspective in which the implementation works. In fact, the fitting algorithm firstly saves the log-transformed values generated by the cohesions, in order to avoid numerical problems and instabilities, and secondly exponentiates and normalizes them into proper scaled probabilities, from which finally draw the cluster assignments.

The first cohesion uses a tessellation idea from [DH01] that considers  $\mathcal{D}_h = \sum_{i \in S_h} \|\mathbf{s}_i - \bar{\mathbf{s}}_h\|$  as the total distance from the units to the cluster centroid  $\bar{\mathbf{s}}_h$ . The computation is then an adjustment of a decreasing function in terms of  $\mathcal{D}_h$ , to give an higher weight on clusters which are denser, i.e. that have lower  $\mathcal{D}_h$ , with an additional parameter  $\alpha$  to provide more control on the penalization.

$$C_1(S_h, \mathbf{s}_h^*) = \begin{cases} \frac{M \cdot \Gamma(|S_h|)}{\Gamma(\alpha \mathcal{D}_h) \mathbb{1}_{[\mathcal{D}_h \geq 1]} + \mathcal{D}_h \mathbb{1}_{[\mathcal{D}_h < 1]}} & \text{if } |S_h| > 1 \\ M & \text{if } |S_h| = 1 \end{cases} \quad (2.12)$$

The second function provides, instead, a hard cluster boundary, where the weight is set to 1, i.e. 0 with the logarithm view, only if all the distances between all possible pairs of points inside the cluster are below the threshold parameter, i.e. if all units are “close enough” to each other. If this does not happen, even for a single pair of points, the returned value is 0, which corresponds to the maximum penalization since it would be  $-\infty$  in the logarithm perspective. The strictness of this requirement can be adjusted through the parameter  $a$ .

$$C_2(S_h, \mathbf{s}_h^*) = M \cdot \Gamma(|S_h|) \cdot \prod_{i,j \in S_h} \mathbb{1}_{[\|\mathbf{s}_i - \mathbf{s}_j\| \leq a]} \quad (2.13)$$



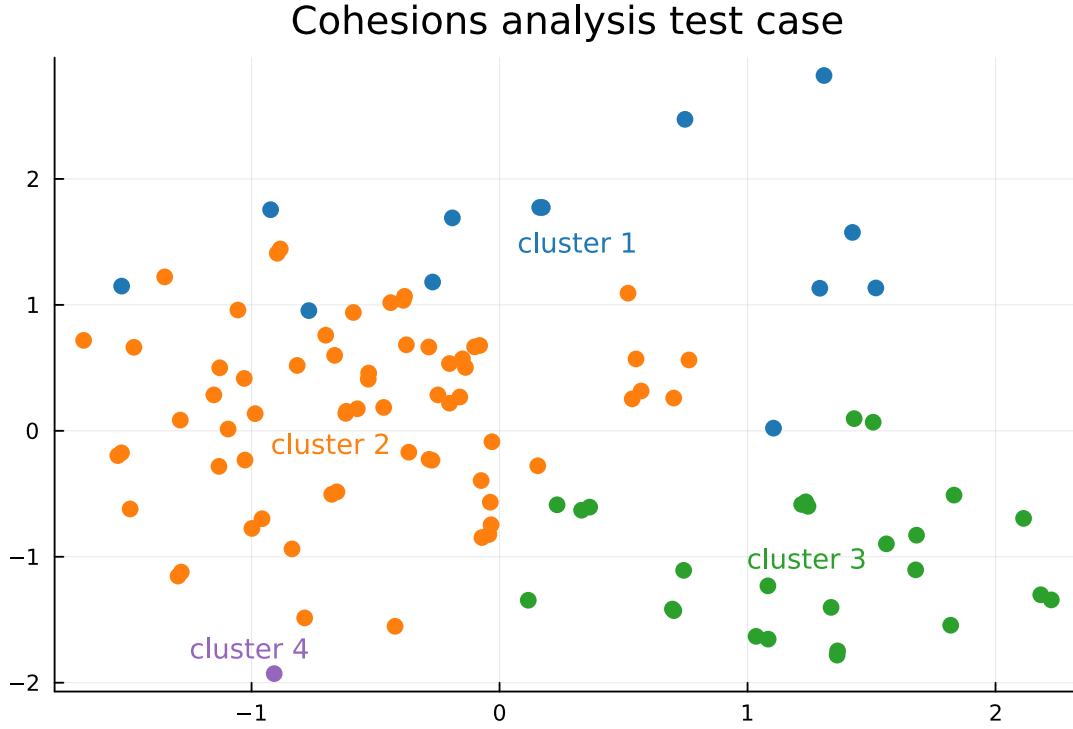


**Figure 2.2:** Partition considered to analyse the spatial cohesions.

According to this function, from Figure 2.3 we can see how the purple cluster is considered the one with the highest cohesion, being a singleton. The runner-up is the green cluster, because it's the first among all the non-singletons which activates cohesion 2 when we increase the parameter  $a$ . The orange and blue clusters, instead, appear to be less dense since they require an higher value of  $a$  to “pass” the distance check.

However, cohesions  $C_1$  and  $C_2$  do not preserve the exchangeability property, meaning that if we would marginalize the random partition model over the last of  $m$  units we would not get to the same model as if we only had  $m - 1$  units. This coherence property, known as sample size consistency or addition rule [De +15], is instead often desirable, for theoretical or computational purposes, and the following two cohesions are able to provide it [MQR11].

Cohesion 3, called marginal likelihood or prior predictive distribution, treats the spatial coordinates  $\mathbf{s}^*$  as if they were random, applying on them a model such as the Normal/Normal-Inverse-Wishart with  $\boldsymbol{\xi} = (\mathbf{m}, V)$ ,  $\mathbf{s}|\boldsymbol{\xi} \sim \mathcal{N}(\mathbf{m}, V)$  and  $\boldsymbol{\xi} \sim \mathcal{NIW}(\boldsymbol{\mu}_0, \kappa_0, \nu_0, \Lambda_0)$ . The idea is to assign a larger weight on clusters which produce large marginal likelihood values, i.e. which according to the modelling are more probable to appear.

$$C_3(S_h, \mathbf{s}_h^*) = M \cdot \Gamma(|S_h|) \cdot \int \prod_{i \in S_h} q(\mathbf{s}_i | \boldsymbol{\xi}_h) q(\boldsymbol{\xi}_h) d\boldsymbol{\xi}_h \quad (2.14)$$

On the same line there is cohesion 4, the double dipper cohesion [QMP15], which now employs the posterior predictive distribution rather than the prior predictive

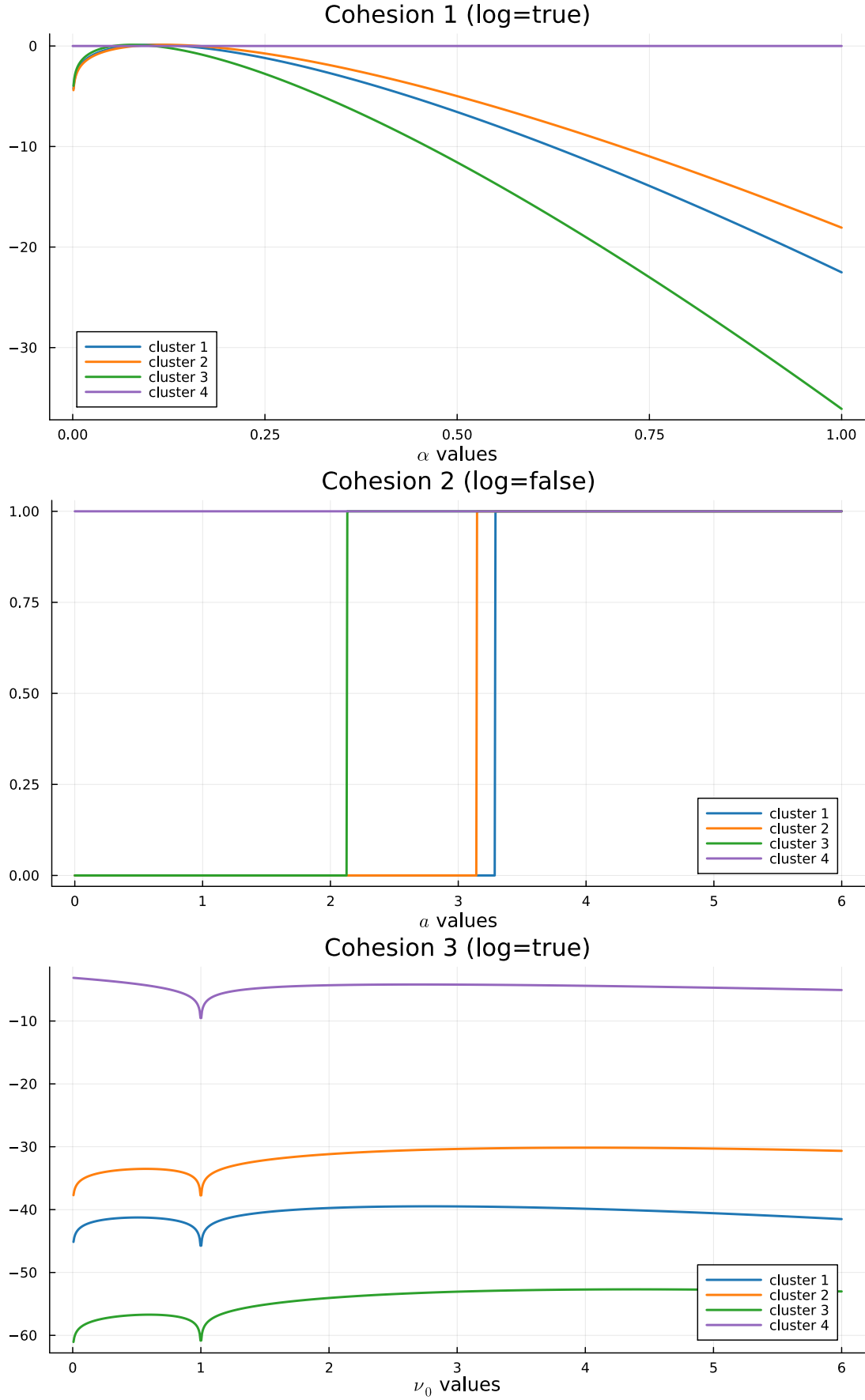


**Figure 2.3:** Cohesions 1, 2, and 3 computed on the test case partition, with respect to different values of their tuning parameter. Cohesion 2 is without the logarithm applied just for plotting purposes, since otherwise the values would have been  $-\infty$  and 0.

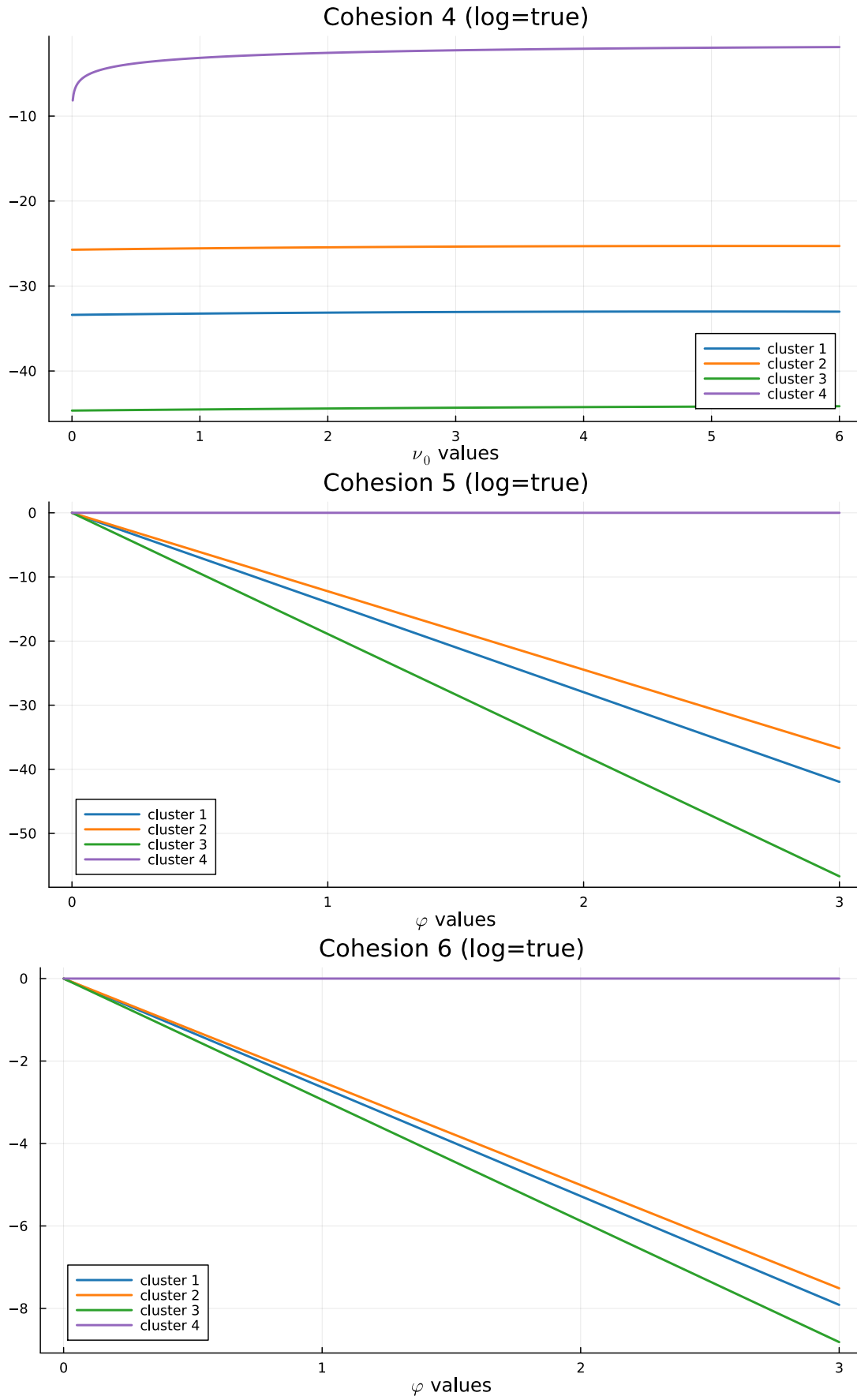


**Figure 2.4:** Cohesions 4, 5, and 6 computed on the test case partition, with respect to different values of their tuning parameter.

distribution of cohesion  $C_3$ .

$$C_4(S_h, \mathbf{s}_h^*) = M \cdot \Gamma(|S_h|) \cdot \int \prod_{i \in S_h} q(\mathbf{s}_i | \boldsymbol{\xi}_h) q(\boldsymbol{\xi}_h | \mathbf{s}_h^*) d\boldsymbol{\xi}_h \quad (2.15)$$

Another final idea comes from the cluster variance/entropy similarity function, a very general methodology to measure the closeness of a set of values which in fact will be used also for the covariates case. As in cohesion  $C_1$ , the idea is to derive a summary of the closeness of the units, summing the distance of the units from the cluster centroid, and then adjust the penalization through the parameter  $\varphi$ , to control how much penalize dissimilar values.

$$C_5(S_h, \mathbf{s}_h^*) = \exp \left\{ -\varphi \sum_{i \in S_h} \|\mathbf{s}_i - \bar{\mathbf{s}}_h\| \right\} \quad (2.16)$$

$$C_6(S_h, \mathbf{s}_h^*) = \exp \left\{ -\varphi \log \left( \sum_{i \in S_h} \|\mathbf{s}_i - \bar{\mathbf{s}}_h\| \right) \right\} \quad (2.17)$$

## 2.3 Covariates similarities analysis

A wide spectrum of choice is also available for covariates similarities [PQ18]. To account for them, the idea consists in extending the PPM to make it function of  $S_{jt}$ ,  $\mathbf{s}_{jt}^*$ , and now also of  $X_{jt}^*$ , being this the  $p \times |S_{jt}|$  matrix storing the covariates of the units belonging to cluster  $j$  at time  $t$ , i.e.  $X_{jt}^* = \{\mathbf{x}_{it}^* = (x_{it1}, \dots, x_{itp})^T : i \in S_{jt}\}$ .

For the current implementation of JDRPM we decided to treat each covariate individually, therefore the PPM will actually be function of the set of unidimensional vectors which record the different  $p$  covariates of the units inside cluster  $S_{jt}$ , meaning  $\mathbf{x}_{jt1}^*, \dots, \mathbf{x}_{jtp}^*$ , of which all contributions will be considered independently one to each other. In this way, the final PPM form will be

$$P(\rho) \propto \prod_{h=1}^{k_t} C(S_{jt}, \mathbf{s}_{jt}^*) \left( \prod_{r=1}^p g(S_{jt}, \mathbf{x}_{jtr}^*) \right) \quad (2.18)$$

where  $\mathbf{x}_{jtr}^*$  represents the vector recording the  $r$ -th covariate values for all the units inside cluster  $S_{jt}$ , i.e. row  $r$  of matrix  $X_{jt}^*$ . This choice is lighter from the theoretical and computational perspectives, and allows a mixture of numerical and categorical covariates without any problem. A unified and multidimensional consideration of the covariates is nonetheless possible, with proper adjustments on the similarities functions, and would have lead to a PPM of the form

$$P(\rho) \propto \prod_{h=1}^{k_t} C(S_{jt}, \mathbf{s}_{jt}^*) g(S_{jt}, X_{jt}^*) \quad (2.19)$$

As in the previous section, we will now discuss all the similarities implemented in the JDRPM model and perform tests on each of them. All the tests will be

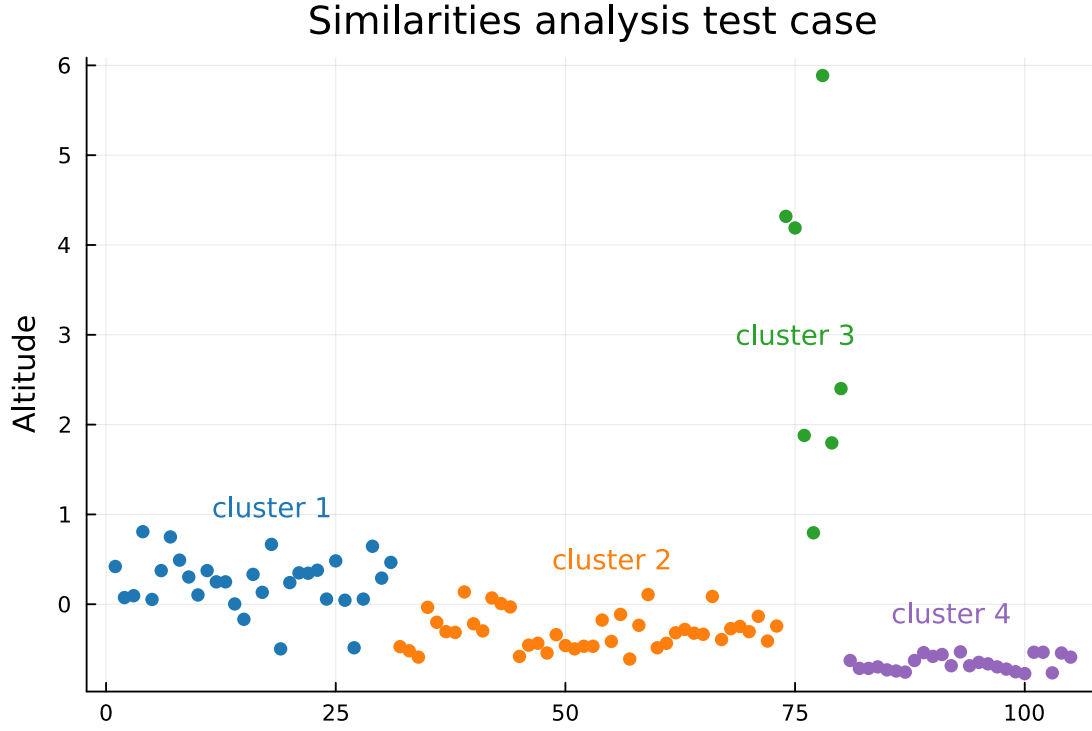


**Figure 2.5:** Partition considered to analyse the covariate similarities. The order of the units has been modified to plot together all units belonging to the same cluster.

referred to the test case partition displayed in Figure 2.5. Regarding the notation, we will again employ the simpler and general one dropping the spatio-temporal context.

The first similarity is the cluster variance/entropy similarity function, which as the name suggest can work with both numerical and categorical variables. The general form is

$$g_1(S_h, \mathbf{x}_h^*) = \exp \{-\varphi H(S_h, \mathbf{x}_h^*)\} \quad (2.20)$$

with  $H(S_h, \mathbf{x}_h^*) = \sum_{i \in S_h} (x_i - \bar{x}_h)^2$  for numerical covariates, being  $\bar{x}_h$  the mean value of the  $\mathbf{x}_h^*$  vector, and  $H(S_h, \mathbf{x}_h^*) = -\sum_{c=1}^C \hat{p}_c \log(\hat{p}_c)$  for categorical covariates, with  $\hat{p}_c$  indicating the relative frequency at which each factor appears. The parameter  $\varphi$  controls the amount of penalization to apply. This function can be extended quite easily to the multidimensional case, at least for the case of numerical covariates only, where the  $H$  function becomes  $H(S_h, X_h^*) = \sum_{r=1}^p \|\mathbf{x}_r - \bar{\mathbf{x}}_h\|$ .

Another popular choice is the Gower similarity function [Gow71], which was originally designed for a multivariate context, where vectors of covariates are compared to each other. As a consequence, some work was required to adapt it to the univariate case. The simple idea of comparing all cluster-specific pair-wise similarities leads to the total Gower similarity.

$$g_2(S_h, \mathbf{x}_h^*) = \exp \left\{ -\alpha \sum_{i,j \in S_h, i \neq j} d(x_i, x_j) \right\} \quad (2.21)$$

This function, however, is strictly increasing with respect to the cluster size, meaning

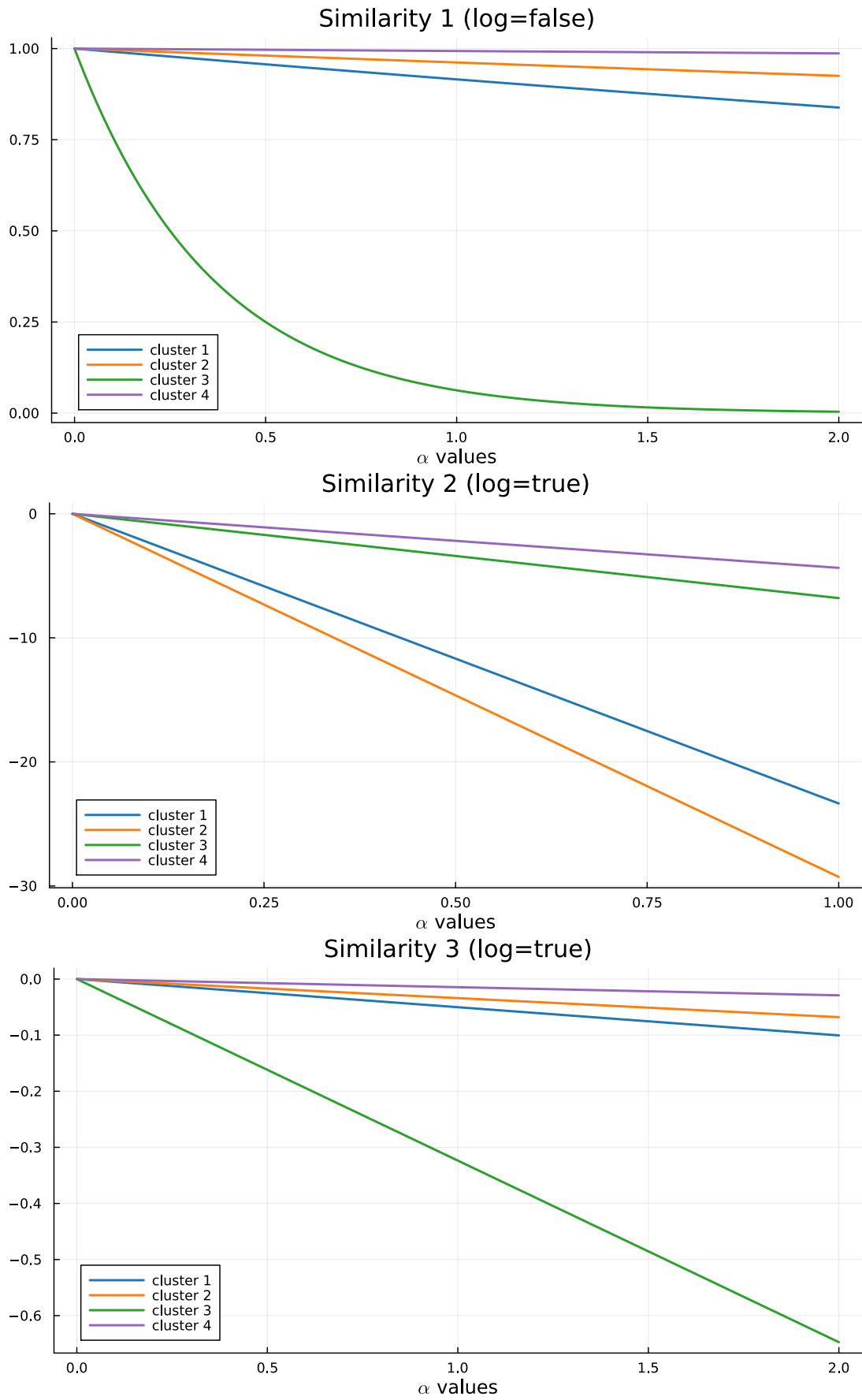


**Figure 2.6:** Similarities 1, 2 and 3 computed on the test case partition, with respect to different values of their tuning parameter. Similarity 1 is without the logarithm applied just for plotting purposes, to see more clearly the gap among the clusters.

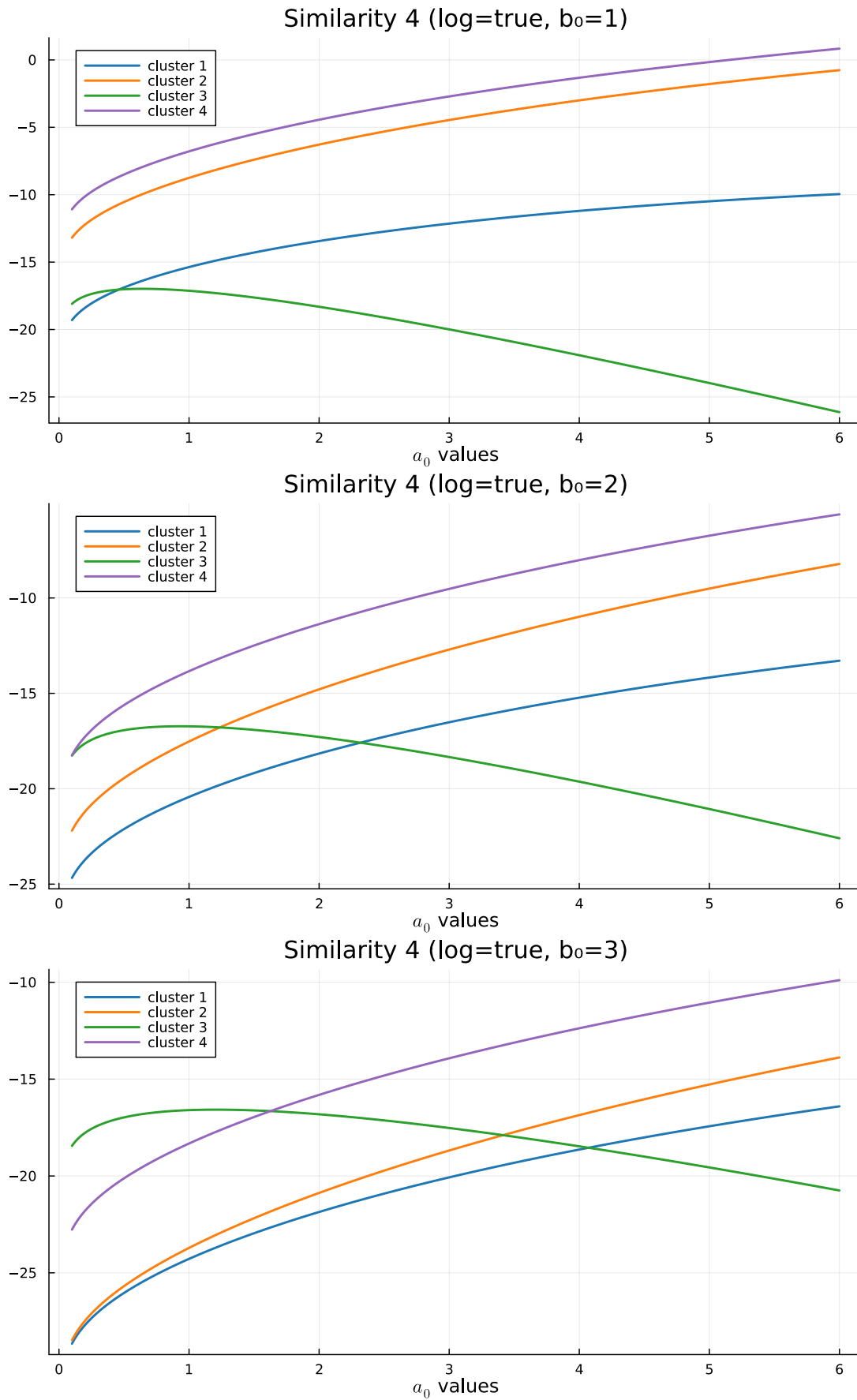


**Figure 2.7:** Similarity 4 computed on the test case partition, with respect to the different values of the tuning parameter  $a_0$  and  $b_0$ . The other parameters has been set to  $\mu_0 = 0$  and  $\lambda_0 = 1$ , with the idea to apply the similarity on scaled (centered and standardized) covariates.

that it will naturally tend to propose a large number of small clusters. For that reason, a correction can be applied, accounting for the size of the cluster  $S_h$ , leading to the average Gower similarity.

$$g_3(S_h, \mathbf{x}_h^*) = \exp \left\{ -\frac{2\alpha}{|S_h|(|S_h| - 1)} \sum_{i,j \in S_h, i \neq j} d(x_i, x_j) \right\} \quad (2.22)$$

In both functions,  $d(x_i, x_j)$  is the Gower dissimilarity between  $x_i$  and  $x_j$ , with  $d(x_i, x_j) = |x_i - x_j|/R$  in the case of numerical covariates, being  $R = \max(\mathbf{x}) - \min(\mathbf{x})$  the range of the covariate values, considering all the units independently from their cluster, while  $d(x_i, x_j) = \mathbb{1}_{[x_i \neq x_j]}$  in the case of categorical covariates. This is a dissimilarity since values closer to 0 refer to similar data, while values closer to 1 to dissimilar data; therefore the minus sign inside  $g_2$  and  $g_3$  exponents converts the function to a similarity. For the multidimensional design there are natural extensions of the  $d(\mathbf{x}_i, \mathbf{x}_j)$  function.

The last similarity recalls the structure of the spatial cohesion  $C_3$ , where now are the covariates to be treated as if they were random variables. However, since we chose to deal with each covariate individually, in this unidimensional setting a Normal/Normal-Inverse-Gamma model is employed, with  $\boldsymbol{\xi} = (\mu, \sigma^2)$ ,  $x|\boldsymbol{\xi} \sim \mathcal{N}(\mu, \sigma^2)$ , and  $\mu \sim \mathcal{N}(\mu_0, \sigma^2/\lambda_0)$ ,  $\sigma^2 \sim \text{invGamma}(a_0, b_0)$ , i.e.  $\boldsymbol{\xi} \sim \mathcal{N}\text{invGamma}(\mu_0, \lambda_0, a_0, b_0)$ . A multivariate extension is thus possible through the same modelling style of the spatial coordinates case.

$$g_4(S_h, \mathbf{x}_h^*) = \int \prod_{i \in S_h} q(x_i|\boldsymbol{\xi}_h) q(\boldsymbol{\xi}_h) d\boldsymbol{\xi}_h \quad (2.23)$$

All the similarities, except for  $g_2$ , agree to classify the clusters with the purple being the one with the highest similarity, followed by the orange, blue, and green, as we can see from Figures 2.6 and 2.7. Intuitively, Figure 2.5 seems to confirm this ranking, by visually reasoning about the sparsity of each cluster. Similarities  $g_4$  and  $g_2$  appears to be the only ones which can give a considerable weight to the green partition, which is indeed sparser but collects all the large, sort of outliers, covariates values.



# Chapter 3

## Implementation and optimizations

To implement our updated model, and to do it efficiently, we decided to opt for the Julia language [Bez+17].

Julia is a relatively new programming language that combines the ease and expressiveness of high-level languages to the efficiency and performance of low-level ones. Such balance largely achieved through the just-in-time (JIT) compilation, implemented using the LLVM framework, together with many nice features like dynamic multiple dispatch and code specialization against run-time types. This design choice allows Julia to be used interactively, in the same fashion to the R, Matlab, or Python consoles, while also supporting the more traditional program execution style of statically compiled languages such as C, C++ and Fortran. This solution provides faster development phases, since for examples code sections can be evaluated and tested line by line, guaranteeing and at the same time efficient implementations. Performances are further enhanced by the native integration of the optimized BLAS [Law+79] and LAPACK libraries for linear algebra operations, which are often at the core of all scientific applications. Regarding productivity, instead, Julia provides an extensive ecosystem, currently comprised by more than ten thousand packages, spanning over almost all branches of science and engineering. Moreover, most of them are already highly tested and optimized, and can therefore reduce the implementation time required to the users. As an example, in this work we employed the `Distributions` [Bes+21] [Lin+19] and `Statistics` packages, while the original C implementation had to write all the statistical functionalities from scratch. Considering all this, the Julia choice was deemed very natural.

### 3.1 Optimizations

As we will see in Section 4, even despite the higher complexity of the model we managed to get better performance in Julia compared to the original C implementation. This at the reasonable cost of a smaller increase in the memory requirements.

In fact, one major issue encountered during the earlier stages of designing the fitting function in Julia was controlling the amount of memory and allocations

that some functions, structures, or algorithms would require. At the beginning of the development and testing, where the correctness of the algorithm was the only priority, we saw that most of the execution time was actually spent by the garbage collector of Julia, which had the burden of tracking all the allocated memory and reclaiming the unused one in order to make it available again for new computations.

Together with avoiding useless allocations, or in general managing more finely the memory, another important aspect to focus on to improve performances is ensuring type stability of the function. Luckily, Julia disposes of several tools to inspect and address both problems.

Regarding the first point, there are packages such as **Cthulhu**, or even the simple `@code_warntype` macro, which allow to ensure that a function is type-stable, i.e. that the types of all variables can be correctly predicted by the compiler and stay consistent throughout the execution. Type stability is crucial for performance as it enables the compiler to generate optimized machine code, removing the load derived from dynamic type checks. In fact, Julia is dynamically typed, which means that variables do not have to be necessarily declared with their type, in contrast to fully statically typed languages such as C, and they could change it during execution. For example a variable initialized as an integer could later become a float, or even a string. However, for performance purposes, these dynamicisms should be avoided, and those tools help to ensure that this happens.

Regarding allocations, we relied on profiling suites such as **ProfileCanvas**. This profiler generates a plot, the *flame graph* of Figure 3.1, which depicts the different sections of code with regions whose size is proportional to a certain metric, e.g. the time spent on them during execution or the number (or size) of allocations that was required. This allows to see if the running time is spent on actual useful operations or instead on “bad” ones, such as garbage collection; highlighting therefore the sections of code which could possibly be optimized. All the modelling variables were of course preallocated, but the key has been to refactor the code to make it work more *in place*, passing directly as arguments the variables which would be modified the function, and modify them inside the function, rather than returning some values and then use them on the initial variables.

More in general, **BenchmarkTools** [CR16] had been also a great ally to quickly analyse and compare whole fits or just small sections of code and simple instructions. For example, we can test different versions of equivalent instructions to see which could be the most efficient, as in this case

```
using BenchmarkTools
nh_tmp = rand(100)
@btime nclus_temp = sum($nh_tmp .> 0)
# 168.956 ns (2 allocations: 112 bytes)
@btime nclus_temp = count(x->(x>0), $nh_tmp)
# 11.612 ns (0 allocations: 0 bytes)
```

or this other one

```
n = 100; rho_tmp = rand((1:5),n); k = 1
@btime findall(j -> ($rho_tmp)[j]==$k, 1:n) # with anonymous function
# 272.302 ns (5 allocations: 384 bytes)
```

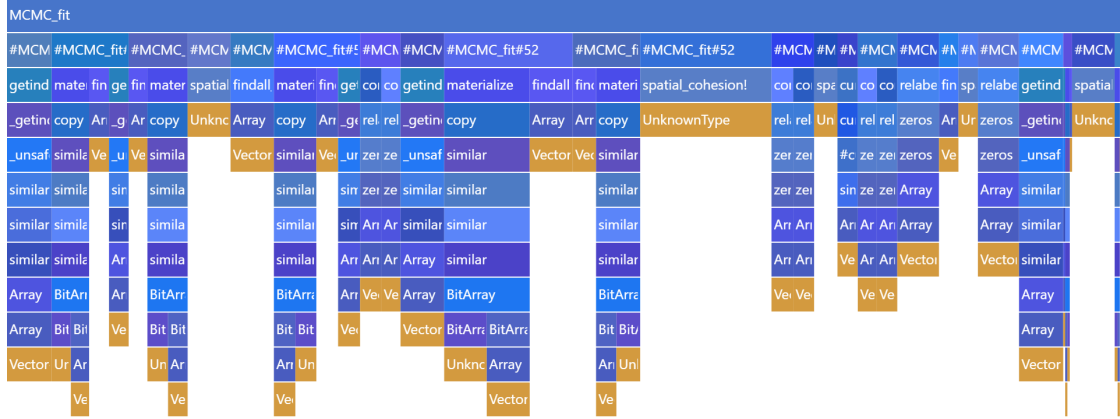


**Figure 3.1:** Flame graph derived from a simple test fit with  $n = 20$ ,  $T = 50$ , ran for 10000 iterates. Each section, identified with a colored box, represents a function call with its stack trace below, i.e. all the other subsequent function calls generated from the initial top one. The widths are proportional to allocation counts, i.e. to how many times a memory allocation was required for their corresponding box. The plot should be read from top to bottom regarding function calls, and from left to right regarding the fitting steps.

```
@btime findall_faster(j -> ($rho_tmp)[j]==$k, 1:n) # custom implementation
# 214.259 ns (3 allocations: 960 bytes)
@btime findall($rho_tmp .== $k) # with element-wise comparison
# 184.112 ns (3 allocations: 320 bytes)
```

where the  $\$$  symbol is used for interpolate the variable, ensuring to treat it as a local variable inside the benchmark and therefore avoiding any bias caused by accessing a global variable. This was a quick and simple comparison, yet very precise and effective, which would be instead more complex to replicate in C.

During the finer and final refinements of the code we even used the surgical `--track-allocation` option, which asks Julia to execute the code and annotate the source file to see at which lines (and of which amount) occur allocations.

### 3.1.1 Optimizing spatial cohesions

The memory allocation problem was especially seen in the spatial cohesion computation. In fact, such computation appears twice in both sections of updating  $\gamma$  and updating  $\rho$ , which are inside of outer loops on draws, time, and units, and involve themselves some other loops on clusters. All this implied that those cohesion computations will be executed possibly millions of times during each fit. A simple and quick inspection suggests a value between  $\Omega(dTn)$  and  $O(dTn^2)$ , being  $d$  the number of iterations,  $T$  the time horizon and  $n$  the number of units. We can't provide a  $\Theta$  estimate due to the variability and randomness of the inside loops, which depend on the distribution of the clusters. With all that in mind, it was crucial to optimize the performance of the cohesion functions.

Function calls in Julia are very cheap, and so the only optimizing task consisted in carefully designing the cohesion function implementations, rather than maybe rethink the whole algorithm. Cohesions 1, 2, 5 and 6 didn't exhibit any complication

or need for optimization. The natural conversion in code from their mathematical models proved to be already optimally performing. The main problem was instead with cohesions 3 and 4, the auxiliary and double dippery, which by nature would involve some linear algebra computations with vectors and matrices.

The first implementation of those cohesions turned out to be really slow, due to the overhead generated by allocating and then freeing, at each call, the memory devoted to all vectors and matrices. This in the end meant that most of the execution time was actually spent by the garbage collector, rather than in the real and useful operations. A first solution was then to resort to a scalar implementation, which would remove the overhead of the more complex memory structures, but in the end we managed to combine the readability of the first idea with the performance of the second one into a final version, as we can see from Listing 1.

**Listing 1:** Sections of the Julia code for the three implementation cases of the spatial cohesions 3 and 4. The first one has the classical vector computations derived from the mathematical formulation, the second one is the conversion to only have scalar variables, while the third one is the final version, keeping the vector form but improved using static structures.

```
# original vector version
sbar = [mean(s1), mean(s2)]
vtmp = sbar - mu_0
Mtmp = vtmp * vtmp'
Psi_n = Psi + S + (k0*sdim) / (k0+sdim) * Mtmp

# scalar-only version
sbar1 = mean(s1); sbar2 = mean(s2)
vtmp_1 = sbar1 - mu_0[1]
vtmp_2 = sbar2 - mu_0[2]
Mtmp_1 = vtmp_1^2
Mtmp_2 = vtmp_1 * vtmp_2
Mtmp_3 = copy(Mtmp_2)
Mtmp_4 = vtmp_2^2
aux1 = k0 * sdim; aux2 = k0 + sdim
Psi_n_1 = Psi[1] + S1 + aux1 / (aux2) * Mtmp_1
Psi_n_2 = Psi[2] + S2 + aux1 / (aux2) * Mtmp_2
Psi_n_3 = Psi[3] + S3 + aux1 / (aux2) * Mtmp_3
Psi_n_4 = Psi[4] + S4 + aux1 / (aux2) * Mtmp_4

# static improved version
sbar1 = mean(s1); sbar2 = mean(s2)
sbar = SVector((sbar1, sbar2))
vtmp = sbar .- mu_0
Mtmp = vtmp * vtmp'
aux1 = k0 * sdim; aux2 = k0 + sdim
Psi_n = Psi .+ S .+ aux1 / (aux2) .* Mtmp
```

This final version exploits the `StaticArrays` package of Julia, which allows to use vectors and matrices more efficiently if their size is known at compile time; which is the case of the spatial cohesions computation, since working with planar spatial coordinates we will always have  $2 \times 1$  vectors and  $2 \times 2$  matrices. The benefits of this final version are that we maintain the natural mathematical form of the first one, improving the clearness of the code, together with the efficiency of

the second one, since now with static structures the compiler is able to optimize all memory allocations as it was doing with the simple scalar variables.

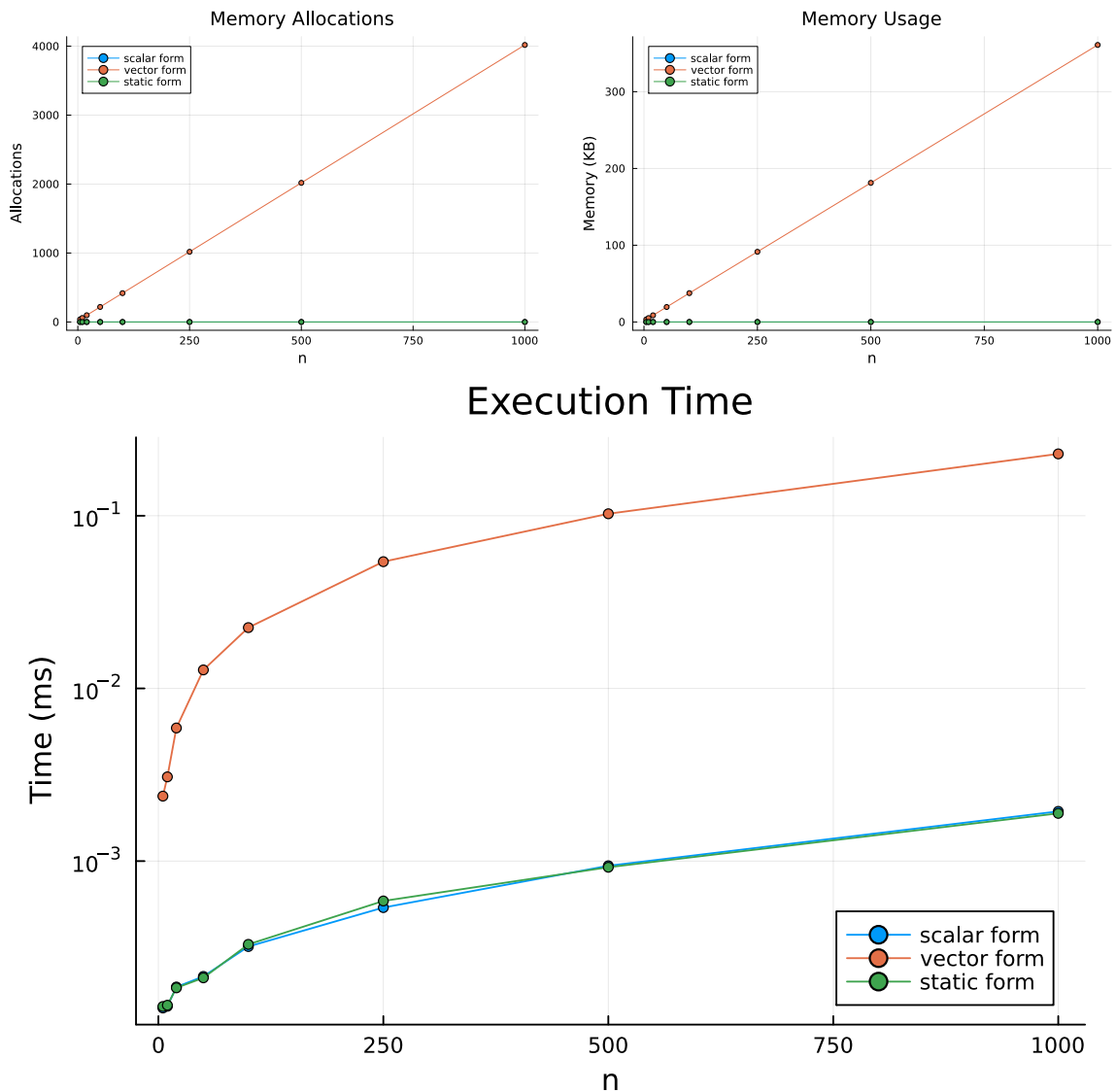


**Figure 3.2:** Performance comparison between the three versions of the cohesion 4 function. Tests ran through the `BenchmarkTools` package of Julia by randomly generating the spatial coordinates of the various test sizes  $n$ , with similar results standing for cohesion 3. The memory allocation and usage plots are constant at zero for both the scalar and vector static cases.

Figure 3.2 shows the comparison of their performances, where we can see how the scalar and static versions indeed perform very similarly.

Noticeably, the C implementation of the model didn't have to worry about all this reasoning, since C can't natively, nor gracefully, work with vectors and matrices.

### 3.1.2 Optimizing covariates similarities

Another problem was how to speed up the computation of the similarity functions, since those would also be called the possibly millions of times as the cohesion ones, considering also that we could incorporate more than one covariate into the clustering process, so there would be an additional loop based on  $p$ , the number of covariates decided to be included.

As in the previous case, some of the functions didn't show any special need or room for relevant optimizations. The fourth one instead, the auxiliary similarity function, was essential to be optimized; not only being one the most frequent choice among all the similarities, but also because it involves a computationally heavy sum of the squares of the covariate values, as we can see in Listing 2.

**Listing 2:** Fully equipped version of the similarity 4 function, i.e. with all the optimizing macros. The performance analysis will focus just on that inside loop, since the rest is not negotiable.

```
function similarity4(X_jt::AbstractVector{<:Real}, mu_c::Real, lambda_c::Real,
↳ a_c::Real, b_c::Real, lg::Bool)
    n = length(X_jt)
    nm = n/2
    xbar = mean(X_jt)
    aux2 = 0.
    @inbounds @fastmath @simd for i in eachindex(X_jt)
        aux2 += X_jt[i]^2
    end
    aux1 = b_c + 0.5 * (aux2 - (n*xbar + lambda_c*mu_c)^2/(n+lambda_c) +
↳ lambda_c*mu_c^2 )
    out = -nm*log2pi + 0.5*log(lambda_c/(lambda_c+n)) + lgamma(a_c+nm) -
↳ lgamma(a_c) + a_c*log(b_c) + (-a_c-nm)*log(aux1)
    return lg ? out : exp(out)
end
```

The idea to optimize it has been to annotate the loop with some macros provided by Julia. They are the following:

- `@inbounds` eliminates the array bounds checking within expressions. This allows to skip the checks, at the cost to guarantee, by code design, that no out-of-bounds or wrong accesses will occur in the code and therefore no undefined behaviour will take place. The above loop is indeed very simple and safe, so this assumption is clearly satisfied.
- `@fastmath` executes a transformed version of the expression, which calls functions that may violate strict IEEE semantics<sup>1</sup>. For example, its use could make  $(a + b) + c \neq a + (b + c)$ , but just in very pathological cases. Again, this is not a problem in our case where we are computing  $\sum X_i^2$ , since it does not have an intrinsically “right order” in which it has to be done.

<sup>1</sup>Institute of Electrical and Electronics Engineers. The IEEE-754 standard defines floating-point formats, i.e. the ways to represent real numbers in hardware, and the expected behavior of arithmetic operations on them, including precision, rounding, and handling of special values (e.g. NaN (Not a Number) and infinity).

- `@simd` (single instruction multiple data) annotate a for loop to allow the compiler to take extra liberties to allow loop re-ordering. This is a sort of parallelism technique, but rather than distributing the computational load on more processors we just *vectorize* the loop, i.e. we enable the CPU to perform that single instruction (summing the square of the  $i$ th component to a reduction variable) on multiple data chunks at once, using vector registers, rather than working on each element of the vector individually.

As we can see from Figure 3.3, the actual performance difference basically derives just from the use of `@simd`, with the other two annotations making not much of a difference. For that reason, and to reassure all pure mathematicians, we decided to remove the `@fastmath` annotation, leaving just `@inbounds` and `@simd`.

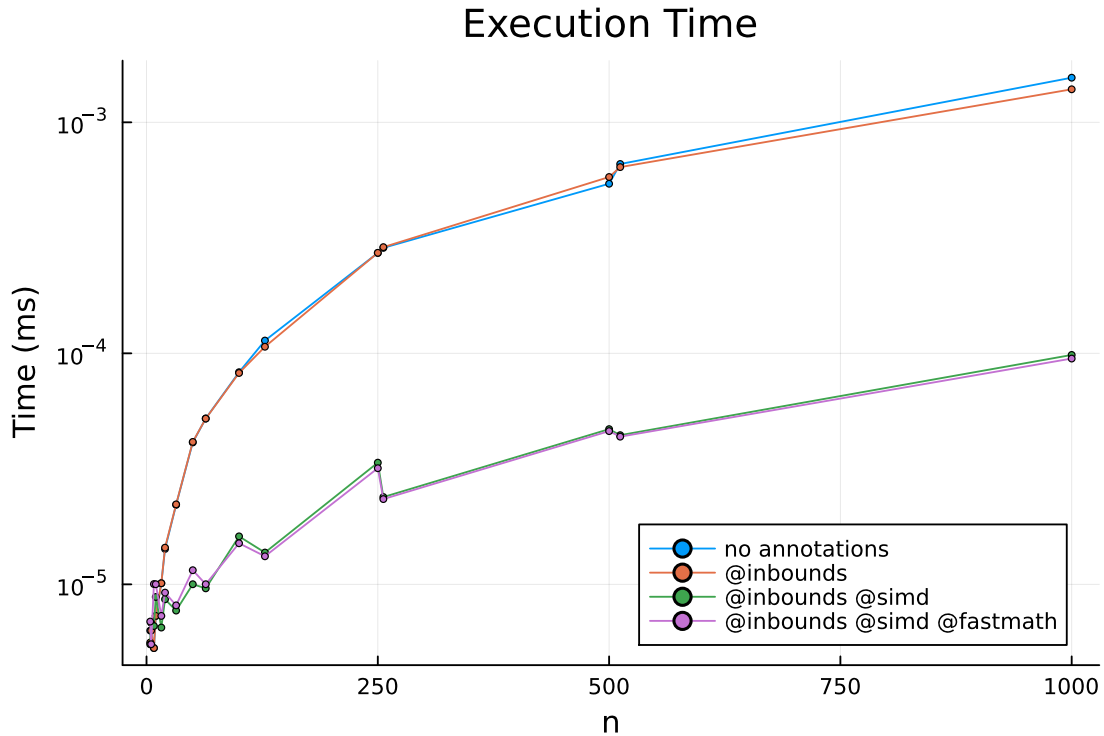


**Figure 3.3:** Comparison of the performances of the different possible loop annotations in the similarity 4 implementation. Their numerical output results are indeed the same for all cases. There are no memory allocation and usage plots since the analysis has been conducted only to evaluate the performances of the inside loop, which has no memory issues.

We can also notice interestingly how the tests with `@simd` annotation runs quicker in the case of  $n$  being a power of two compared to its closest rounded integer (e.g. 256 against 250 or 512 against 500), despite having some more data. This is a proof of the effectiveness of the SIMD paradigm: according to the different architectures, the CPUs can provide different register sizes (e.g. 64, 128, 256 or 512 bits) and therefore the data subdivision can fit perfectly in them when the total memory occupied by the elements is a multiple of that register size (i.e. the number of data values is a power of two). Otherwise there will be some “leftovers chunks”, which will of course be processed, but will also cause, as a consequence of the imperfect fit, a bit of overhead.





# Chapter 4

## Testing

### 4.1 Assessing the equivalence of the models

Our model, and the corresponding Julia code, is just an improvement of the original DRPM with his relative C implementation. These improvements, as described in the previous chapters, refer to the insertion of covariates, both at the clustering and likelihood levels, the handling of missing values in the target variable, and the computational efficiency. In this sense, our updates are just add-ons to the original model, and therefore at a common testing level they should perform similarly by agreeing in the clusters that they produce on a given dataset.

To assess this ideally equivalent behaviour we ran two tests: the first one with only the target values, using synthetic data, while the second including spatial information, using a real spatio-temporal dataset. For the sake of clarity, also in these sections we will refer to CDRPM for the original model and implementation from [PQD22], while to JDRPM for the updated version derived from this thesis work.

In the following analysis we will heavily rely on the Adjusted Random Index (ARI) [HA85] to compare the partitions generated by the models. The ARI index is a correlation index to measure similarities between clusterings. More precisely, given two partitions  $\rho_1$  and  $\rho_2$ , the  $\text{ARI}(\rho_1, \rho_2)$  returns a value between  $[-1, 1]$  where higher values indicates higher levels of agreement between the partitions, i.e. they produced similar clusters. Being a *random* index it has an expected value and it is equal to zero, which corresponds to the case of comparing two randomly generated partitions.

We will use this index both to study the time evolution of the clusterings, to see e.g. if  $\rho_{t+k}$  is correlated to  $\rho_t$ , that is, if the clusters show the time dependent structure that the models implement, and also to check the level of agreement between the two models, comparing the clusters produced by CDRPM and JDRPM.

### 4.1.1 Target variable only

For the first test we generated a dataset of  $n = 10$  units and  $T = 12$  time instants, and fitted both models collecting 1000 iterates derived from 10000 total iterations, discarding the first 5000 as burnin and thinning by 5. Those parameters, as well as the generating function, were the same of [PQD22]. The generating function allowed to create data points with temporal dependence, which could be tuned through some dedicated parameters. Both models were fitted using the full formulation, i.e. including and updating also the optional autoregression parameters  $\eta_{1i}$ , and  $\varphi_1$ , and using a time specific  $\alpha$ .

**Table 4.1:** Summary of the comparison between the two fits. The MSE columns refer to the accuracy between the fitted values generated by the models (estimated by taking the mean and the median of the returned 1000 iterates) and the true values of the target variable. Higher LPML and lower WAIC indicate a better fit.

	MSE mean	MSE median	LPML	WAIC	execution time
CDRPM	1.6731	1.5861	-249.61	469.69	4.8s
JDRPM	<b>1.2628</b>	<b>1.2181</b>	<b>-227.83</b>	<b>415.03</b>	<b>2.5s</b>

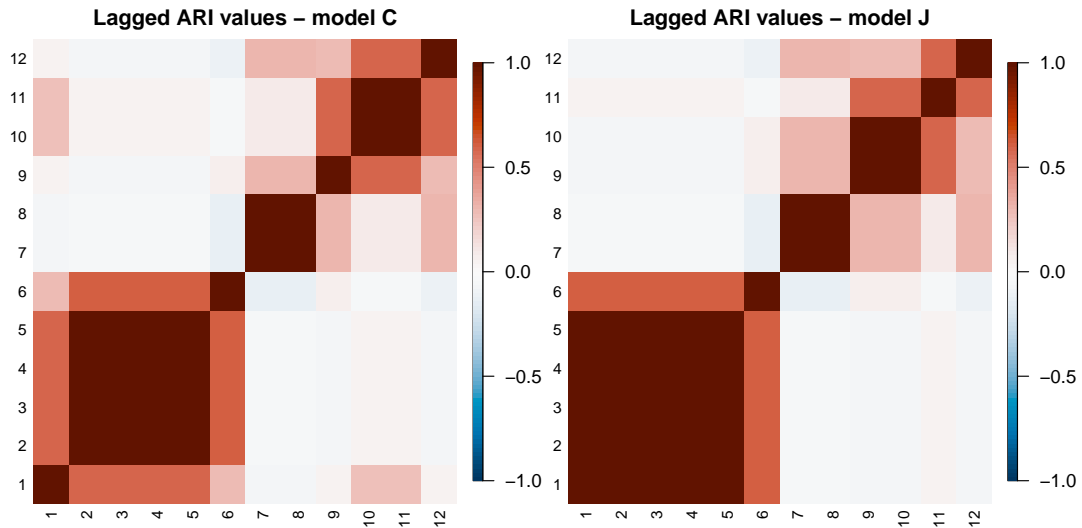


**Figure 4.1:** Lagged ARI values for the two models, on the fit with target only data. The partitions were estimated using the `salso` function from the corresponding R library.

At this testing stage there were just the target values from  $Y_{it}$  to dictate the clusters definition, and both models managed to provide good fits, as we can read from Table 4.1. The JDRPM model had better fit metrics (lower WAIC and higher LPML) and also faster execution time, which is however not really relevant in this small-sized fit. Regarding the fitted values, displayed in Figure 4.4 together with the original data, they turned out to be also more precise than the one generated by CDRPM, having lower mean squared errors.

The resulting clusters were indeed very similar. Figure 4.1 shows how they manifest the same temporal trend, while Figure 4.2 highlights how the clusters

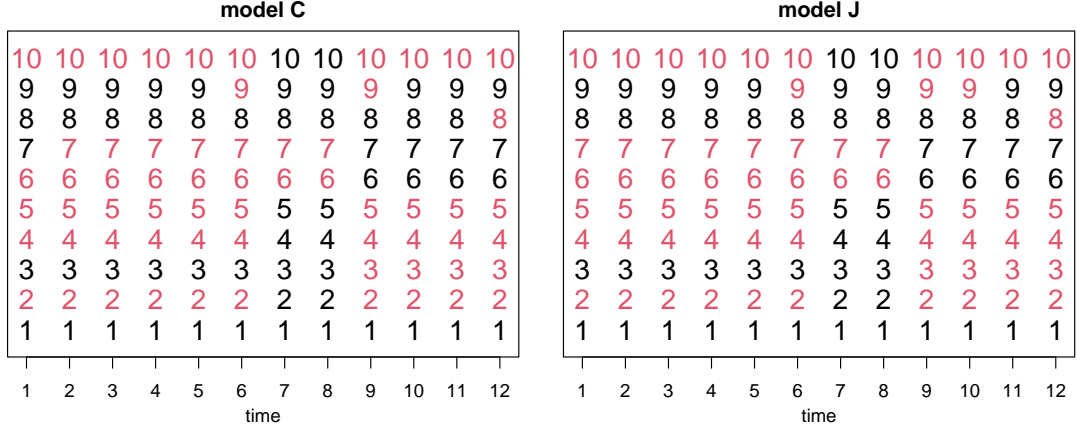


**Figure 4.2:** Clustering produced by the two models, with time points on the  $x$  axis, units indicated vertically by their number, and colors representing the cluster label.

produced are effectively the same except for two differences occurred at times 1 and 10. By visually inspecting the clusters from Figure 4.3, we can see how at  $t = 1$  the JDRPM model assigned a red label to a unit closer to the black pack, to which in fact model CDRPM assigned a black label. However, that same unit in the following time instants would be clearly part of the red cluster, thus making the JDRPM choice very reasonable. The opposite happens at  $t = 10$ , where now the CDRPM model seems to give more importance to the temporal trend, assigning a black label to a unit really closer to the red pack but that is destined to enter the black cluster in the following two time instants.

#### 4.1.2 Target variable plus space

We now consider a more realistic scenario in which we fit the models using a spatio-temporal dataset. In particular, we used the AgrImOnIA [Fas+23] dataset which stores measurements about air pollutants, together with many other environmental variables, in the Lombardy region from 2016 to 2021. For the following testing fits, we employed a summary dataset composed by weekly averages of the data from year 2018.

The chosen target variable was  $\text{PM}_{10}$  whose values had been log-transformed, to recover a normal distribution, and centered with respect to time-wise means. More precisely, each unit  $Y_{it}$  was corrected by subtracting the mean  $\bar{Y}_t$  of all the observations of that time instant. This procedure, which was the same employed by the authors of the original DRPM during their spatial tests, helps to emphasizes the variations within each time point rather than across the entire dataset. This can be particularly useful to understand how units deviate from their typical behavior at specific times, potentially highlighting temporal trends and anomalies. This method also removes any temporal bias, e.g. time instants in which all target values were particularly high or low for any particular reason. In contrast, the more traditional choice of centering with respect to the global mean  $\bar{Y}$  of the dataset would be useful to just detect global trends, without inspecting deeply into each step. From some

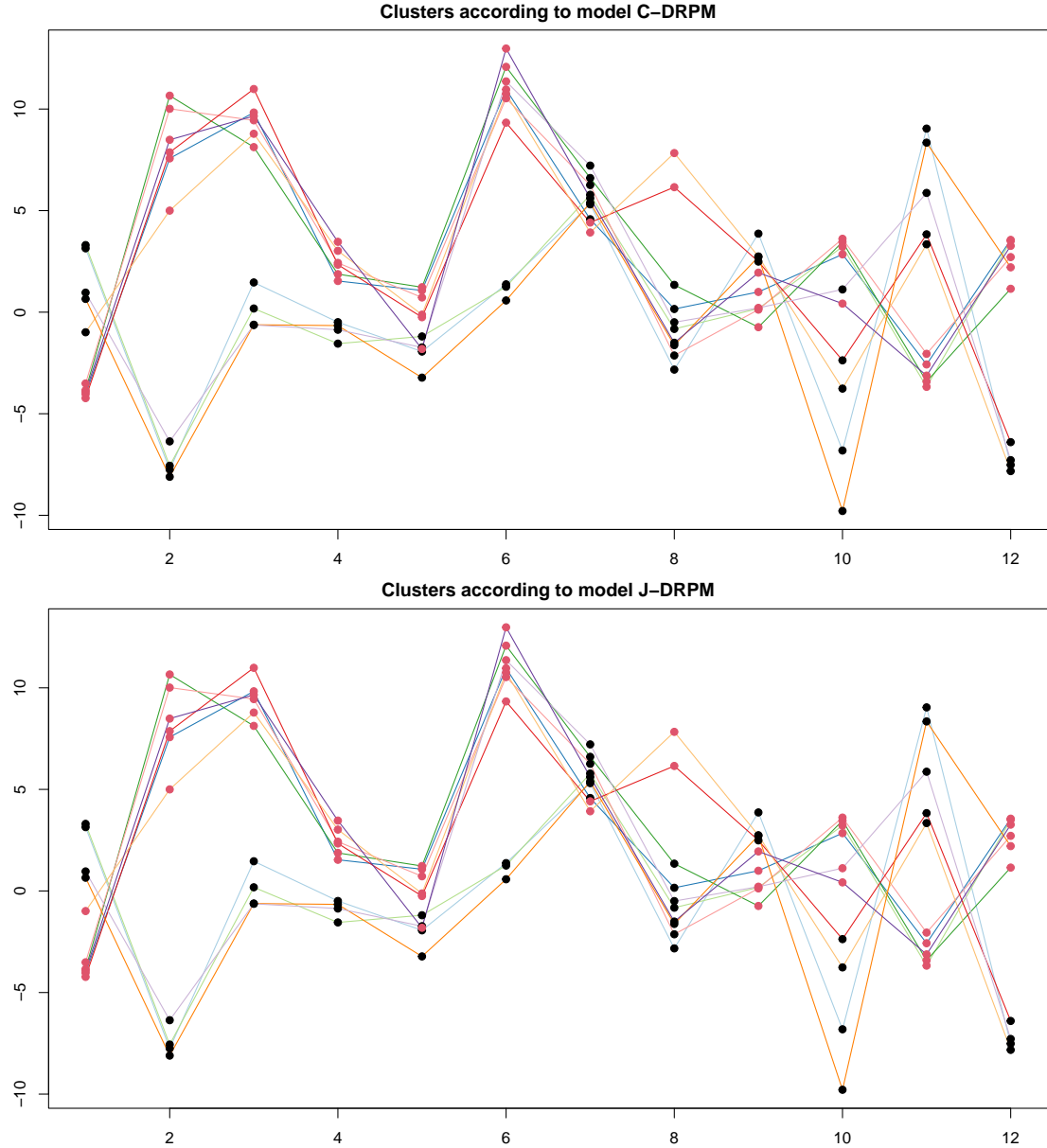


**Figure 4.3:** Visual representation of the clusters produced by the models, on the fit with target only data, with units' labels represented as colored dots overlaid to the trend of the generated target variable. The only differences occur at times 1 and 10.

test fits performed on the target values with the classical global centering indeed only three clusters appeared, for all time instants. This is of course correct, in some sense, since it's reasonable according to the trend displayed in the top image of Figure 4.5. However, as we will see shortly, the other version was able to produce several clusters, or at least different partitions at different time instants, improving the specializations of the clusters and the interpretability of the obtained results.

We took all the  $n = 105$  stations available in the dataset but we limited the time horizon to  $T = 12$ , which corresponds to a three-month monitoring period, just to reduce the time needed to perform all tests. We ran both CDRPM and JDRPM models using the same complete modelling setup, as in Section 4.1.1, and

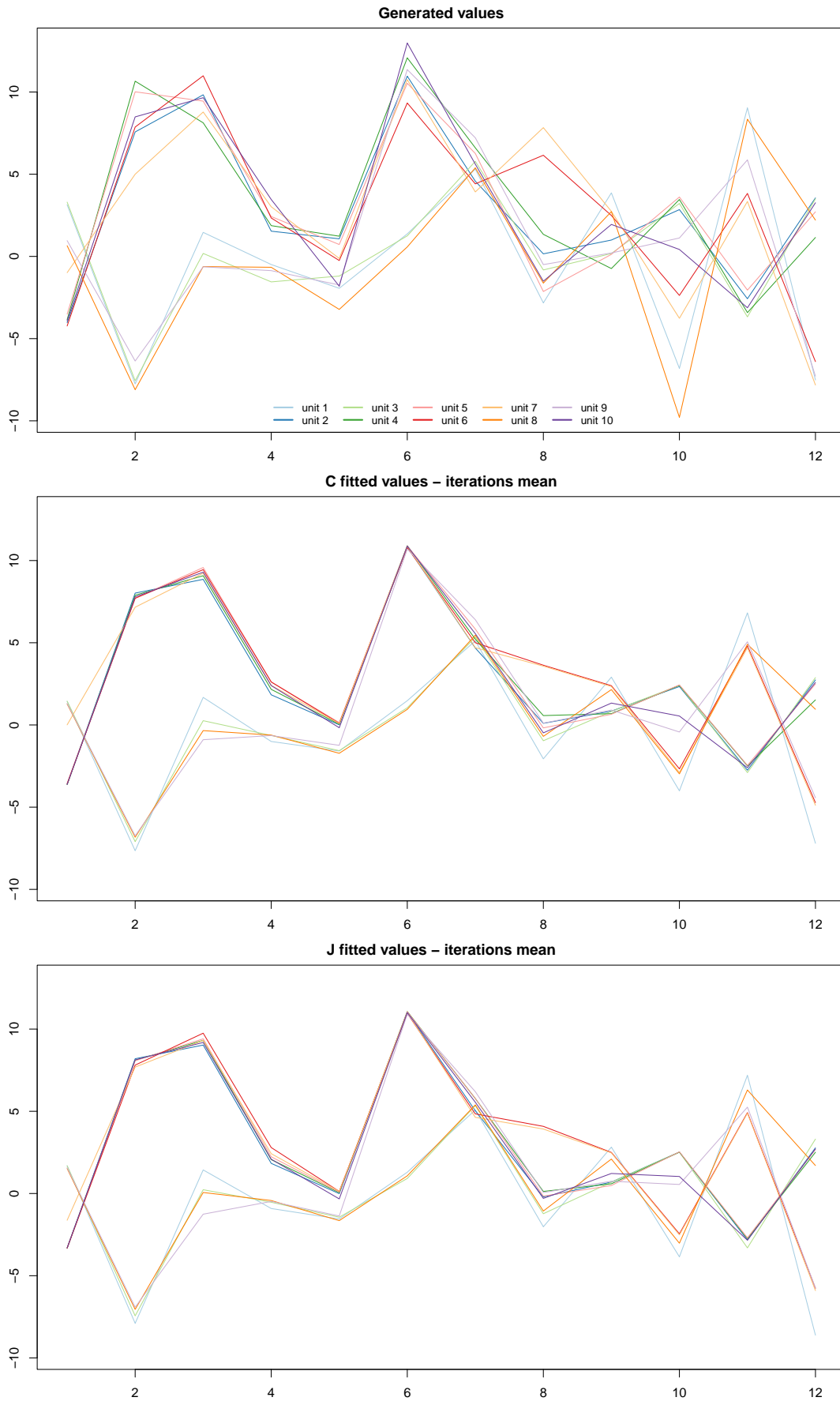


**Figure 4.4:** Generated target values (top), together with their fitted values estimate trough the mean of the 1000 iterates generated by model CDRPM (middle) and JDRPM (bottom).

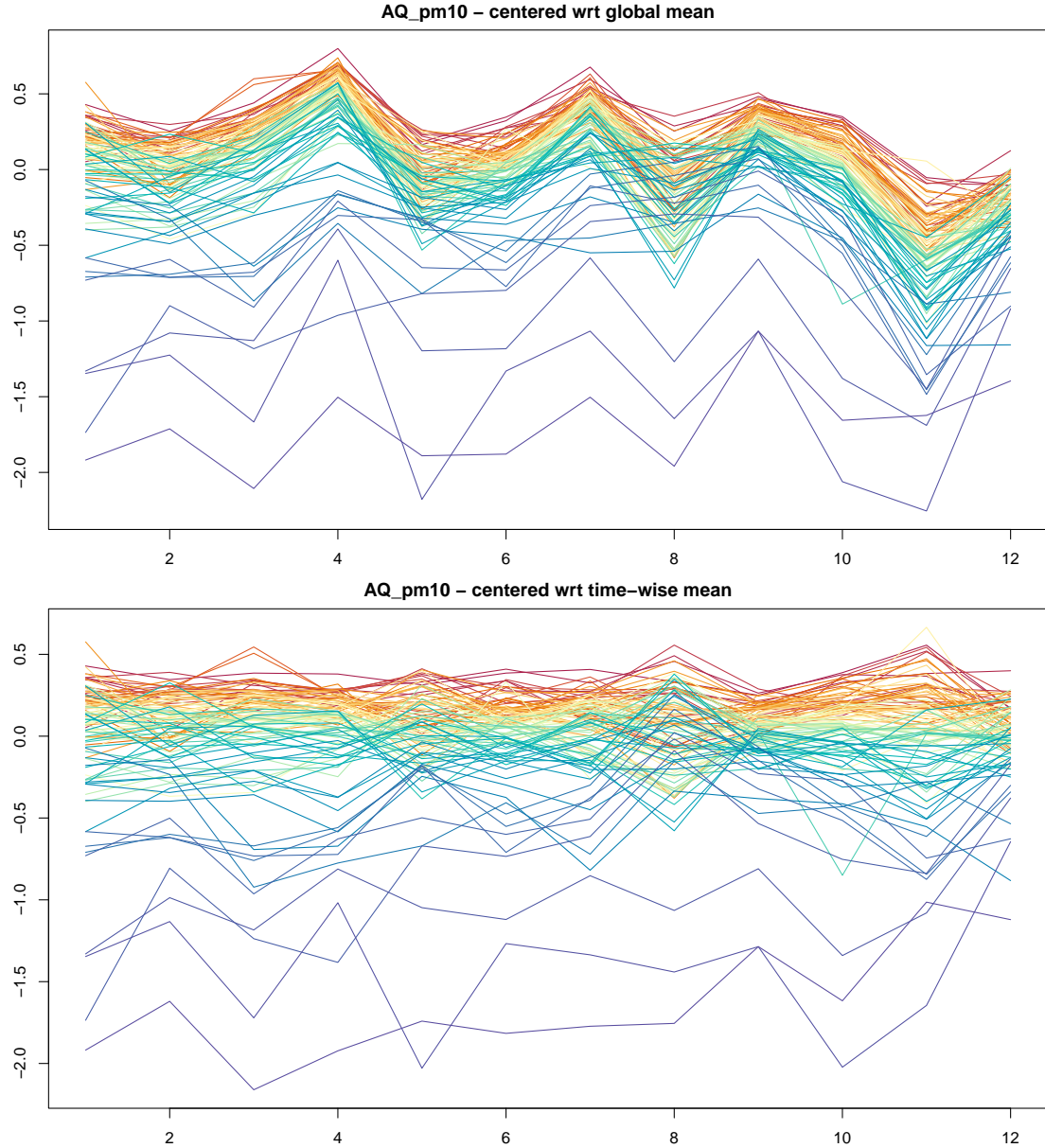


**Figure 4.5:** Values of the target variable AQ\_pm10 corrected using the global mean (top) and using the time-wise mean (bottom). This second choice helps to adjust the values range while keeping, or even highlighting, the clustering structural information. Coloring is based on the ranking of PM<sub>10</sub> values of the units according to their median, from highest (red) to lowest (blue).

using a time specific  $\alpha$ . Convergence was ensured visually by inspecting trace plots and, for the JDRPM model, by numerical diagnostics such as ESS and  $\hat{R}$ , which instead the CDRPM model is not able to provide directly from the fit. We collected 4000 iterates, from 110000 total iterates with a burnin of 90000 and thinning by 5.

Table 4.2 shows how both model managed to be accurate not only with respect to the fitting metrics of LPML and WAIC but also in terms of the fitted values. Execution times are also reported, but they are somewhat altered since during the fitting I was busy in writing this thesis, meaning that not all the computational resources of my laptop were devoted to the fitting task. The reported times are

**Table 4.2:** Summary of the comparison between the two fits. The MSE columns refer to the accuracy between the fitted values generated by the models (estimated by taking the mean and the median of the returned 4000 iterates) and the true values of the target variable. Higher LPML and lower WAIC indicate a better fit.

	MSE mean	MSE median	LPML	WAIC	execution time
CDRPM	0.0142	0.0149	<b>694.81</b>	-1768.42	$\approx$ 1h30m
JDRPM	<b>0.0131</b>	<b>0.0138</b>	624.91	<b>-1898.05</b>	$\approx$ 30m

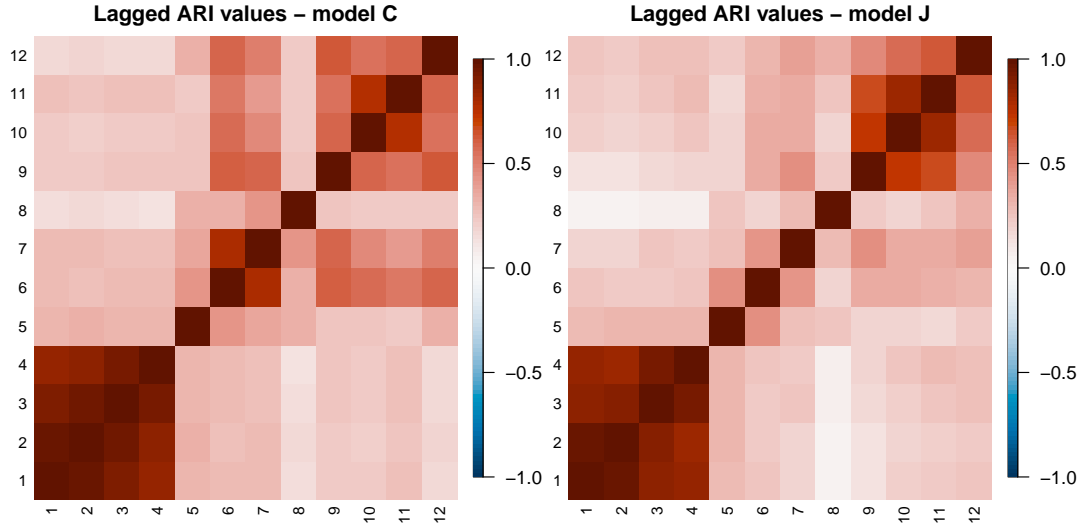


**Figure 4.6:** Lagged ARI values for the two models, on the fit with target plus space data. The partitions were estimated using the `salso` function from the corresponding R library.

therefore just estimates, but in any case more accurate performance evaluations on the timings will be conducted in Section 4.4.

From Figure 4.6 we can see how the temporal trend was very similar, confirming again the correctness of the JDRPM implementation. Regarding the similarity of the produced clusters, the partition plot as the one of Figure 4.2 would now be more crowded due to the high number of units. For this reason, in order to still convey that information, we computed  $\text{ARI}(\rho_{\text{JDRPM}}(t), \rho_{\text{CDRPM}}(t))$  for all time instants  $t = 1, \dots, 12$ , and we obtained a mean of 0.80 and a median of 0.86, denoting high levels of agreement in the clusters produced.

A visual representation of the clusters is provided in Figure 4.8, but will be further detailed and commented in Section 4.3.2 together with the fits including covariates in the clustering.

## 4.2 Performance with missing values

We now repeat the tests of the previous section on the same datasets but this time with missing values, to see how the JDRPM model reacts to the absence of a full dataset and check if it can still perform well. Based on the amount of



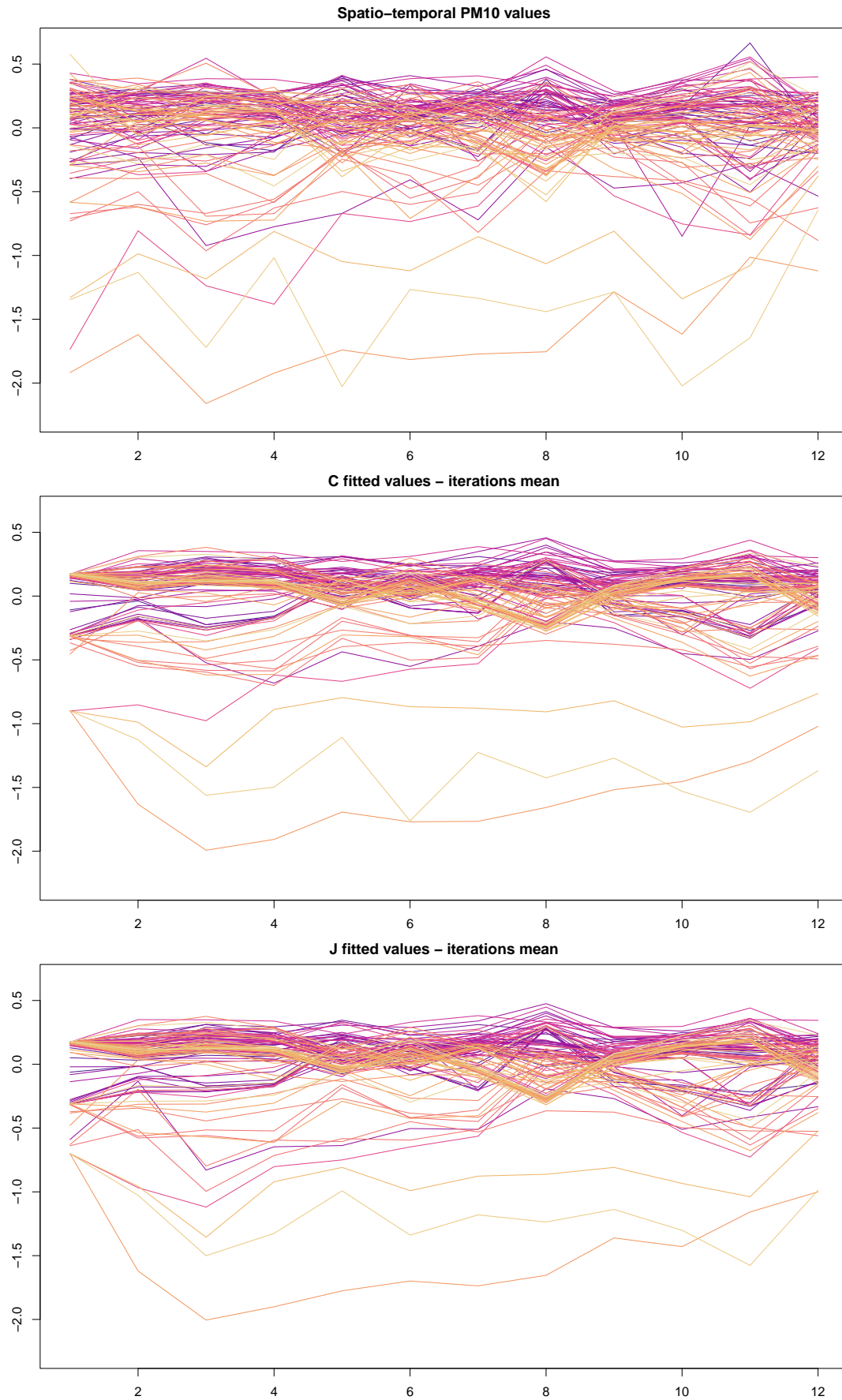


**Figure 4.7:** Target  $Y_{it}$  values (top), together with their fitted values estimate trough the mean of the 4000 iterates generated by model CDRPM (middle) and JDRPM (bottom).



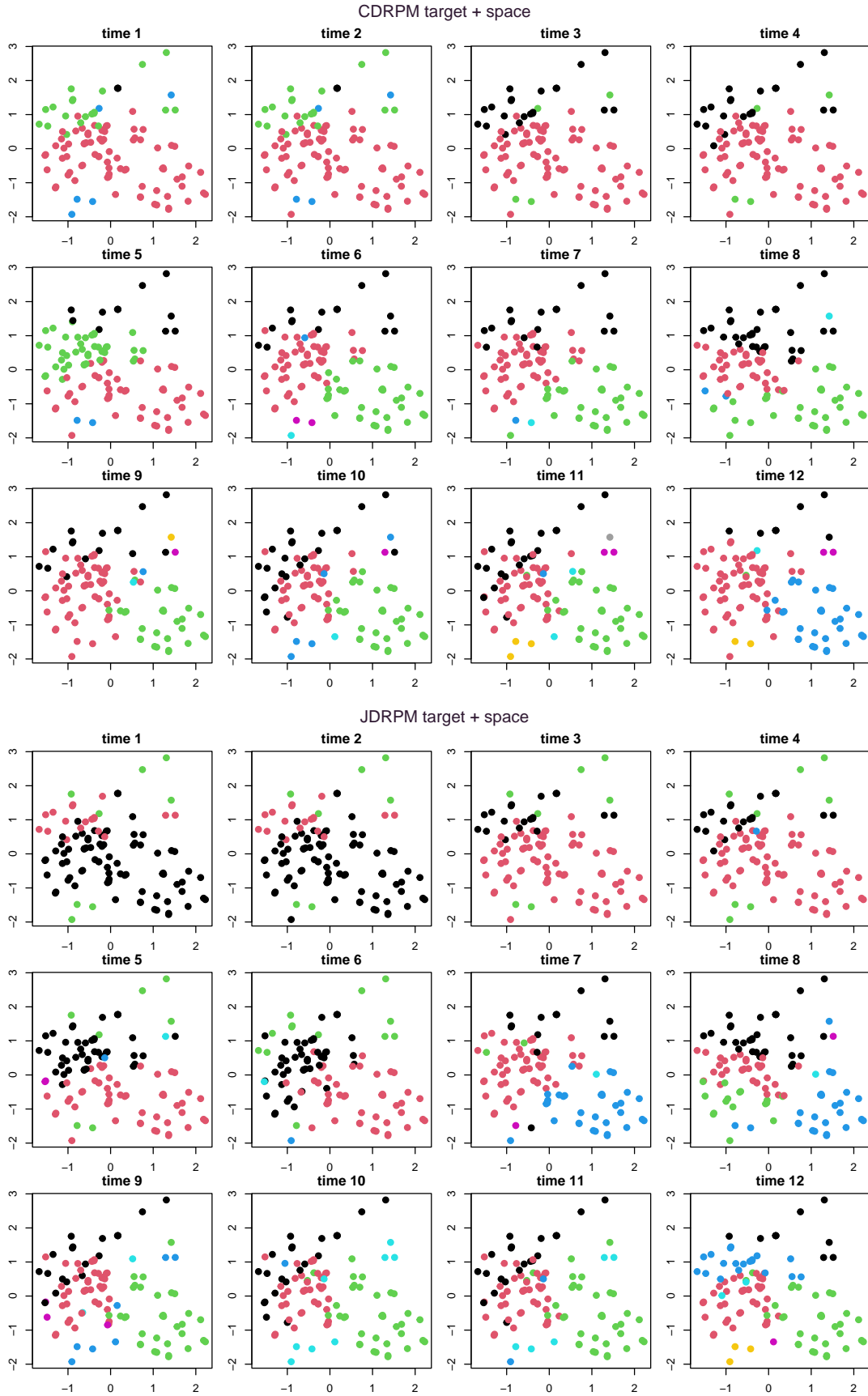


**Figure 4.8:** Clusters generated by the CDRPM and JDRPM fits with target plus space values.

missing values in the AgrImOnIA [Fas+23] dataset, used for the spatio-temporal tests, we chose to set at 10% the amount of values that would be replaced by NAs. To perform such replacements, we randomly drew  $nT/10$  indexes from the sets  $[1, \dots, n]$  and  $[1, \dots, T]$  to get all the pairs  $(i, t)$  which would become missing values in the target variable  $Y_{it}$ . The dealing of NAs was an upgrade brought by the JDRPM model, so we can't perform these tests with the original CDRPM model since it cannot handle missing data.

All the following fits have been conducted under the same conditions of their full-dataset counterpart, i.e. using the same models formulation and parameters.

### 4.2.1 Target variable only (NA case)

The JDRPM seems to exhibit good performance also with missing values. From Table 4.3 we can see how the performances, naturally worse than the fit in the full case, are still good. The MSE is inevitably higher since the model did not have all the data points, and so we get less precise fitted values for the corresponding missing spots in the dataset, but the fitted values of Figure 4.9 are still close the one obtained with the fit on full dataset.

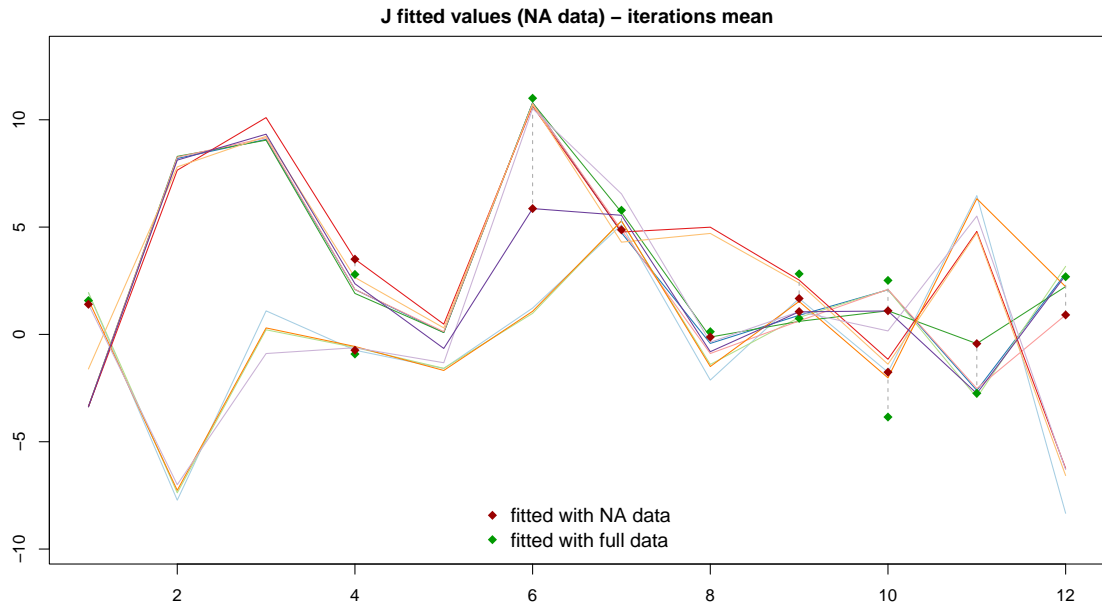


**Figure 4.9:** Fitted values estimate through the mean of the 1000 iterates generated by model JDRPM. The generated target values were the same of Figure 4.4. Special point markers are used for the data points which were missing, to highlight the gaps between the fitted values on the full dataset (green squares) and the fitted ones on the NA dataset (red squares).

From Figures 4.11 and 4.10 we can see how we get almost the same temporal trend which we saw in the case without missing data, and indeed the assigned clusters are almost the same. The only difference occurs on a single unit at time 10, where now the JDRPM model does the same thing that CDRPM did in its corresponding fit of Section 4.1.1.

**Table 4.3:** Summary of the comparison between the two Julia fits on target values only. The MSE columns refer to the accuracy between the fitted values generated by the models (estimated by taking the mean and the median of the returned 1000 iterates) and the true values of the target variable. Higher LPML and lower WAIC indicate a better fit.

<i>JDRPM</i>	MSE mean	MSE median	LPML	WAIC	execution time
NA data	2.1819	1.7876	-239.21	417.21	3.0s
full data	1.2628	1.2181	-227.83	415.03	2.5s

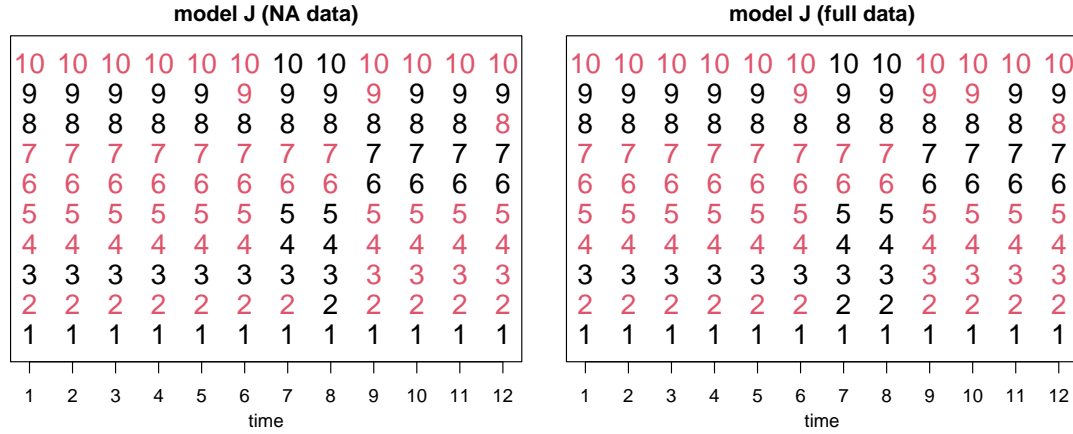


**Figure 4.10:** Clustering produced by the two tests on the JDRPM model, with time points on the  $x$  axis, units indicated vertically by their number, and colors representing the cluster label.

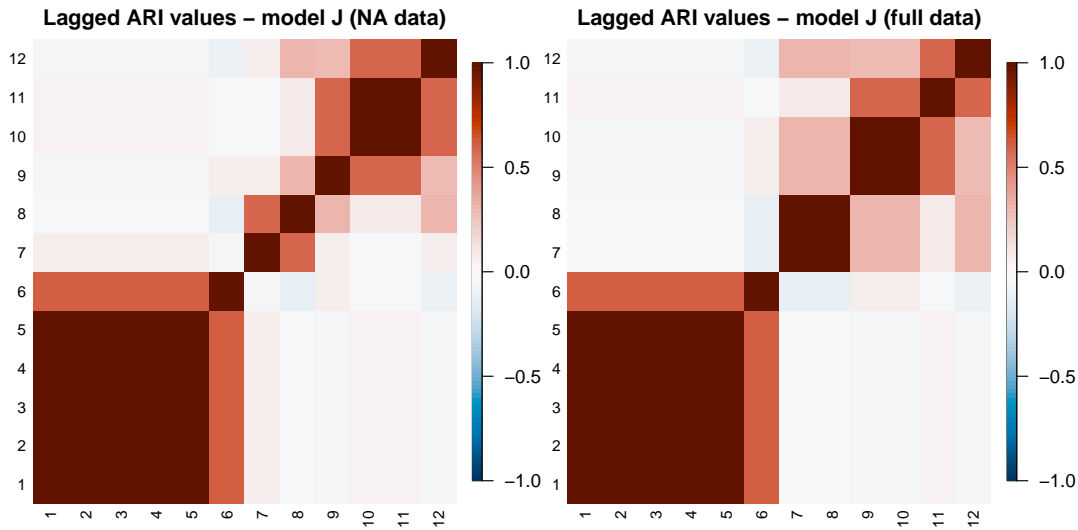


**Figure 4.11:** Lagged ARI values for the two fits on the JDRPM model with target values only. The partitions were estimated using the `salso` function from the corresponding R library.

### 4.2.2 Target variable plus space (NA case)

The JDRPM model seems able to perform well also in the case of fits including spatial information. Table 4.4 shows how the accuracy reduces, which again is inevitable since we are fitting with missing data, but not drastically. In fact, the

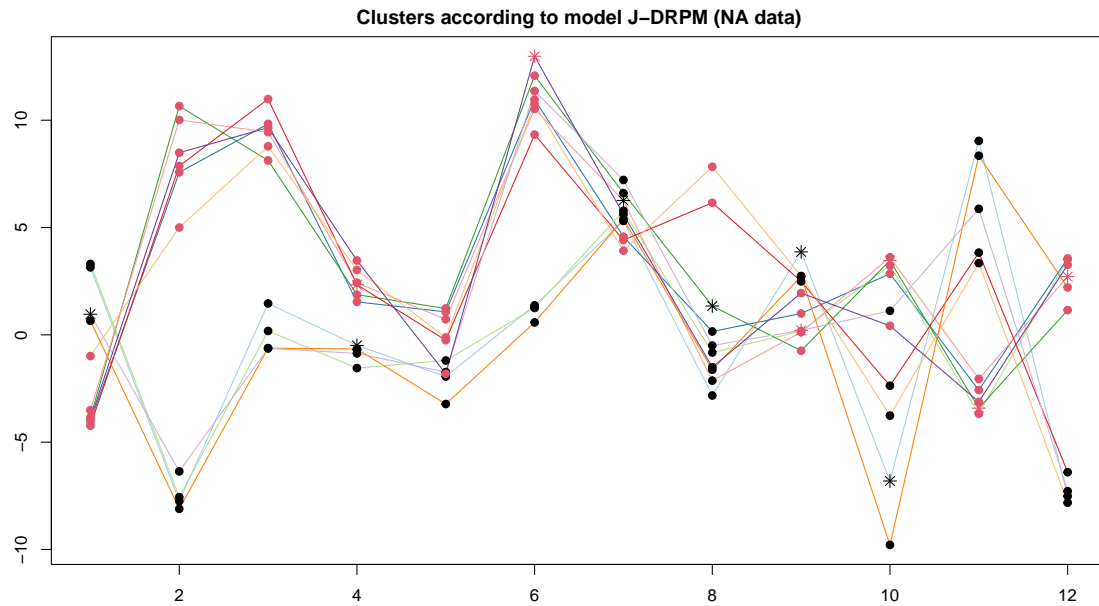


**Figure 4.12:** Visual representation of the clusters produced by the model, with units' labels represented as colored dots overlaid to the trend of the original generated target variables. Special point markers are used for the data points corresponding to missing values.

**Table 4.4:** Summary of the comparison between the two Julia fits on target plus space values. The MSE columns refer to the accuracy between the fitted values generated by the models (estimated by taking the mean and the median of the returned 4000 iterates) and the true values of the target variable. Higher LPML and lower WAIC indicate a better fit.

<i>JDRPM</i>	MSE mean	MSE median	LPML	WAIC	execution time
NA data	0.0160	0.0170	502.86	-1793.64	$\approx 40\text{m}$
full data	0.0131	0.0138	624.91	-1898.05	$\approx 30\text{m}$

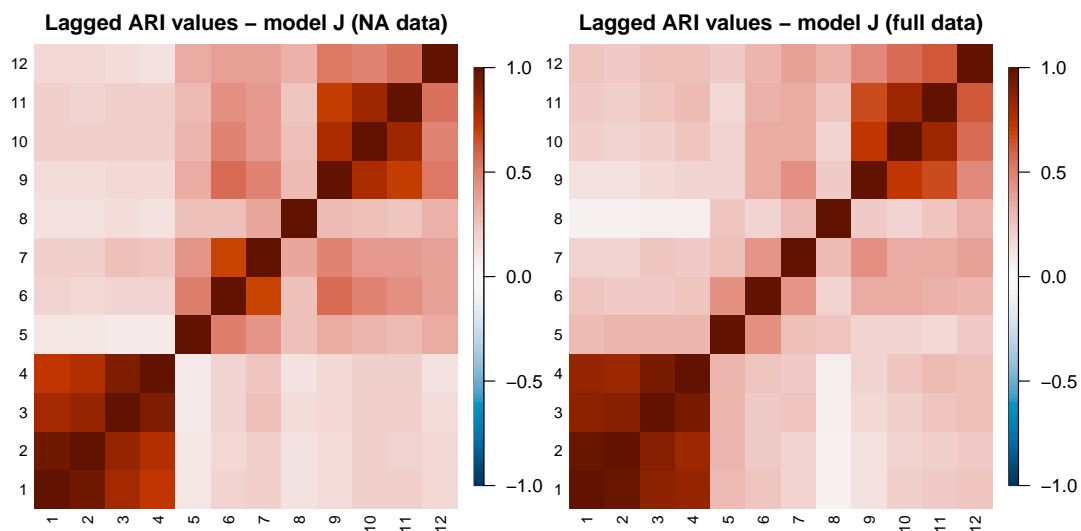


**Figure 4.13:** Lagged ARI values for the two fits on the JDRPM model with target plus space values. The partitions were estimated using the `salso` function from the corresponding R library.

drops in LPML and WAIC metrics are just of 3.16% and 0.95% respectively.

The temporal trend managed as well to remain similar to the trend we saw in Section 4.1.2, as proved by Figure 4.13. Regarding the similarity of the produced clusters, we computed the values  $\text{ARI}(\rho_{\text{JDRPM\_NA}}(t), \rho_{\text{JDRPM\_full}}(t))$  for all time instants  $t = 1, \dots, 12$ , and we obtained a mean of 0.82 and a median of 0.86, denoting still a relatively high level of agreement in the partitions despite the loss of quite some data (121 points out of the 1260 of the full dataset).

## 4.3 Effects of the covariates

To perform the fits that will now follow, all the included covariates were treated in the same way as the target value, with the time-wise centering procedure and reasoning described in Section 4.1.2. Figure 4.14 provides an exemplification of the effect of this transformation on one of the covariates.

### 4.3.1 Covariates in the likelihood

Continuing on the line of the previous section, we can test if the insertion of covariates in the likelihood can help to recover some accuracy in the case of fits with missing data. In fact, the addition of the regression parameter  $\beta_t$  had the main goal of improving the accuracy of the model when estimating the target values  $Y_{it}$ , without affecting too much the cluster generation. With that in mind, the most natural use case of such parameter would be when fitting with missing values.

Indeed, after including one or multiple covariates in the likelihood, and repeating the fit on the NA dataset under the same conditions, apart from this addition, we saw some improvements. To better illustrate them, we also ran the corresponding fit using the same covariates set in the likelihood, but this time on the full dataset. Results are summarized in Table 4.5 which also includes, as a reference, the results of the previous fits without the regressor component.

**Table 4.5:** Summary of the comparison between the Julia fits on target plus space values. The MSE columns refer to the accuracy between the fitted values generated by the models (estimated by taking the mean and the median of the returned 4000 iterates) and the true values of the target variable. Higher LPML and lower WAIC indicate a better fit.

<i>JDRPM</i>	MSE mean	MSE median	LPML	WAIC	execution time
full data	0.0131	0.0138	624.91	-1898.05	$\approx$ 30m
full data + Xlk	<b>0.0112</b>	<b>0.0113</b>	<b>778.96</b>	<b>-2029.84</b>	$\approx$ 50m
NA data	0.0160	0.0170	502.86	-1793.64	$\approx$ 40m
NA data + Xlk	<b>0.0127</b>	<b>0.0130</b>	<b>625.81</b>	<b>1902.74</b>	$\approx$ 60m

We can see how clearly the insertion of covariates in the likelihood managed to improve all fitting metrics with, as expected, a decrease in the MSEs, especially in the fits with NA data, proving how that insertion can indeed recover some performance in the case of missing values.

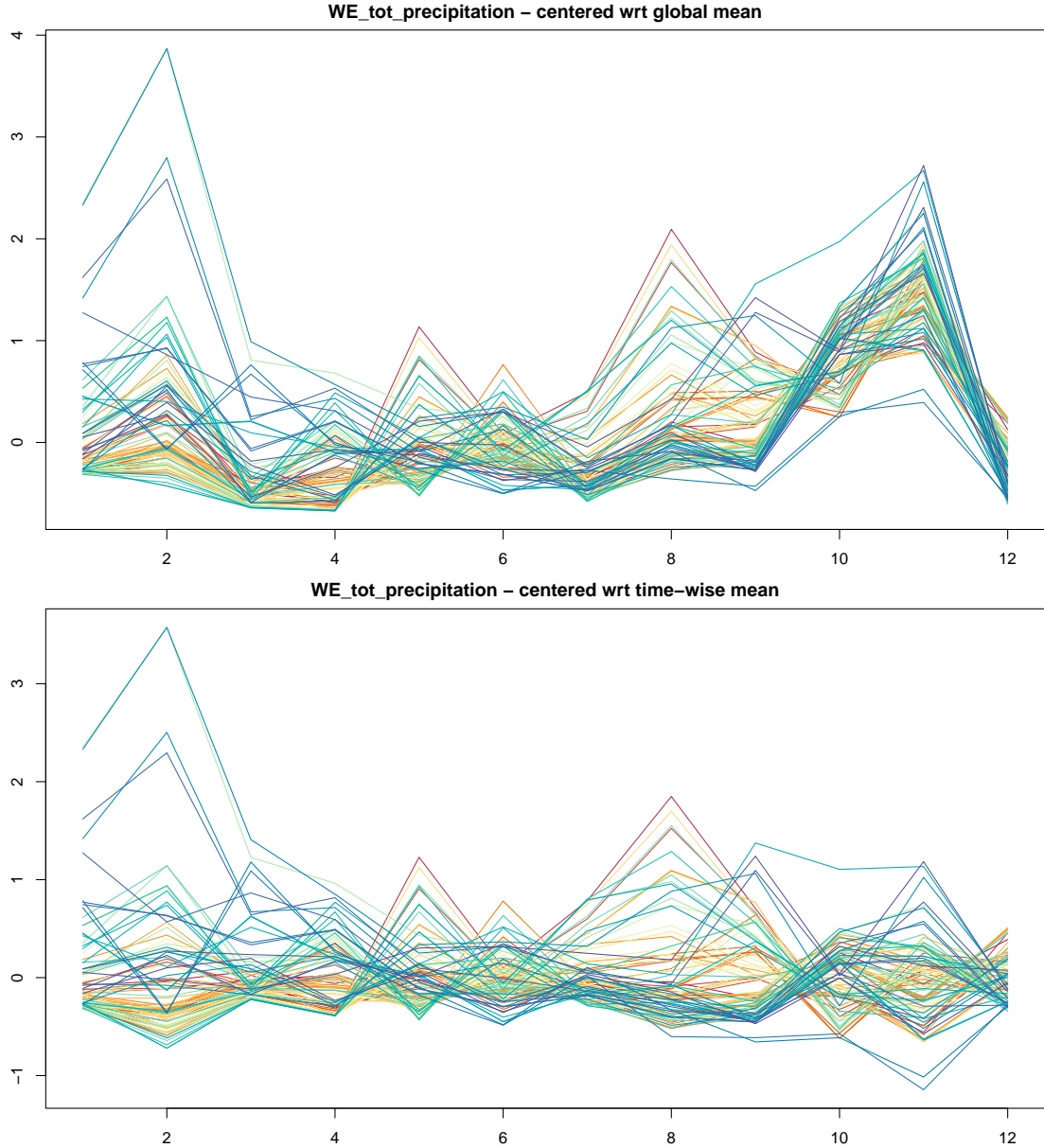


**Figure 4.14:** Values of the `WE_tot_precipitation` covariate corrected using the global mean (top) and using the time-wise mean (bottom). Coloring is based on the ranking of PM<sub>10</sub> values of the units according to their median, from highest (red) to lowest (blue).

Regarding the generated partitions, they also remained substantially unchanged, as briefly depicted in Figure ??, and with a similar spatio-temporal trend, displayed in Figure 4.18, but for a generally higher dependence trend in the second part of the time interval, after the same identified “change point” at  $t = 4$ .

The JDRPM fitting function also includes a `beta_update_threshold` argument, defaulted to zero, to set after which iteration the algorithm should start to update the  $\beta_t$  parameter. This was an harmless and simple addition, which was considered useful to firstly let the model update and improve the more delicate and relevant parameters for the clustering, such as  $\mu_{jt}^*$  and  $\sigma_{jt}^{2*}$ , and secondly tune also the less impactful  $\beta_t$ . Otherwise, maybe, the initial development of the model parameters

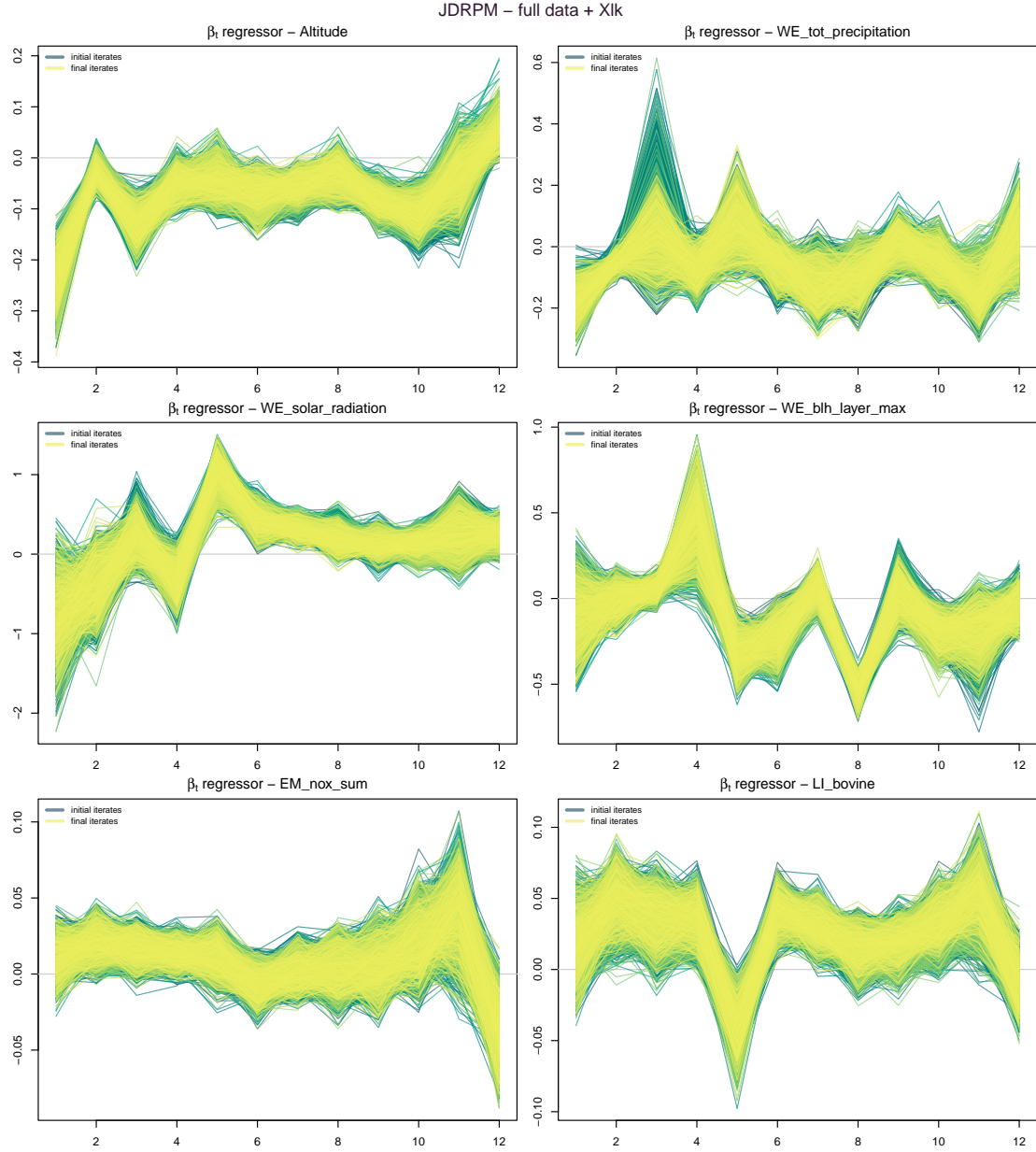


**Figure 4.15:** Regression vector  $\beta_t$  for the  $p = 6$  covariates inserted in the likelihood in the full data spatio-temporal fit test, with time instants  $t = 1, \dots, 12$  are on the  $x$  axis.

and clusterings could be biased by early inaccurate samples of the likelihood regressor.

Finally, Figure 4.17 encloses the fitted values of these two runs, with multiple covariates in the likelihood on the NA and full datasets, with respect to the real  $\text{PM}_{10}$  values. We can see how indeed, visually but also as proved by the better MSEs, these fitted values resemble more the ones of the original target variable, especially if compared to the case of Figure 4.7, in which both fits were without any “external suggestion” of covariates in the likelihood. In the end, this analysis denotes how the addition of this regression parameter  $\beta_t$  could be beneficial to recover more accurate results, and also help the clustering process since the regressor contribution manifests when using variables computed from the target values inside the update



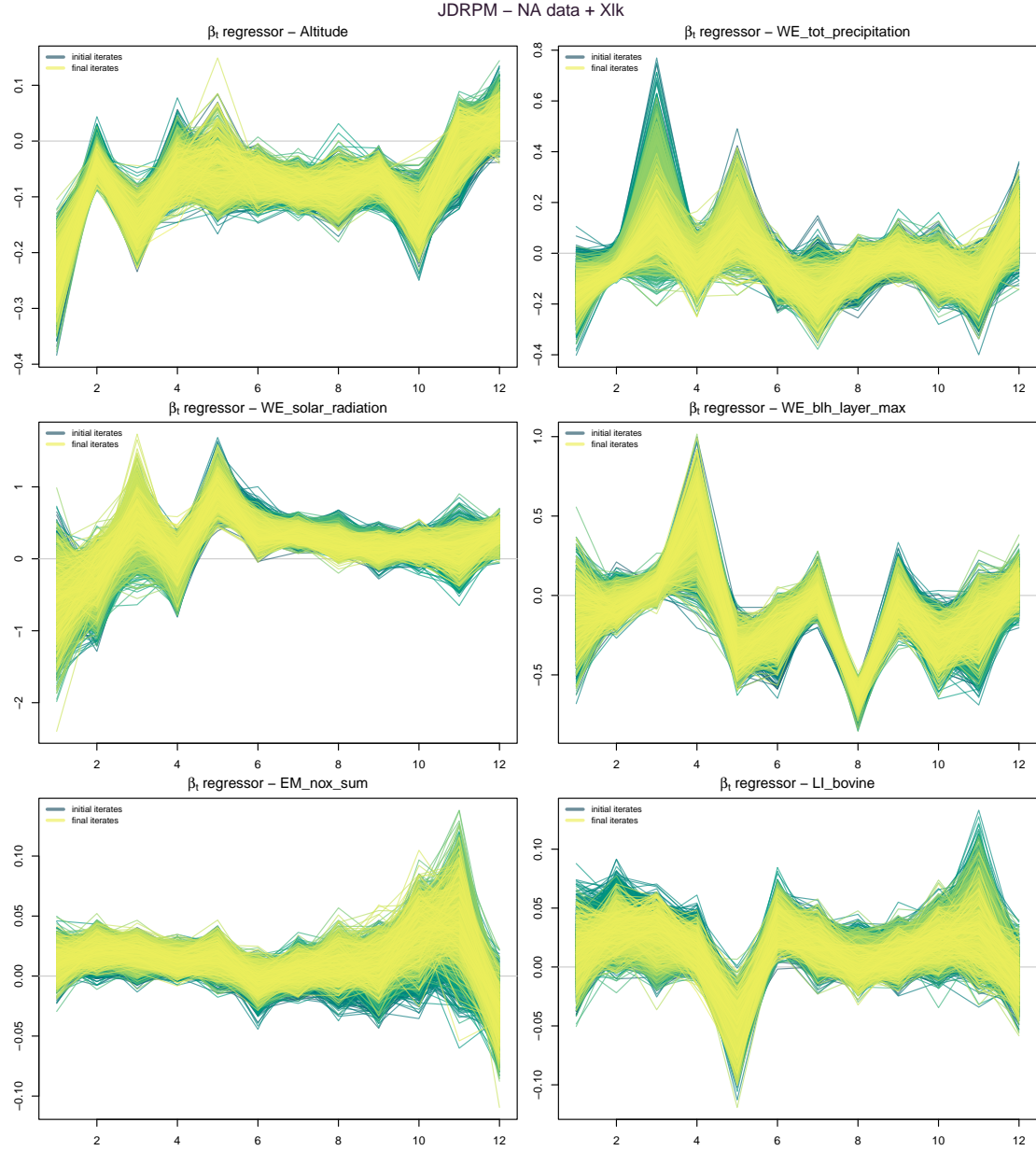


**Figure 4.16:** Regression vector  $\beta_t$  for the  $p = 6$  covariates inserted in the likelihood in the NA data spatio-temporal fit test, with time instants  $t = 1, \dots, 12$  are on the  $x$  axis.

steps of the parameters.

### 4.3.2 Covariates in the clustering

Now we consider the more effective and impactful addition of covariates in the clustering process.



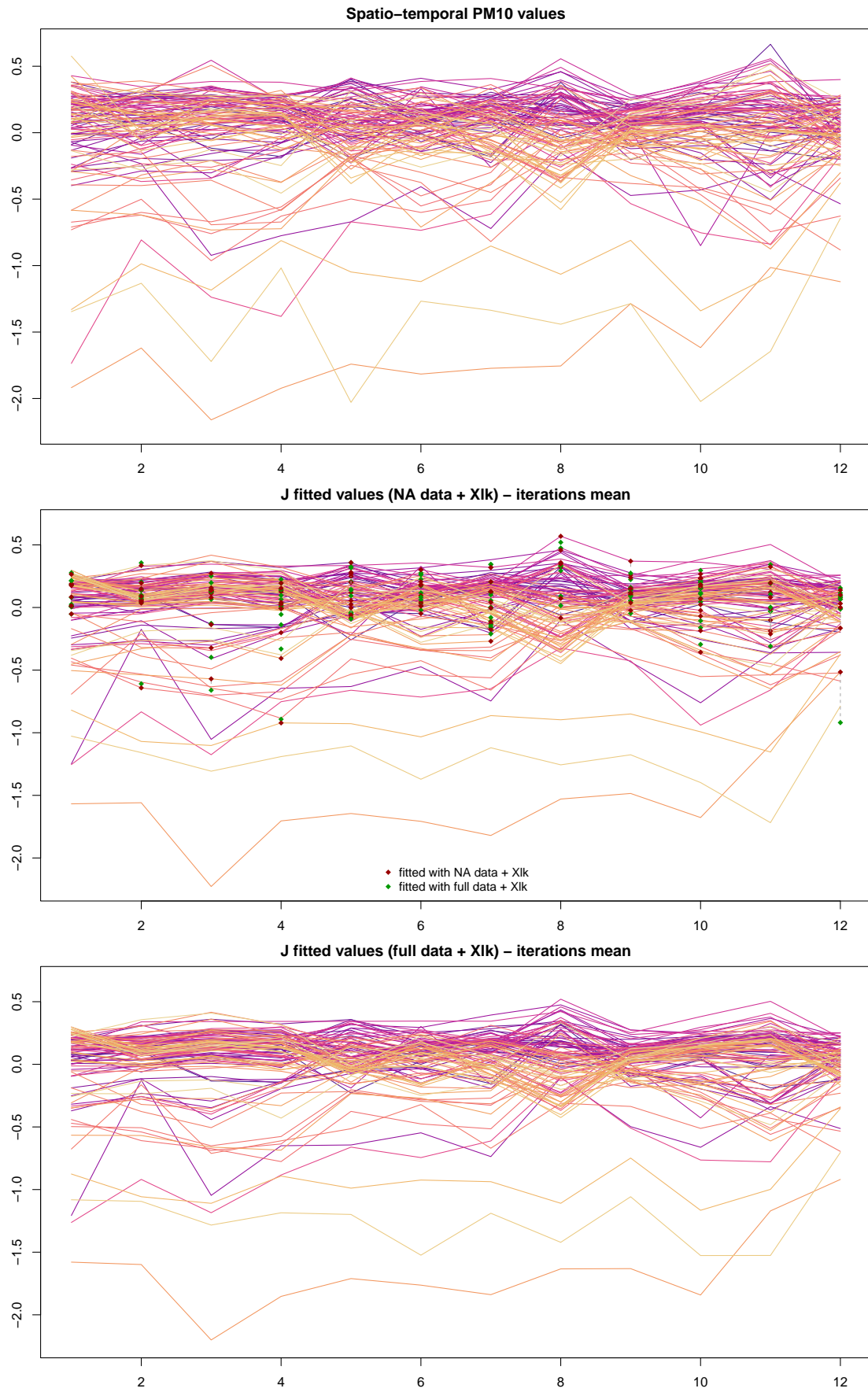


**Figure 4.17:** Target and fitted values of the JDRPM fits with target plus space values, on the NA and full dataset, to see the effects of the insertion of covariates in the likelihood.

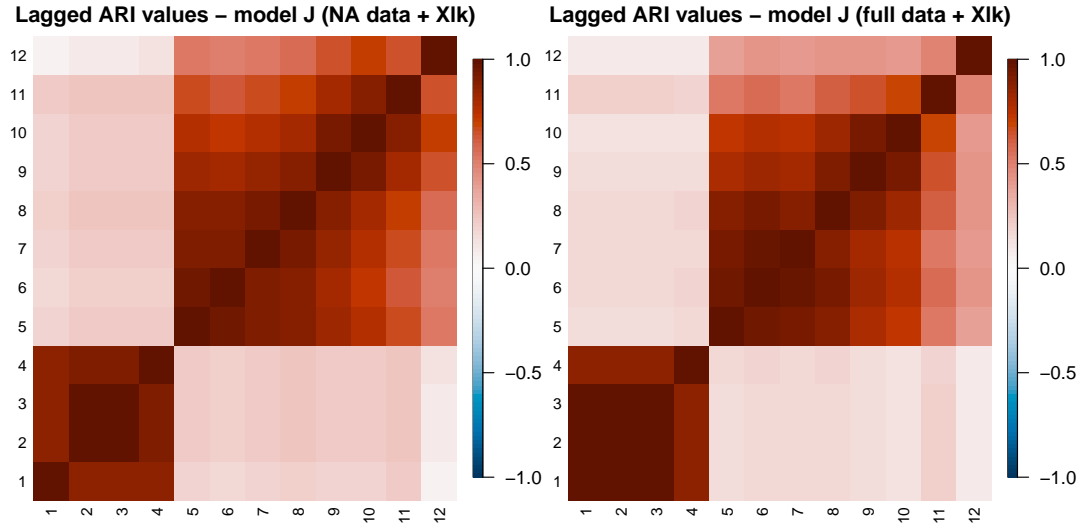


**Figure 4.18:** Lagged ARI values of the two JDRPM fits with target plus space values on the full and NA datasets, with covariates in the likelihood.

## 4.4 Scaling performances

To really assess if the goal of faster fits was reached, we setup several tests to compare the two models and the different information levels at which they could be called. The original CDRPM allowed to perform clustering using just the target values or by also including spatial information. In addition to them, the options introduced by JDRPM are the inclusion of covariates at clustering and/or likelihood levels.

Apart, of course, from the target values, all the other information levels are indeed independent: one could perform the fit ignoring space and accounting just for covariates, for example; but with an additive perspective in mind we decide to perform incremental tests, adding new layers on top of the base ones. Therefore, in what follows, we will see comparisons of fits using just the target values, then those plus space, then those two plus covariates in the clustering, and finally all those plus covariates in the likelihood.

As it appeared from Section 3, the Julia implementation seemed to be a little more eager for memory than the C one. This meant that when we ran the larger tests my system could have ran out of RAM memory, resulting in some data needing to be stored in the slower swap space on the disk, and therefore losing performance. However, on newer or just more technical-oriented machines than my simple laptop, this memory limitation should not be an issue.

Accounting all this, in what follows we should consider really accurate just the intermediate-values tests, i.e. the ones with  $n$  or  $T$  being 10, 50 or 100, and take with a pinch of salt the extreme one of 250, for which my laptop hardware limitations could have concealed the true results. Nonetheless, the analysis is really encouraging for the JDRPM model.

The tests were conducted on randomly generated values, according to  $n$  and  $T$ ,

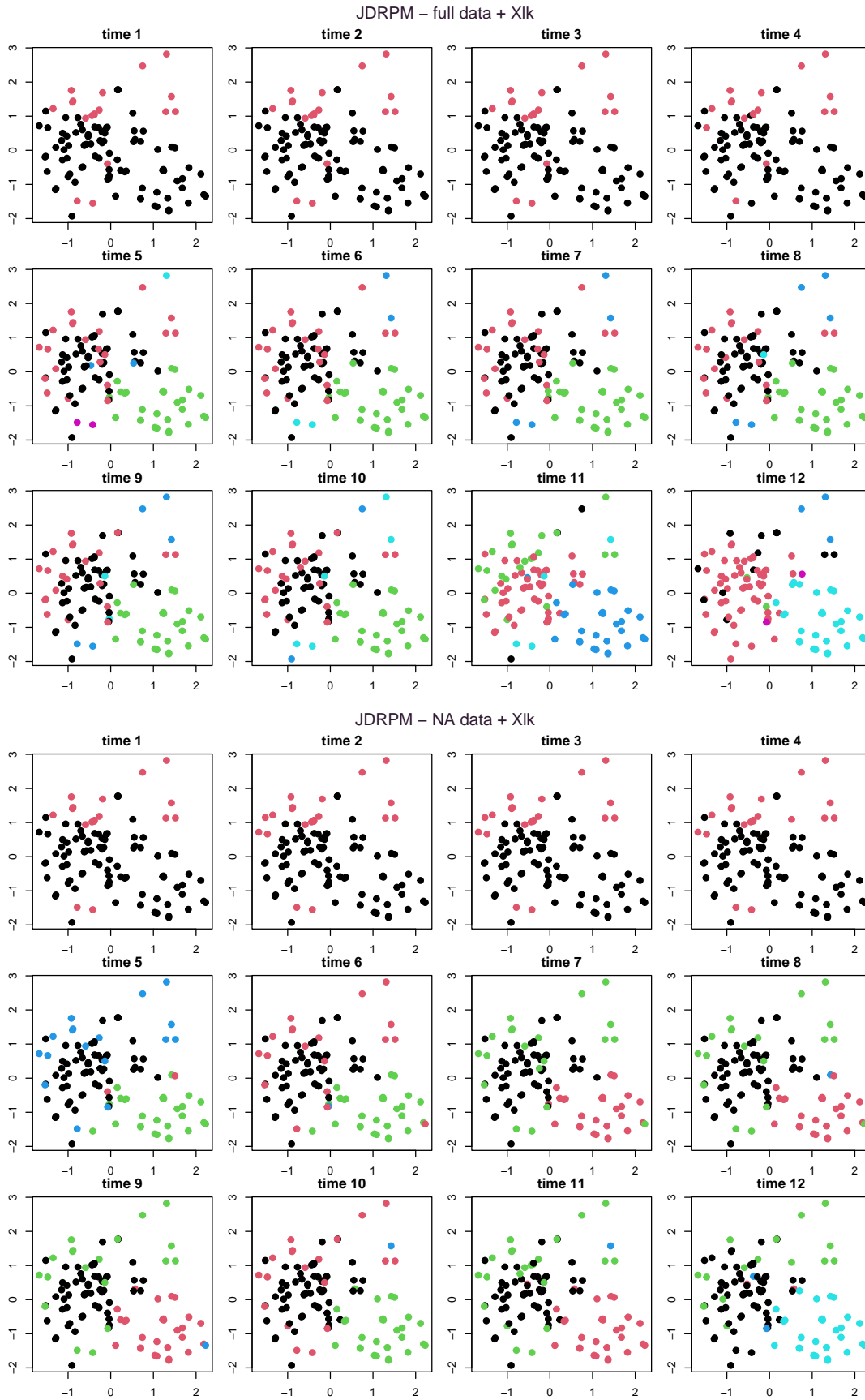


**Figure 4.19:** Clusters generated by the two JDRPM fits with target plus space values fits on the full and NA datasets, with covariates in the likelihood.

for the target data  $Y_{it}$  and the spatial coordinates  $s_i$ . In this way, we produced a sort of “mesh” of possible fitting parameters, ranging from small number of units and time horizons to larger ones. To record the expected execution time per iteration of each case we ran each fit with a number of iterations inversely proportional to the size of the test, e.g. 10000 iterations for the case  $(n, T) = (10, 10)$  and 16 iterations for  $(n, T) = (250, 250)$ . This ensured that each fit lasted approximately the same time. Each fit was ran four times, to then save the minimum time observed during those multiple runs. Such practice, common in benchmarking, helps to eliminate bias from the results due to the system computational demands and fluctuations, filtering in this way just the “ideal” execution time in which all the system performance are devoted to that task.

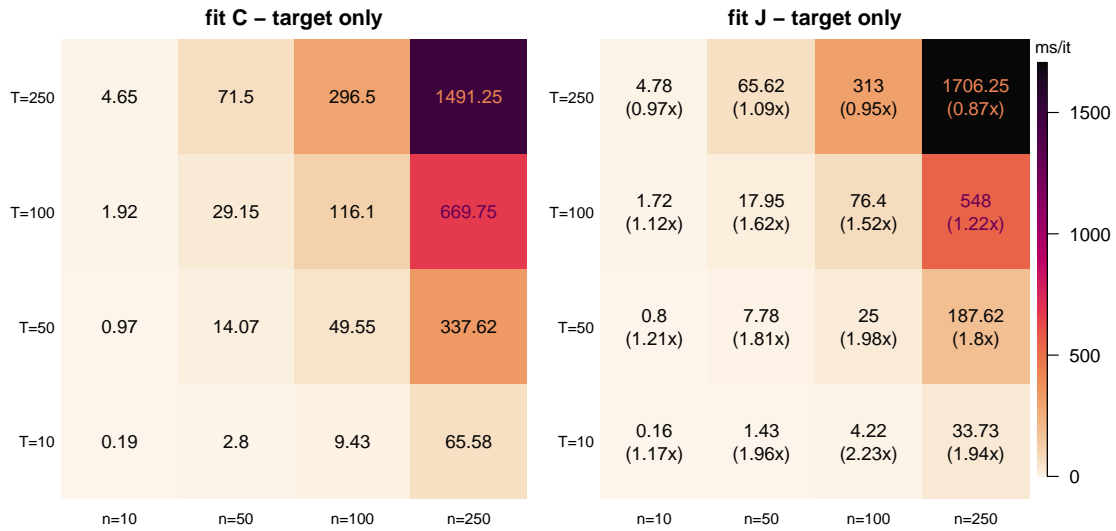


**Figure 4.20:** Execution times, measured in milliseconds per iteration, when fitting the models using just the target values to generate the clusters. On the JDRPM plot (on the right), in brackets, are reported the speedups relative to the CDRPM timings (on the left), where higher values indicate better performance.

From Figure 4.20 we can see how the basic fit, with just the target values, perform very quickly in Julia, with peaks even around a 2x speedup. Similar improvements appeared in the case of fits including also the spatial information, as Figure 4.21 shows. Therefore, especially looking at the more reliable non-extreme tests, we can confidently claim that the JDRPM implementation is faster than the CDRPM one.

Regarding fits with covariates, we also generated them randomly by creating matrices of dimensions  $n \times p \times T$ . For these tests, we avoided to treat different values of  $p$ : the previous figures summarizing the fits up to spatial information were in fact projection of 3d information ( $n$ ,  $T$ , and execution time), while if we extended the mesh to also account for  $p$ , the number of covariates, we would have ended up with 4d information, or even 5d if we considered separately clustering and likelihood covariates. Therefore, to keep things tidy and understandable, we just fixed  $p = 5$  for both cases.

Figure 4.22 shows how fits including covariates saw a drop of performance, which

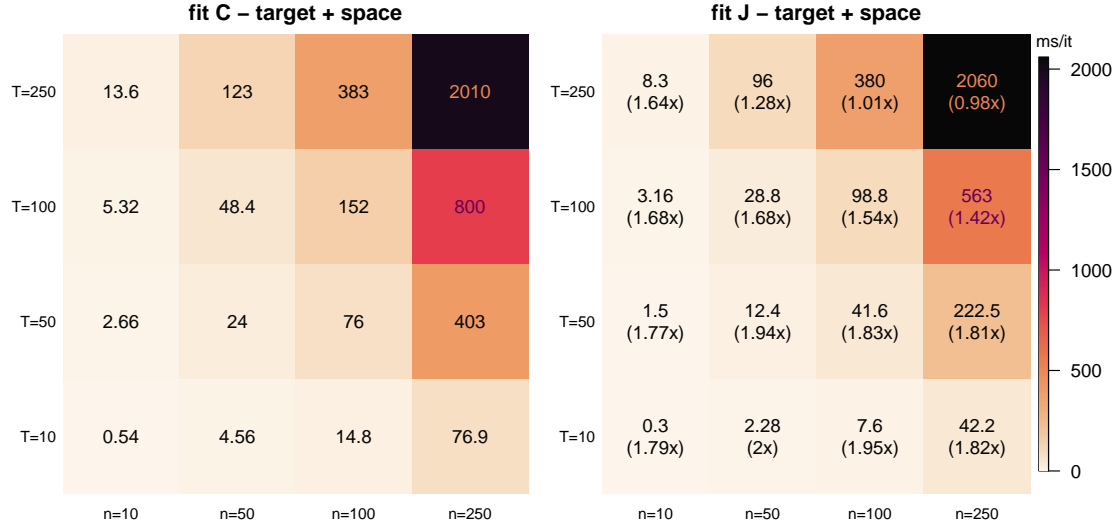


**Figure 4.21:** Execution times, measured in milliseconds per iteration, when fitting the models using the target values plus the spatial information to generate the clusters. On the JDRPM plot (on the right), in brackets, are reported the speedups relative to the CDRPM timings (on the left), where higher values indicate better performance.

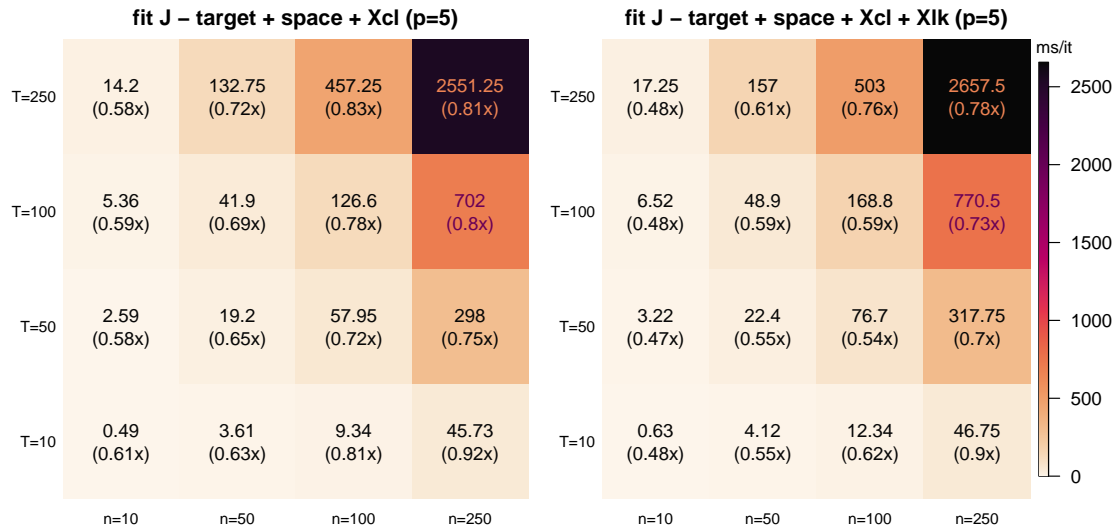


**Figure 4.22:** Execution times, measured in milliseconds per iteration, when fitting the JDRPM model using target values, spatial information, covariates in the clustering level (left), and covariates in both clustering and likelihood levels (right). In brackets are reported the speedups relative to the JDRPM timings of the fitting with target and space, with higher values still indicating better performance.

was inevitable due to the additional work to perform, but they still remain at a good performance level. Indeed, Figure 4.23 will point out how some of the fits with all information levels in Julia were actually faster than the basic fits in C.

We can also notice how with larger fits the performance drop reduces to just around 0.8x, rather than the 0.6x of the small cases: this indicates that on fits with heavy  $n$  and  $T$  the bottleneck is no more the algorithm complexity, meaning the

choice of which information levels to include in the clusters generation, but rather the available hardware resources.

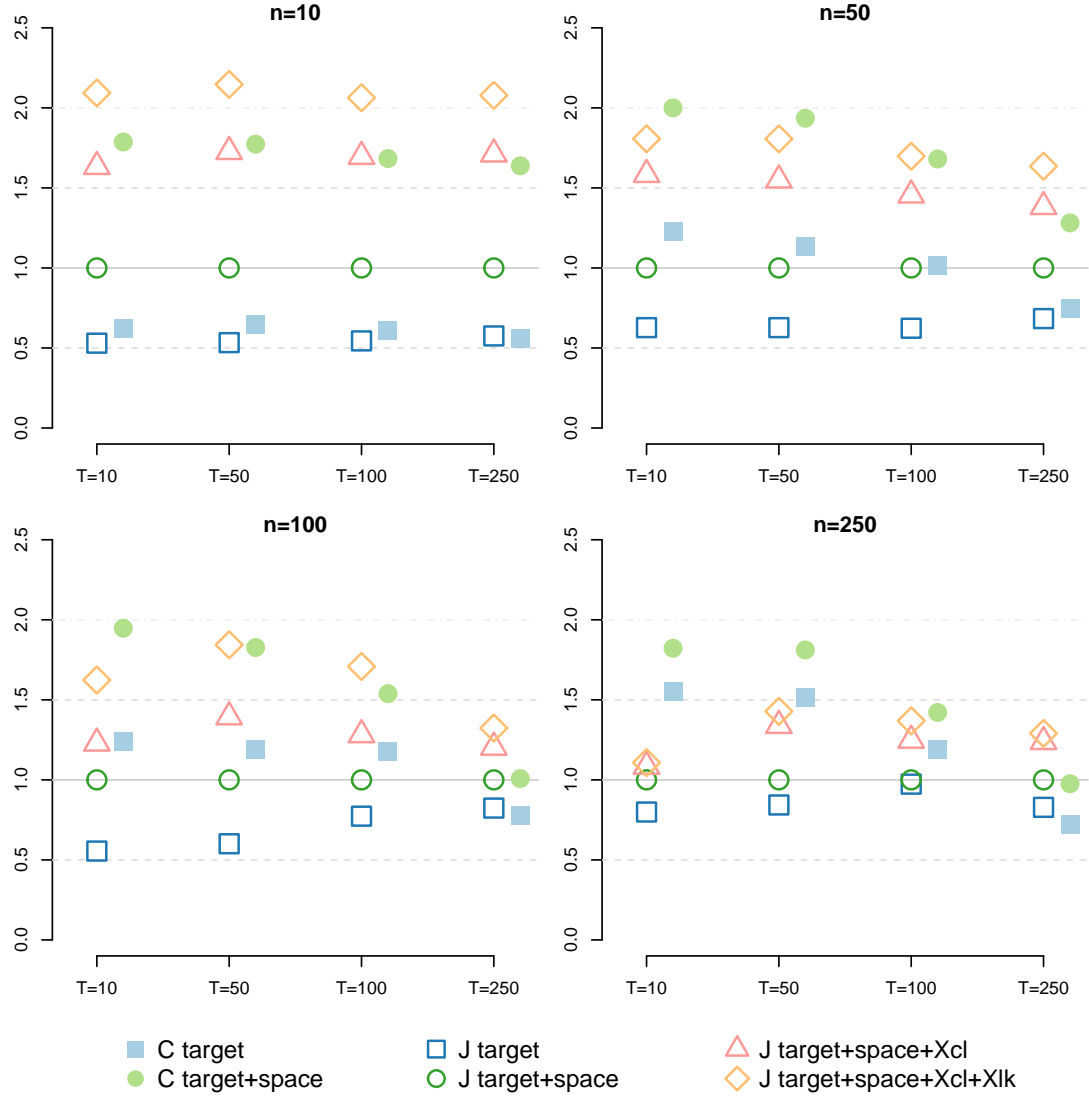


**Figure 4.23:** Visual representation of the performance of all the fits, for all the  $n$  and  $T$  cases, relatively to the JDRPM fit using target values and spatial information. Namely, the execution time per iteration metric of that fit has been taken as a reference, to which then all other fits have been compared to derive their speedup (or slowdown) factor. Points above the reference line indicate slower fits, while points below denote faster fits.

# Chapter 5

## Conclusion

*And what in human reckoning seems still afar off,  
may by the Divine ordinance be close at hand, on the  
eve of its appearance. And so be it, so be it!*

— Fëdor Dostoevskij, *Brothers Karamazov*

In the end, we can confidently assert that the JDRPM model is a valid improvement of the original DRPM formulation.

From a theoretical point of view, it offers the same structure, with an addition of a possible regression term in the likelihood, while also enhancing the quality of the sampled values of the parameters by having the laws of the variance parameters changed from  $\mathcal{U}$  to  $\text{invGamma}$ . In fact, this choice recovers conjugacy in the model and therefore improves the mixing of the chain during the fitting of the model. And, of course, the insertion of covariates in the clustering should provide even more accurate results in the clustering generation with respect to just having the spatio-temporal information.

A possible drawback, inevitable with the increased model complexity, could be the tuning of the parameters, for example in the cohesions and similarities function to find the right balance between the different contributes of the information levels. However, in this regards, an hopefully helpful analysis was conducted in Chapter 2, where the effects of the tuning parameters for all cohesions and similarities have been explored. Moreover, the Julia `MCMC_fit` function provides an optional argument `cv_weight`, defaulted to 1, which can be used to scale up (or down) the contribute of the covariates similarities, e.g. to make them closer to the interval of values to which the spatial cohesions values belong.

This higher complexity appeared also in the tuning of the  $\text{invGamma}(a, b)$  parameters, which are indeed more delicate than a simple  $\mathcal{U}(l, u)$ . To this end, a possible solution could be to run an initial fit with the original CDRPM model, to see where the values of the variances tend to gather, and according to that fixing the  $\text{invGamma}$  parameters. For example, in the spatio-temporal tests of Section 4.1.2 we saw, from the CDRPM fits, very low values for the variances parameters, and as such we assigned, for  $\lambda^2$  and  $\tau_t^2$  parameters in the JDRPM model, an  $\text{invGamma}(a =$

1.9,  $b = 0.4$ ), which has 90% of his density in the interval  $[0.109151, 1.58222]$ . The more relevant  $\sigma_{jt}^{2*}$  parameter had also pretty low values, however on that we attached a more uninformative prior of  $\text{invGamma}(a = 0.01, b = 0.01)$ , which despite being not always suggested [Gel04] turned out to be fine and very precise, relatively to the sampled “reference” values of CDRPM. An alternative solution, probably less theoretically appealing but possibly effective, could be to truncate the  $\text{invGamma}$  laws to a certain region in order to avoid sampling extremely high values, which can happen when uninformative priors get not properly adjusted by the data, and to resemble more the density of a  $\mathcal{U}$  random variable. This choice can be seamlessly implemented in the Julia code by e.g. swapping `rand(InverseGamma(a,b))` to `rand(truncated(InverseGamma(a,b),l,u))`, with  $l$  and  $u$  being the lower and upper bounds of the designed truncation interval.

From a computational point of view, the goal of faster fits was also reached, reducing the execution times up to a factor of two with respect to the original implementation. This at the cost of a small increase in the memory requirements which however, nowadays, is not a big deal.

A final drawback can be the time needed to convert back the results from Julia to R, since the `juliaGet` function from the `JuliaConnectoR` package can take up to some minutes, especially in fits where lots of iterations are saved. In any case, this latency becomes negligible with respect to the time saved from the previous implementation on the DRPM package.

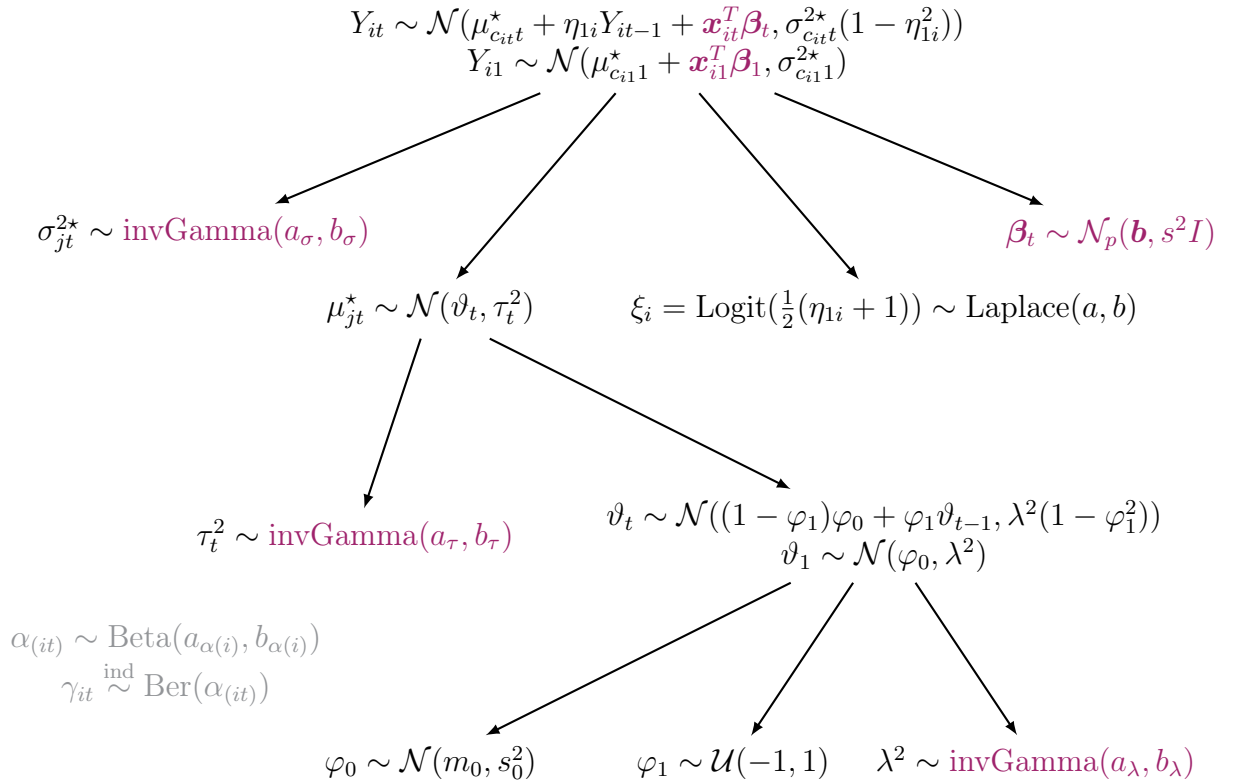


# Appendix A

## Theoretical details

### A.1 Extended computations of the full conditionals

We propose here the extended computations which allowed to extract the full conditionals presented in Chapter 2. We report also the model graph to make it quickly accessible as a reference for the laws involved in the following computations.



- update  $\sigma_{jt}^{2*}$

for  $t = 1$ :

$$f(\sigma_{jt}^{2*} | -) \propto f(\sigma_{jt}^{2*}) f(\{Y_{it} : c_{it} = j\} | \sigma_{jt}^{2*}, -)$$

$$\begin{aligned}
&= \mathcal{L}_{\text{invGamma}(a_\sigma, b_\sigma)}(\sigma_{jt}^{2*}) \prod_{i \in S_{jt}} \mathcal{L}_{\mathcal{N}(\mu_{c_{it}t}^* + \mathbf{x}_{it}^T \boldsymbol{\beta}_t, \sigma_{c_{it}1}^{2*})}(Y_{it}) \\
&\propto \left[ \left( \frac{1}{\sigma_{jt}^{2*}} \right)^{a_\sigma + 1} \exp \left\{ -\frac{1}{\sigma_{jt}^{2*}} b \right\} \right] \\
&\quad \cdot \left[ \prod_{i \in S_{jt}} \left( \frac{1}{\sigma_{jt}^{2*}} \right)^{1/2} \exp \left\{ -\frac{1}{2\sigma_{jt}^{2*}} (Y_{it} - \mu_{jt}^* - \mathbf{x}_{it}^T \boldsymbol{\beta}_t)^2 \right\} \right] \\
&\propto \left( \frac{1}{\sigma_{jt}^{2*}} \right)^{(a_\sigma + |S_{jt}|/2) + 1} \exp \left\{ -\frac{1}{\sigma_{jt}^{2*}} \left( b_\sigma + \frac{1}{2} \sum_{i \in S_{jt}} (Y_{it} - \mu_{jt}^* - \mathbf{x}_{it}^T \boldsymbol{\beta}_t)^2 \right) \right\} \\
&\implies f(\sigma_{jt}^{2*} | -) \propto \text{kernel of a invGamma}(a_{\sigma(\text{post})}, b_{\sigma(\text{post})}) \text{ with} \\
&\quad a_{\tau(\text{post})} = a_\sigma + \frac{|S_{jt}|}{2} \\
&\quad b_{\tau(\text{post})} = b_\sigma + \frac{1}{2} \sum_{i \in S_{jt}} (Y_{it} - \mu_{jt}^* - \mathbf{x}_{it}^T \boldsymbol{\beta}_t)^2 \tag{A.1}
\end{aligned}$$

for  $t > 1$ :

$$\begin{aligned}
&f(\sigma_{jt}^{2*} | -) \propto f(\sigma_{jt}^{2*}) f(\{Y_{it} : c_{it} = j\} | \sigma_{jt}^{2*}, -) \\
&= \mathcal{L}_{\text{invGamma}(a_\sigma, b_\sigma)}(\sigma_{jt}^{2*}) \prod_{i \in S_{jt}} \mathcal{L}_{\mathcal{N}(\mu_{c_{it}t}^* + \eta_{1i} Y_{it-1} + \mathbf{x}_{it}^T \boldsymbol{\beta}_t, \sigma_{c_{it}1}^{2*})}(Y_{it}) \\
&\propto \left[ \left( \frac{1}{\sigma_{jt}^{2*}} \right)^{a_\sigma + 1} \exp \left\{ -\frac{1}{\sigma_{jt}^{2*}} b \right\} \right] \\
&\quad \cdot \left[ \prod_{i \in S_{jt}} \left( \frac{1}{\sigma_{jt}^{2*}} \right)^{1/2} \exp \left\{ -\frac{1}{2\sigma_{jt}^{2*}} (Y_{it} - \mu_{jt}^* - \eta_{1i} Y_{it-1} - \mathbf{x}_{it}^T \boldsymbol{\beta}_t)^2 \right\} \right] \\
&\propto \left( \frac{1}{\sigma_{jt}^{2*}} \right)^{(a_\sigma + |S_{jt}|/2) + 1} \\
&\quad \cdot \exp \left\{ -\frac{1}{\sigma_{jt}^{2*}} \left( b_\sigma + \frac{1}{2} \sum_{i \in S_{jt}} (Y_{it} - \eta_{1i} Y_{it-1} - \mu_{jt}^* - \mathbf{x}_{it}^T \boldsymbol{\beta}_t)^2 \right) \right\} \\
&\implies f(\sigma_{jt}^{2*} | -) \propto \text{kernel of a invGamma}(a_{\sigma(\text{post})}, b_{\sigma(\text{post})}) \text{ with} \\
&\quad a_{\tau(\text{post})} = a_\sigma + \frac{|S_{jt}|}{2} \\
&\quad b_{\tau(\text{post})} = b_\sigma + \frac{1}{2} \sum_{i \in S_{jt}} (Y_{it} - \mu_{jt}^* - \eta_{1i} Y_{it-1} - \mathbf{x}_{it}^T \boldsymbol{\beta}_t)^2 \tag{A.2}
\end{aligned}$$

- update  $\mu_{jt}^*$

for  $t = 1$ :

$$f(\mu_{jt}^* | -) \propto f(\mu_{jt}^*) f(\{Y_{it} : c_{it} = j\} | \mu_{jt}^*, -)$$

$$\begin{aligned}
&= \mathcal{L}_{\mathcal{N}(\vartheta_t, \tau_t^2)}(\mu_{jt}^*) \prod_{i \in S_{jt}} \mathcal{L}_{\mathcal{N}(\mu_{c_{it}t}^* + \mathbf{x}_{it}^T \boldsymbol{\beta}_t, \sigma_{c_{it}1}^{2*})}(Y_{it}) \\
&\propto \exp \left\{ -\frac{1}{2\tau_t^2} (\mu_{jt}^* - \vartheta_t)^2 \right\} \exp \left\{ -\frac{1}{2\sigma_{jt}^{2*}} \left( \sum_{i \in S_{jt}} (\mu_{jt}^* - (Y_{i1} - \mathbf{x}_{it}^T \boldsymbol{\beta}_t))^2 \right) \right\} \\
&\propto \exp \left\{ -\frac{1}{2\tau_t^2} (\mu_{jt}^* - \vartheta_t)^2 \right\} \exp \left\{ -\frac{|S_{jt}|}{2\sigma_{jt}^{2*}} \left( \mu_{jt}^* - \frac{\text{SUM}_y}{|S_{jt}|} \right)^2 \right\} \\
&\text{where } \text{SUM}_y = \sum_{i \in S_{jt}} Y_{i1} - \mathbf{x}_{it}^T \boldsymbol{\beta}_t \\
\Rightarrow f(\mu_{jt}^* | -) &\propto \text{kernel of a } \mathcal{N}(\mu_{\mu_{jt}^*}^*(\text{post}), \sigma_{\mu_{jt}^*}^2(\text{post})) \text{ with} \\
\sigma_{\mu_{jt}^*}^2(\text{post}) &= \frac{1}{\frac{1}{\tau_t^2} + \frac{|S_{jt}|}{\sigma_{jt}^{2*}}} \\
\mu_{\mu_{jt}^*}^*(\text{post}) &= \sigma_{\mu_{jt}^*}^2(\text{post}) \left( \frac{\vartheta_t}{\tau_t^2} + \frac{\text{SUM}_y}{\sigma_{jt}^{2*}} \right) \tag{A.3}
\end{aligned}$$

for  $t > 1$ :

$$\begin{aligned}
f(\mu_{jt}^* | -) &\propto f(\mu_{jt}^*) f(\{Y_{it} : c_{it} = j\} | \mu_{jt}^*, -) \\
&= \mathcal{L}_{\mathcal{N}(\vartheta_1, \tau_1^2)}(\mu_{jt}^*) \prod_{i \in S_{jt}} \mathcal{L}_{\mathcal{N}(\mu_{c_{it}t}^* + \eta_{1i} Y_{i,t-1} + \mathbf{x}_{it}^T \boldsymbol{\beta}_t, \sigma_{c_{it}1}^{2*})}(Y_{it}) \\
&\propto \exp \left\{ -\frac{1}{2\tau_t^2} (\mu_{jt}^* - \vartheta_t)^2 \right\} \\
&\cdot \exp \left\{ -\frac{1}{2\sigma_{jt}^{2*}} \left( \sum_{i \in S_{jt}} \frac{1}{1 - \eta_{1i}^2} (\mu_{jt}^* - (Y_{it} - \eta_{1i} Y_{i,t-1} - \mathbf{x}_{it}^T \boldsymbol{\beta}_t))^2 \right) \right\} \\
&\propto \exp \left\{ -\frac{1}{2\tau_t^2} (\mu_{jt}^* - \vartheta_t)^2 \right\} \exp \left\{ -\frac{\text{SUM}_{e2}}{2\sigma_{jt}^{2*}} \left( \mu_{jt}^* - \frac{\text{SUM}_y}{\text{SUM}_{e2}} \right)^2 \right\} \\
&\text{where } \text{SUM}_y = \sum_{i \in S_{jt}} \frac{Y_{it} - \eta_{1i} Y_{i,t-1} - \mathbf{x}_{it}^T \boldsymbol{\beta}_t}{1 - \eta_{1i}^2}, \text{SUM}_{e2} = \sum_{i \in S_{jt}} \frac{1}{1 - \eta_{1i}^2} \\
\Rightarrow f(\mu_{jt}^* | -) &\propto \text{kernel of a } \mathcal{N}(\mu_{\mu_{jt}^*}^*(\text{post}), \sigma_{\mu_{jt}^*}^2(\text{post})) \text{ with} \\
\sigma_{\mu_{jt}^*}^2(\text{post}) &= \frac{1}{\frac{1}{\tau_t^2} + \frac{\text{SUM}_{e2}}{\sigma_{jt}^{2*}}} \\
\mu_{\mu_{jt}^*}^*(\text{post}) &= \sigma_{\mu_{jt}^*}^2(\text{post}) \left( \frac{\vartheta_t}{\tau_t^2} + \frac{\text{SUM}_y}{\sigma_{jt}^{2*}} \right) \tag{A.4}
\end{aligned}$$

- update  $\boldsymbol{\beta}_t$

for  $t = 1$ :

$$\begin{aligned}
f(\boldsymbol{\beta}_t | -) &\propto f(\boldsymbol{\beta}_t) f(\{Y_{1t}, \dots, Y_{nt}\} | \boldsymbol{\beta}_t, -) \\
&= \mathcal{L}_{\mathcal{N}(\mathbf{b}, s^2 I)}(\boldsymbol{\beta}_t) \prod_{i=1}^n \mathcal{L}_{\mathcal{N}(\mu_{c_{it}t}^* + \mathbf{x}_{it}^T \boldsymbol{\beta}_t, \sigma_{c_{it}t}^{2*})}(Y_{it})
\end{aligned}$$

$$\begin{aligned}
& \propto \exp \left\{ -\frac{1}{2} \left[ (\boldsymbol{\beta}_t^T - \mathbf{b})^T \frac{1}{s^2} (\boldsymbol{\beta}_t - \mathbf{b}) \right] \right\} \\
& \cdot \exp \left\{ -\frac{1}{2} \sum_{i=1}^n (Y_{it} - \mu_{c_{it}}^* - \mathbf{x}_{it}^T \boldsymbol{\beta}_t)^2 \right\} \\
& \propto \exp \left\{ -\frac{1}{2} \left[ \boldsymbol{\beta}_t^T \left( \frac{1}{s^2} I + \sum_{i=1}^n \frac{\mathbf{x}_{it} \mathbf{x}_{it}^T}{\sigma_{c_{it}}^{2*}} \right) \boldsymbol{\beta}_t \right. \right. \\
& \quad \left. \left. - 2 \left( \frac{\mathbf{b}}{s^2} + \sum_{i=1}^n \frac{(Y_{it} - \mu_{c_{it}}^*) \mathbf{x}_{it}}{\sigma_{c_{it}}^{2*}} \right) \cdot \boldsymbol{\beta}_t \right] \right\} \\
& \implies f(\boldsymbol{\beta}_t | -) \propto \text{kernel of a } \mathcal{N}(\mathbf{b}_{(\text{post})}, A_{(\text{post})}) \text{ with} \\
& A_{(\text{post})} = \left( \frac{1}{s^2} I + \sum_{i=1}^n \frac{\mathbf{x}_{it} \mathbf{x}_{it}^T}{\sigma_{c_{it}}^{2*}} \right)^{-1} \\
& \mathbf{b}_{(\text{post})} = A_{(\text{post})} \left( \frac{\mathbf{b}}{s^2} + \sum_{i=1}^n \frac{(Y_{it} - \mu_{c_{it}}^*) \mathbf{x}_{it}}{\sigma_{c_{it}}^{2*}} \right) \\
& \iff f(\boldsymbol{\beta}_t | -) \propto \text{kernel of a } \mathcal{N}\text{Canon}(\mathbf{h}_{(\text{post})}, J_{(\text{post})}) \text{ with} \\
& \mathbf{h}_{(\text{post})} = \left( \frac{\mathbf{b}}{s^2} + \sum_{i=1}^n \frac{(Y_{it} - \mu_{c_{it}}^*) \mathbf{x}_{it}}{\sigma_{c_{it}}^{2*}} \right) \\
& J_{(\text{post})} = \left( \frac{1}{s^2} I + \sum_{i=1}^n \frac{\mathbf{x}_{it} \mathbf{x}_{it}^T}{\sigma_{c_{it}}^{2*}} \right) \tag{A.5}
\end{aligned}$$

for  $t > 1$ :

$$\begin{aligned}
& f(\boldsymbol{\beta}_t | -) \propto f(\boldsymbol{\beta}_t) f(\{Y_{1t}, \dots, Y_{nt}\} | \boldsymbol{\beta}_t, -) \\
& = \mathcal{L}_{\mathcal{N}(\mathbf{b}, s^2 I)}(\boldsymbol{\beta}_t) \prod_{i=1}^n \mathcal{L}_{\mathcal{N}(\mu_{c_{it}}^* + \eta_{1i} Y_{it-1} + \mathbf{x}_{it}^T \boldsymbol{\beta}_t, \sigma_{c_{it}}^{2*})}(Y_{it}) \\
& \propto \exp \left\{ -\frac{1}{2} \left[ (\boldsymbol{\beta}_t^T - \mathbf{b})^T \frac{1}{s^2} (\boldsymbol{\beta}_t - \mathbf{b}) \right] \right\} \\
& \cdot \exp \left\{ -\frac{1}{2} \sum_{i=1}^n (Y_{it} - \mu_{c_{it}}^* - \eta_{1i} Y_{it-1} - \mathbf{x}_{it}^T \boldsymbol{\beta}_t)^2 \right\} \\
& \propto \exp \left\{ -\frac{1}{2} \left[ \boldsymbol{\beta}_t^T \left( \frac{1}{s^2} I + \sum_{i=1}^n \frac{\mathbf{x}_{it} \mathbf{x}_{it}^T}{\sigma_{c_{it}}^{2*}} \right) \boldsymbol{\beta}_t \right. \right. \\
& \quad \left. \left. - 2 \left( \frac{\mathbf{b}}{s^2} + \sum_{i=1}^n \frac{(Y_{it} - \mu_{c_{it}}^* - \eta_{1i} Y_{it-1}) \mathbf{x}_{it}}{\sigma_{c_{it}}^{2*}} \right) \cdot \boldsymbol{\beta}_t \right] \right\} \\
& \implies f(\boldsymbol{\beta}_t | -) \propto \text{kernel of a } \mathcal{N}(\mathbf{b}_{(\text{post})}, A_{(\text{post})}) \text{ with} \\
& A_{(\text{post})} = \left( \frac{1}{s^2} I + \sum_{i=1}^n \frac{\mathbf{x}_{it} \mathbf{x}_{it}^T}{\sigma_{c_{it}}^{2*}} \right)^{-1} \\
& \mathbf{b}_{(\text{post})} = A_{(\text{post})} \left( \frac{\mathbf{b}}{s^2} + \sum_{i=1}^n \frac{(Y_{it} - \mu_{c_{it}}^* - \eta_{1i} Y_{it-1}) \mathbf{x}_{it}}{\sigma_{c_{it}}^{2*}} \right)
\end{aligned}$$

$$\begin{aligned}
&\Longleftrightarrow f(\beta_t|-) \propto \text{kernel of a } \mathcal{N}\text{Canon}(\mathbf{h}_{(\text{post})}, J_{(\text{post})}) \text{ with} \\
&\mathbf{h}_{(\text{post})} = \left( \frac{\mathbf{b}}{s^2} + \sum_{i=1}^n \frac{(Y_{it} - \mu_{c_{it}}^* - \eta_{1i} Y_{it-1}) \mathbf{x}_{it}}{\sigma_{c_{it}}^{2*}} \right) \\
&J_{(\text{post})} = \left( \frac{1}{s^2} I + \sum_{i=1}^n \frac{\mathbf{x}_{it} \mathbf{x}_{it}^T}{\sigma_{c_{it}}^{2*}} \right)
\end{aligned} \tag{A.6}$$

- update  $\tau_t^2$

$$\begin{aligned}
&f(\tau_t^2|-) \propto f(\tau_t^2) f((\mu_{1t}^*, \dots, \mu_{k_{it}}^*) | \tau_t^2, -) \\
&= \mathcal{L}_{\text{invGamma}(a_\tau, b_\tau)}(\tau_t^2) \prod_{j=1}^{k_t} \mathcal{L}_{\mathcal{N}(\vartheta_t, \tau_t^2)}(\mu_{jt}^*) \\
&\propto \left[ \left( \frac{1}{\tau_t^2} \right)^{a_\tau+1} \exp \left\{ -\frac{b_\tau}{\tau_t^2} \right\} \right] \left[ \prod_{j=1}^{k_t} \left( \frac{1}{\tau_t^2} \right)^{1/2} \exp \left\{ -\frac{1}{2\tau_t^2} (\mu_{jt}^* - \vartheta_t)^2 \right\} \right] \\
&\propto \left( \frac{1}{\tau_t^2} \right)^{\left( \frac{k_t}{2} + a_\tau \right) + 1} \exp \left\{ -\frac{1}{\tau_t^2} \left( \frac{\sum_{j=1}^{k_t} (\mu_{jt}^* - \vartheta_t)^2}{2} + b_\tau \right) \right\} \\
&\implies f(\tau_t^2|-) \propto \text{kernel of a } \text{invGamma}(a_{\tau(\text{post})}, b_{\tau(\text{post})}) \text{ with} \\
&a_{\tau(\text{post})} = \frac{k_t}{2} + a_\tau \\
&b_{\tau(\text{post})} = \frac{\sum_{j=1}^{k_t} (\mu_{jt}^* - \vartheta_t)^2}{2} + b_\tau
\end{aligned} \tag{A.7}$$

- update  $\vartheta_t$

for  $t = T$ :

$$\begin{aligned}
&f(\vartheta_t|-) \propto f(\vartheta_t) f((\mu_{1t}^*, \dots, \mu_{k_{it}}^*) | \vartheta_t, -) \\
&= \mathcal{L}_{\mathcal{N}((1-\varphi_1)\varphi_0 + \varphi_1\vartheta_{t-1}, \lambda^2(1-\varphi_1^2))}(\vartheta_t) \prod_{j=1}^{k_t} \mathcal{L}_{\mathcal{N}(\vartheta_t, \tau_t^2)}(\mu_{jt}^*) \\
&\propto \exp \left\{ -\frac{1}{2(\lambda^2(1-\varphi_1^2))} \left( \vartheta_t - ((1-\varphi_1)\varphi_0 + \varphi_1\vartheta_{t-1}) \right)^2 \right\} \\
&\quad \cdot \exp \left\{ -\frac{k_t}{2\tau_t^2} \left( \vartheta_t - \frac{\sum_{j=1}^{k_t} \mu_{jt}^*}{k_t} \right)^2 \right\} \\
&\implies f(\vartheta_t|-) \propto \text{kernel of a } \mathcal{N}(\mu_{\vartheta_t(\text{post})}, \sigma_{\vartheta_t(\text{post})}^2) \text{ with} \\
&\sigma_{\vartheta_t(\text{post})}^2 = \frac{1}{\frac{1}{\lambda^2(1-\varphi_1^2)} + \frac{k_t}{\tau_t^2}} \\
&\mu_{\vartheta_t(\text{post})} = \sigma_{\vartheta_t(\text{post})}^2 \left( \frac{\sum_{j=1}^{k_t} \mu_{jt}^*}{\tau_t^2} + \frac{(1-\varphi_1)\varphi_0 + \varphi_1\vartheta_{t-1}}{\lambda^2(1-\varphi_1^2)} \right)
\end{aligned} \tag{A.8}$$

for  $1 < t < T$ :

$$\begin{aligned}
f(\vartheta_t|-) &\propto \underbrace{f(\vartheta_t)f((\mu_{1t}^*, \dots, \mu_{k_t t}^*)|\vartheta_t, -)}_{\text{as in the case } t=T} f(\vartheta_{t+1}|\vartheta_t, -) \\
&= \mathcal{L}_{\mathcal{N}(\mu_{\vartheta_t(\text{post})}, \sigma_{\vartheta_t(\text{post})}^2)}(\vartheta_t) \mathcal{L}_{\mathcal{N}((1-\varphi_1)\varphi_0 + \varphi_1\vartheta_t, \lambda^2(1-\varphi_1^2))}(\vartheta_{t+1}) \\
&\propto \exp\left\{-\frac{1}{2\sigma_{\vartheta_t(\text{post})}^2}(\vartheta_t - \mu_{\vartheta_t(\text{post})})^2\right\} \\
&\quad \cdot \exp\left\{-\frac{1}{2\frac{\lambda^2(1-\varphi_1^2)}{\varphi_1^2}}\left(\vartheta_t - \frac{\vartheta_{t+1} - (1-\varphi_1)\varphi_0}{\varphi_1}\right)^2\right\} \\
&\Rightarrow f(\vartheta_t|-) \propto \text{kernel of a } \mathcal{N}(\mu_{\vartheta_t(\text{post})}, \sigma_{\vartheta_t(\text{post})}^2) \text{ with} \\
&\quad \sigma_{\vartheta_t(\text{post})}^2 = \frac{1}{\frac{1+\varphi_1^2}{\lambda^2(1-\varphi_1^2)} + \frac{k_t}{\tau_t^2}} \\
&\quad \mu_{\vartheta_t(\text{post})} = \sigma_{\vartheta_t(\text{post})}^2 \left( \frac{\sum_{j=1}^{k_t} \mu_{jt}^*}{\tau_t^2} + \frac{\varphi_1(\vartheta_{t-1} + \vartheta_{t+1}) + \varphi_0(1-\varphi_1)^2}{\lambda^2(1-\varphi_1^2)} \right) \quad (\text{A.9})
\end{aligned}$$

for  $t = 1$ :

$$\begin{aligned}
f(\vartheta_t|-) &\propto f(\vartheta_t)f(\vartheta_{t+1}|\vartheta_t, -)f(\mu_t^*|\vartheta_t, -) \\
&= \mathcal{L}_{\mathcal{N}(\varphi_0, \lambda^2)}(\vartheta_t) \mathcal{L}_{\mathcal{N}((1-\varphi_1)\varphi_0 + \varphi_1\vartheta_{t-1}, \lambda^2(1-\varphi_1^2))}(\vartheta_{t+1}) \prod_{j=1}^{k_t} \mathcal{L}_{\mathcal{N}(\vartheta_t, \tau_t^2)}(\mu_{jt}^*) \\
&\propto \exp\left\{-\frac{1}{2\lambda^2}(\vartheta_t - \varphi_0)^2\right\} \\
&\quad \cdot \exp\left\{-\frac{1}{2\frac{\lambda^2(1-\varphi_1^2)}{\varphi_1^2}}\left(\vartheta_t - \frac{\vartheta_{t+1} - (1-\varphi_1)\varphi_0}{\varphi_1}\right)^2\right\} \\
&\quad \cdot \exp\left\{-\frac{k_t}{2\tau_t^2}\left(\vartheta_t - \frac{\sum_{j=1}^{k_t} \mu_{jt}^*}{k_t}\right)^2\right\} \\
&\Rightarrow f(\vartheta_t|-) \propto \text{kernel of a } \mathcal{N}(\mu_{\vartheta_t(\text{post})}, \sigma_{\vartheta_t(\text{post})}^2) \text{ with} \\
&\quad \sigma_{\vartheta_t(\text{post})}^2 = \frac{1}{\frac{1}{\lambda^2} + \frac{\varphi_1^2}{\lambda^2(1-\varphi_1^2)} + \frac{k_t}{\tau_t^2}} \\
&\quad \mu_{\vartheta_t(\text{post})} = \sigma_{\vartheta_t(\text{post})}^2 \left( \frac{\varphi_0}{\lambda^2} + \frac{\varphi_1(\vartheta_{t+1} - (1-\varphi_1)\varphi_0)}{\lambda^2(1-\varphi_1^2)} + \frac{\sum_{j=1}^{k_t} \mu_{jt}^*}{\tau_t^2} \right) \quad (\text{A.10})
\end{aligned}$$

- update  $\varphi_0$

$$\begin{aligned}
f(\varphi_0|-) &\propto f(\varphi_0)f((\vartheta_1, \dots, \vartheta_T)|\varphi_0, -) \\
&= \mathcal{L}_{\mathcal{N}(m_0, s_0^2)}(\varphi_0) \mathcal{L}_{\mathcal{N}(\varphi_0, \lambda^2)}(\vartheta_1) \prod_{t=2}^T \mathcal{L}_{\mathcal{N}((1-\varphi_1)\varphi_0 + \varphi_1\vartheta_{t-1}, \lambda^2(1-\varphi_1^2))}(\vartheta_t) \\
&\propto \exp\left\{\left\{-\frac{1}{2s_0^2}(\varphi_0 - m_0)^2\right\}\right\} \exp\left\{\left\{-\frac{1}{2\lambda^2}(\varphi_0 - \vartheta_1)^2\right\}\right\}
\end{aligned}$$

$$\begin{aligned}
& \cdot \exp \left\{ \left\{ -\frac{1}{2 \frac{\lambda^2(1-\varphi_1^2)}{(T-1)(1-\varphi_1)^2}} \left( \varphi_0 - \frac{(1-\varphi_1)(\text{SUM}_t)}{(T-1)(1-\varphi_1)^2} \right)^2 \right\} \right\} \\
& \text{where } \text{SUM}_t = \sum_{t=2}^T (\vartheta_t - \varphi_1 \vartheta_{t-1}) \\
\Rightarrow f(\varphi_0 | -) & \propto \text{kernel of a } \mathcal{N}(\mu_{\varphi_0(\text{post})}, \sigma_{\varphi_0(\text{post})}^2) \text{ with} \\
\sigma_{\varphi_0(\text{post})}^2 &= \frac{1}{\frac{1}{s_0^2} + \frac{1}{\lambda^2} + \frac{(T-1)(1-\varphi_1)^2}{\lambda^2(1-\varphi_1^2)}} \\
\mu_{\varphi_0(\text{post})} &= \sigma_{\varphi_0(\text{post})}^2 \left( \frac{m_0}{s_0^2} + \frac{\vartheta_1}{\lambda^2} + \frac{1-\varphi_1}{\lambda^2(1-\varphi_1^2)} \text{SUM}_t \right) \tag{A.11}
\end{aligned}$$

- update  $\lambda^2$

$$\begin{aligned}
f(\lambda^2 | -) & \propto f(\lambda^2) f(\vartheta_1, \dots, \vartheta_T | \lambda^2, -) \\
&= \mathcal{L}_{\text{invGamma}(a_\lambda, b_\lambda)}(\lambda^2) \mathcal{L}_{\mathcal{N}(\varphi_0, \lambda^2)}(\vartheta_1) \prod_{t=2}^T \mathcal{L}_{\mathcal{N}((1-\varphi_1)\varphi_0 + \varphi_1 \vartheta_{t-1}, \lambda^2(1-\varphi_1^2))}(\vartheta_t) \\
&\propto \left[ \left( \frac{1}{\lambda_t^2} \right)^{a_\lambda+1} \exp \left\{ -\frac{b_\lambda}{\lambda^2} \right\} \right] \left[ \left( \frac{1}{\lambda^2} \right)^{1/2} \exp \left\{ -\frac{1}{2\lambda^2} (\vartheta_1 - \varphi_0)^2 \right\} \right] \\
&\cdot \left[ \prod_{t=2}^T \left( \frac{1}{\lambda^2} \right)^{1/2} \exp \left\{ -\frac{1}{2\lambda^2} (\vartheta_t - (1-\varphi_1)\varphi_0 - \varphi_1 \vartheta_{t-1})^2 \right\} \right] \\
&\propto \left( \frac{1}{\lambda^2} \right)^{\left( \frac{T}{2} + a_\lambda \right) + 1} \\
&\cdot \exp \left\{ -\frac{1}{\lambda^2} \left( \frac{(\vartheta_1 - \varphi_0)^2}{2} + \sum_{t=2}^T \frac{(\vartheta_t - (1-\varphi_1)\varphi_0 - \varphi_1 \vartheta_{t-1})^2}{2} + b_\lambda \right) \right\} \\
\Rightarrow f(\lambda^2 | -) & \propto \text{kernel of a invGamma}(a_{\lambda(\text{post})}, b_{\lambda(\text{post})}) \text{ with} \\
a_{\lambda(\text{post})} &= \frac{T}{2} + a_\lambda \\
b_{\lambda(\text{post})} &= \frac{(\vartheta_1 - \varphi_0)^2}{2} + \sum_{t=2}^T \frac{(\vartheta_t - (1-\varphi_1)\varphi_0 - \varphi_1 \vartheta_{t-1})^2}{2} + b_\lambda \tag{A.12}
\end{aligned}$$

- update  $\alpha$

$$\begin{aligned}
& \text{if global } \alpha: \text{ prior is } \alpha \sim \text{Beta}(a_\alpha, b_\alpha) \\
f(\alpha | -) & \propto f(\alpha) f((\gamma_{11}, \dots, \gamma_{1T}, \dots, \gamma_{n1}, \dots, \gamma_{nT}) | \alpha) \\
&\propto \alpha^{a_\alpha-1} (1-\alpha)^{b_\alpha-1} \prod_{i=1}^n \prod_{t=1}^T \alpha^{\gamma_{it}} (1-\alpha)^{1-\gamma_{it}} \\
&= \alpha^{(a_\alpha + \sum_{i=1}^n \sum_{t=1}^T \gamma_{it})-1} (1-\alpha)^{(b_\alpha + nT - \sum_{i=1}^n \sum_{t=1}^T \gamma_{it})-1} \\
\Rightarrow f(\alpha | -) & \propto \text{kernel of a Beta}(a_{\alpha(\text{post})}, b_{\alpha(\text{post})}) \text{ with}
\end{aligned}$$

$$a_{\alpha(\text{post})} = a_{\alpha} + \sum_{i=1}^n \sum_{t=1}^T \gamma_{it} \quad b_{\alpha(\text{post})} = b_{\alpha} + nT - \sum_{i=1}^n \sum_{t=1}^T \gamma_{it} \quad (\text{A.13})$$

if time specific  $\alpha$ : prior is  $\alpha_t \sim \text{Beta}(a_{\alpha}, b_{\alpha})$

$$\begin{aligned} f(\alpha_t | -) &\propto f(\alpha_t) f((\gamma_{1t}, \dots, \gamma_{nt}) | \alpha_t) \\ &\propto \alpha_t^{a_{\alpha}-1} (1 - \alpha_t)^{b_{\alpha}-1} \prod_{i=1}^n \alpha_t^{\gamma_{it}} (1 - \alpha_t)^{1-\gamma_{it}} \\ &= \alpha_t^{(a_{\alpha} + \sum_{i=1}^n \gamma_{it})-1} (1 - \alpha_t)^{(b_{\alpha} + n - \sum_{i=1}^n \gamma_{it})-1} \\ \implies f(\alpha_t | -) &\propto \text{kernel of a Beta}(a_{\alpha(\text{post})}, b_{\alpha(\text{post})}) \text{ with} \\ a_{\alpha(\text{post})} &= a_{\alpha} + \sum_{i=1}^n \gamma_{it} \quad b_{\alpha(\text{post})} = b_{\alpha} + n - \sum_{i=1}^n \gamma_{it} \end{aligned} \quad (\text{A.14})$$

if unit specific  $\alpha$ : prior is  $\alpha_i \sim \text{Beta}(a_{\alpha i}, b_{\alpha i})$

$$\begin{aligned} f(\alpha_i | -) &\propto f(\alpha_i) f((\gamma_{i1}, \dots, \gamma_{iT}) | \alpha_i) \\ &\propto \alpha_i^{a_{\alpha i}-1} (1 - \alpha_i)^{b_{\alpha i}-1} \prod_{t=1}^T \alpha_i^{\gamma_{it}} (1 - \alpha_i)^{1-\gamma_{it}} \\ &= \alpha_i^{(a_{\alpha i} + \sum_{t=1}^T \gamma_{it})-1} (1 - \alpha_i)^{(b_{\alpha i} + T - \sum_{t=1}^T \gamma_{it})-1} \\ \implies f(\alpha_i | -) &\propto \text{kernel of a Beta}(a_{\alpha(\text{post})}, b_{\alpha(\text{post})}) \text{ with} \\ a_{\alpha(\text{post})} &= a_{\alpha i} + \sum_{t=1}^T \gamma_{it} \quad b_{\alpha(\text{post})} = b_{\alpha i} + T - \sum_{t=1}^T \gamma_{it} \end{aligned} \quad (\text{A.15})$$

if time and unit specific  $\alpha$ : prior is  $\alpha_{it} \sim \text{Beta}(a_{\alpha i}, b_{\alpha i})$

$$\begin{aligned} f(\alpha_{it} | -) &\propto f(\alpha_{it}) f(\gamma_{it} | \alpha_{it}) \\ &\propto \alpha_{it}^{a_{\alpha i}-1} (1 - \alpha_{it})^{b_{\alpha i}-1} \alpha_{it}^{\gamma_{it}} (1 - \alpha_{it})^{1-\gamma_{it}} \\ &= \alpha_{it}^{(a_{\alpha i} + \gamma_{it})-1} (1 - \alpha_{it})^{(b_{\alpha i} + 1 - \gamma_{it})-1} \\ \implies f(\alpha_{it} | -) &\propto \text{kernel of a Beta}(a_{\alpha(\text{post})}, b_{\alpha(\text{post})}) \text{ with} \\ a_{\alpha(\text{post})} &= a_{\alpha i} + \gamma_{it} \quad b_{\alpha(\text{post})} = b_{\alpha i} + 1 - \gamma_{it} \end{aligned} \quad (\text{A.16})$$

- update a missing observation  $Y_{it}$

for  $t = 1$ :

$$\begin{aligned} f(Y_{it} | -) &\propto f(Y_{it}) f(Y_{it+1} | Y_{it}, -) \\ &= \mathcal{L}_{\mathcal{N}(\mu_{c_{it}t}^* + \mathbf{x}_{it}^T \boldsymbol{\beta}_t, \sigma_{c_{it}t}^{2*})}(Y_{it}) \\ &\quad \cdot \mathcal{L}_{\mathcal{N}(\mu_{c_{it+1}t+1}^* + \eta_{1i} Y_{it} + \mathbf{x}_{it+1}^T \boldsymbol{\beta}_{t+1}, \sigma_{c_{it+1}t+1}^{2*} (1 - \eta_{1i}^2))}(Y_{it+1}) \\ &\propto \exp \left\{ -\frac{1}{2\sigma_{c_{it}t}^{2*}} (Y_{it} - \mu_{c_{it}t}^* - \mathbf{x}_{it}^T \boldsymbol{\beta}_t)^2 \right\} \\ &\quad \cdot \exp \left\{ -\frac{1}{2\sigma_{c_{it+1}t+1}^{2*} (1 - \eta_{1i}^2)} (Y_{it+1} - \mu_{c_{it+1}t+1}^* - \eta_{1i} Y_{it} - \mathbf{x}_{it+1}^T \boldsymbol{\beta}_{t+1})^2 \right\} \end{aligned}$$



$$\begin{aligned}
&= \exp \left\{ -\frac{1}{2\sigma_{c_{it}t}^{2*}} (Y_{it} - (\mu_{c_{it}t}^* + \mathbf{x}_{it}^T \boldsymbol{\beta}_t))^2 \right\} \\
&\cdot \exp \left\{ -\frac{\eta_{1i}^2}{2\sigma_{c_{it+1}t+1}^{2*}(1-\eta_{1i}^2)} \left( Y_{it} - \frac{Y_{it+1} - \mu_{c_{it+1}t+1}^* - \mathbf{x}_{it+1}^T \boldsymbol{\beta}_{t+1}}{\eta_{1i}} \right)^2 \right\} \\
\Rightarrow f(Y_{it}|-) &\propto \text{kernel of a } \mathcal{N}(\mu_{Y_{it}(\text{post})}, \sigma_{Y_{it}(\text{post})}^2) \text{ with} \\
\sigma_{Y_{it}(\text{post})}^2 &= \frac{1}{\frac{1}{\sigma_{c_{it}t}^{2*}} + \frac{\eta_{1i}^2}{2\sigma_{c_{it+1}t+1}^{2*}(1-\eta_{1i}^2)}} \\
\mu_{Y_{it}(\text{post})} &= \sigma_{Y_{it}(\text{post})}^2 \left( \frac{\mu_{c_{it}t}^* + \mathbf{x}_{it}^T \boldsymbol{\beta}_t}{\sigma_{c_{it}t}^{2*}} + \frac{\eta_{1i}(Y_{it+1} - \mu_{c_{it+1}t+1}^* - \mathbf{x}_{it+1}^T \boldsymbol{\beta}_{t+1})}{\sigma_{c_{it+1}t+1}^{2*}(1-\eta_{1i}^2)} \right)
\end{aligned} \tag{A.17}$$

for  $1 < t < T$ :

$$\begin{aligned}
f(Y_{it}|-) &\propto f(Y_{it})f(Y_{it+1}|Y_{it}, -) \\
&= \mathcal{L}_{\mathcal{N}(\mu_{c_{it}t}^* + \eta_{1i}Y_{it-1} + \mathbf{x}_{it}^T \boldsymbol{\beta}_t, \sigma_{c_{it}t}^{2*})}(Y_{it}) \\
&\cdot \mathcal{L}_{\mathcal{N}(\mu_{c_{it+1}t+1}^* + \eta_{1i}Y_{it} + \mathbf{x}_{it+1}^T \boldsymbol{\beta}_{t+1}, \sigma_{c_{it+1}t+1}^{2*}(1-\eta_{1i}^2))}(Y_{it+1}) \\
&\propto \exp \left\{ -\frac{1}{2\sigma_{c_{it}t}^{2*}(1-\eta_{1i}^2)} (Y_{it} - \mu_{c_{it}t}^* - \eta_{1i}Y_{it-1} - \mathbf{x}_{it}^T \boldsymbol{\beta}_t)^2 \right\} \\
&\cdot \exp \left\{ -\frac{1}{2\sigma_{c_{it+1}t+1}^{2*}(1-\eta_{1i}^2)} (Y_{it+1} - \mu_{c_{it+1}t+1}^* - \eta_{1i}Y_{it} - \mathbf{x}_{it+1}^T \boldsymbol{\beta}_{t+1})^2 \right\} \\
&= \exp \left\{ -\frac{1}{2\sigma_{c_{it}t}^{2*}(1-\eta_{1i}^2)} (Y_{it} - (\mu_{c_{it}t}^* + \eta_{1i}Y_{it-1} + \mathbf{x}_{it}^T \boldsymbol{\beta}_t))^2 \right\} \\
&\cdot \exp \left\{ -\frac{\eta_{1i}^2}{2\sigma_{c_{it+1}t+1}^{2*}(1-\eta_{1i}^2)} \left( Y_{it} - \frac{Y_{it+1} - \mu_{c_{it+1}t+1}^* - \mathbf{x}_{it+1}^T \boldsymbol{\beta}_{t+1}}{\eta_{1i}} \right)^2 \right\} \\
\Rightarrow f(Y_{it}|-) &\propto \text{kernel of a } \mathcal{N}(\mu_{Y_{it}(\text{post})}, \sigma_{Y_{it}(\text{post})}^2) \text{ with} \\
\sigma_{Y_{it}(\text{post})}^2 &= \frac{1 - \eta_{1i}^2}{\frac{1}{\sigma_{c_{it}t}^{2*}} + \frac{\eta_{1i}^2}{\sigma_{c_{it+1}t+1}^{2*}}} \\
\mu_{Y_{it}(\text{post})} &= \sigma_{Y_{it}(\text{post})}^2 \left( \frac{\mu_{c_{it}t}^* + \eta_{1i}Y_{it-1} + \mathbf{x}_{it}^T \boldsymbol{\beta}_t}{\sigma_{c_{it}t}^{2*}(1-\eta_{1i}^2)} + \frac{\eta_{1i}(Y_{it+1} - \mu_{c_{it+1}t+1}^* - \mathbf{x}_{it+1}^T \boldsymbol{\beta}_{t+1})}{\sigma_{c_{it+1}t+1}^{2*}(1-\eta_{1i}^2)} \right)
\end{aligned} \tag{A.18}$$

for  $t = T$ :

$$\begin{aligned}
f(Y_{it}|-) &\propto f(Y_{it}) \\
&= \mathcal{L}_{\mathcal{N}(\mu_{c_{it}t}^* + \eta_{1i}Y_{it-1} + \mathbf{x}_{it}^T \boldsymbol{\beta}_t, \sigma_{c_{it}t}^{2*}(1-\eta_{1i}^2))}(Y_{it}) \\
\Rightarrow f(Y_{it}|-) &\text{ is just the likelihood of } Y_{it}
\end{aligned} \tag{A.19}$$



# Appendix B

## Computational details

### B.1 Fitting algorithm code

We report here part of the code of the `MCMC_fit` function which implements the updated DRPM model described in this work. We include it to let the readers appreciate the ease, clarity and even elegance of the Julia language in translating the mathematical formulation into code. Together with what said in Chapter 3, we also note that the productivity offered by the Julia language is not only obtained through the vast land of packages and documentation, but even through an online active forum<sup>1</sup>, where I wrote myself some questions (and received answers) during the development of the thesis.

All this with the hope for Julia to become the new natural choice in the statistical, or in general scientific, computing field, giving to it a refreshing approach.

**Listing 3:** Julia code which implements the fitting model algorithm. We report here just the “functional” part, i.e. not all the setup lines regarding the function definition, variable preallocations, input arguments checks, etc.

```
##### start MCMC algorithm #####
println("Starting MCMC algorithm")

t_start = now()
progresso = Progress(round{Int64}(draws)),
    showspeed=true,
    output=stdout, # not stderr, to make it work nicer on R
    dt=1, # every how many seconds update the feedback
    barlen=0 # no progress bar, just time feedback
)

for i in 1:draws

    ##### sample the missing values #####
    # from the "update rho" section onwards also the Y[j,t] will be needed (to
    ↪ compute weights, update laws, etc)
    # so we need now to simulate the values (from their full conditional) for the
    ↪ data which are missing
    if Y_has_NA
```

---

<sup>1</sup><https://discourse.julialang.org/>

```

# we have to use the missing_idx to remember which units and at which
# times had a missing value,
# in order to simulate just them and instead use the given value for the
# other units and times
for (j,t) in missing_idx
  # What if when filling a NA we occur in another NA value? eg when we
  # also need Y[j,t+1]?
  # I decided here to set that value to 0, if occurs, since anyway target
  # should be centered
  # so it seems a reasonable patch, and I think there was no other
  # solution

  c_it = Si_iter[j,t]
  Xlk_term_t = (lk_xPPM ? dot(view(Xlk_covariates,j,:,t), beta_iter[t]) :
    0)
  aux1 = eta1_iter[j]^2

  if t==1
    c_itp1 = Si_iter[j,t+1]
    Xlk_term_tp1 = (lk_xPPM ? dot(view(Xlk_covariates,j,:,t+1),
    beta_iter[t+1]) : 0)

    sig2_post = 1 / (1/sig2h_iter[c_it,t] +
    aux1/(sig2h_iter[c_itp1,t+1]*(1-aux1)))
    mu_post = sig2_post * (
      (1/sig2h_iter[c_it,t])*(muh_iter[c_it,t] + Xlk_term_t) +
      (eta1_iter[j]/(sig2h_iter[c_itp1,t+1]*(1-aux1))*((ismissing(Y[j,t+1])
      ? 0 : Y[j,t+1]) - muh_iter[c_itp1,t+1] - Xlk_term_tp1)
    )

    Y[j,t] = rand(Normal(mu_post,sqrt(sig2_post)))

  elseif 1<t<T
    c_itp1 = Si_iter[j,t+1]
    Xlk_term_tp1 = (lk_xPPM ? dot(view(Xlk_covariates,j,:,t+1),
    beta_iter[t+1]) : 0)

    sig2_post = (1-aux1) / (1/sig2h_iter[c_it,t] +
    aux1/sig2h_iter[c_itp1,t+1])
    mu_post = sig2_post * (
      (1/(sig2h_iter[c_it,t]*(1-aux1)))*(muh_iter[c_it,t] +
      eta1_iter[j]*(ismissing(Y[j,t-1]) ? 0 : Y[j,t-1]) +
      Xlk_term_t) +
      (eta1_iter[j]/(sig2h_iter[c_itp1,t+1]*(1-aux1))*((ismissing(Y[j,t+1])
      ? 0 : Y[j,t+1]) - muh_iter[c_itp1,t+1] - Xlk_term_tp1)
    )

    Y[j,t] = rand(Normal(mu_post,sqrt(sig2_post)))

  else # t==T
    Y[j,t] = rand(Normal(
      muh_iter[c_it,t] + eta1_iter[j]*(ismissing(Y[j,t-1]) ? 0 :
      Y[j,t-1]) + Xlk_term_t,
      sqrt(sig2h_iter[c_it,t]*(1-aux1))
    ))
  end
end
end

for t in 1:T
  ##### update gamma #####

```

```

for j in 1:n
  if t==1
    gamma_iter[j,t] = 0
    # at the first time units get reallocated
  else
    # we want to find  $\rho_{t-\{R_t(-j)\}}$  ...
    indexes = findall_faster(jj -> jj != j && gamma_iter[jj, t] == 1,
      ↪ 1:n)
    Si_red = Si_iter[indexes, t]
    copy!(Si_red1, Si_red)
    push!(Si_red1, Si_iter[j,t]) # ... and  $\rho_{t-\{R_t(+j)\}}$ 

    # get also the reduced spatial info if sPPM model
    if sPPM
      sp1_red = @view sp1[indexes]
      sp2_red = @view sp2[indexes]
    end
    # and the reduced covariates info if cl_xPPM model
    if cl_xPPM
      Xcl_covariates_red = @view Xcl_covariates[indexes,:,t]
    end

    # compute n_red's and nclus_red's and relabel
    n_red = length(Si_red) # = "n" relative to here, i.e. the
    ↪ sub-partition size
    n_red1 = length(Si_red1)
    relabel!(Si_red, n_red)
    relabel!(Si_red1, n_red1)
    nclus_red = isempty(Si_red) ? 0 : maximum(Si_red) # = number of
    ↪ clusters
    nclus_red1 = maximum(Si_red1)

    # save the label of the current working-on unit j
    j_label = Si_red1[end]

    # compute also nh_red's
    nh_red .= 0
    nh_red1 .= 0
    for jj in 1:n_red
      nh_red[Si_red[jj]] += 1 # = numerosities for each cluster label
      nh_red1[Si_red1[jj]] += 1
    end
    nh_red1[Si_red1[end]] += 1 # account for the last added unit j, not
    ↪ included in the above loop

    # start computing weights
    lg_weights .= 0

    # unit j can enter an existing cluster...
    for k in 1:nclus_red
      aux_idx = findall(Si_red == k) # fast
      lC .= 0.
      if sPPM
        # filter the spatial coordinates of the units of label k
        copy!(s1o, sp1_red[aux_idx])
        copy!(s2o, sp2_red[aux_idx])
        copy!(s1n, s1o); push!(s1n, sp1[j])
        copy!(s2n, s2o); push!(s2n, sp2[j])
        spatial_cohesion!(spatial_cohesion_idx, s1o, s2o,
          ↪ sp_params_struct, true, M_dp, S, 1, false, lC)
        spatial_cohesion!(spatial_cohesion_idx, s1n, s2n,
          ↪ sp_params_struct, true, M_dp, S, 2, false, lC)
      end
    end
  end
end

```

```

end
lS .= 0.
if cl_xPPM
    # and the covariates of the units of label k
    for p in 1:p_cl
        copy!(Xo, @view Xcl_covariates_red[aux_idx, p])
        copy!(Xn, Xo); push!(Xn, Xcl_covariates[j, p, t])
        covariate_similarity!(covariate_similarity_idx, Xo,
            ↪ cv_params, true, 1, true, lS)
        covariate_similarity!(covariate_similarity_idx, Xn,
            ↪ cv_params, true, 2, true, lS)
    end
end
lg_weights[k] = log(nh_red[k]) + lC[2] - lC[1] + lS[2] - lS[1]
end
# ... or unit j can create a singleton
lC .= 0.
if sPPM
    spatial_cohesion!(spatial_cohesion_idx, SVector(sp1[j]),
        ↪ SVector(sp2[j]), sp_params_struct, true, M_dp, S, 2, false,
        ↪ lC)
end
lS .= 0.
if cl_xPPM
    for p in 1:p_cl
        covariate_similarity!(covariate_similarity_idx,
            ↪ SVector(Xcl_covariates[j, p, t]), cv_params, true, 2, true,
            ↪ lS)
    end
end
lg_weights[nclus_red+1] = log_Mdp + lC[2] + lS[2]

# now use the weights towards sampling the new gamma_jt
max_ph = maximum(@view lg_weights[1:(nclus_red+1)])
sum_ph = 0.0
# exponentiate...
for k in 1:(nclus_red+1)
    # for numerical purposes we subtract max_ph
    lg_weights[k] = exp(lg_weights[k] - max_ph)
    sum_ph += lg_weights[k]
end
# ... and normalize
lg_weights ./= sum_ph

# compute probh
probh = 0.0
if time_specific_alpha==false && unit_specific_alpha==false
    probh = alpha_iter / (alpha_iter + (1 - alpha_iter) *
        ↪ lg_weights[j_label])
elseif time_specific_alpha==true && unit_specific_alpha==false
    probh = alpha_iter[t] / (alpha_iter[t] + (1 - alpha_iter[t]) *
        ↪ lg_weights[j_label])
elseif time_specific_alpha==false && unit_specific_alpha==true
    probh = alpha_iter[j] / (alpha_iter[j] + (1 - alpha_iter[j]) *
        ↪ lg_weights[j_label])
elseif time_specific_alpha==true && unit_specific_alpha==true
    probh = alpha_iter[j, t] / (alpha_iter[j, t] + (1 -
        ↪ alpha_iter[j, t]) * lg_weights[j_label])
end

# compatibility check for gamma transition
if gamma_iter[j, t] == 0

```

```

    # we want to find  $\rho_{t-1} \sim \{R_t(+j)\}$  ...
    indexes = findall_faster(jj -> jj==j gamma_iter[jj, t]==1, 1:n)
    Si_comp1 = @view Si_iter[indexes, t-1]
    Si_comp2 = @view Si_iter[indexes, t] # ... and  $\rho_t \sim R_t(+j)$ 

    rho_comp = compatibility(Si_comp1, Si_comp2)
    if rho_comp == 0
        probh = 0.0
    end
end
# sample the new gamma
gt = rand(Bernoulli(probh))
gamma_iter[j, t] = gt
end
end # for j in 1:n

##### update rho #####
# we only update the partition for the units which can move (i.e. with
↪ gamma_jt=0)
movable_units = findall(gamma_iter[:,t] .== 0)

for j in movable_units
    # remove unit j from the cluster she is currently in

    if nh[Si_iter[j,t],t] > 1 # unit j does not belong to a singleton
        ↪ cluster
        nh[Si_iter[j,t],t] -= 1
        # no nclus_iter[t] change since j's cluster is still alive
    else # unit j belongs to a singleton cluster
        j_label = Si_iter[j,t]
        last_label = nclus_iter[t]

        if j_label < last_label
            # here we enter if j_label is not the last label, so we need to
            # relabel clusters in order to then remove j's cluster
            # eg: units 1 2 3 4 5 j 7 -> units 1 2 3 4 5 j 7
            #          label 1 1 2 2 2 3 4      label 1 1 2 2 2 4 3

            # swap cluster labels...
            for jj in 1:n
                if Si_iter[jj, t] == last_label
                    Si_iter[jj, t] = j_label
                end
            end
            Si_iter[j, t] = last_label
            # ... and cluster-specific parameters
            sig2h_iter[j_label, t], sig2h_iter[last_label, t] =
                ↪ sig2h_iter[last_label, t], sig2h_iter[j_label, t]
            muh_iter[j_label, t], muh_iter[last_label, t] =
                ↪ muh_iter[last_label, t], muh_iter[j_label, t]
            nh[j_label, t] = nh[last_label, t]
            nh[last_label, t] = 1

        end
        # remove the j-th observation and the last cluster (being j in a
        ↪ singleton)
        nh[last_label, t] -= 1
        nclus_iter[t] -= 1
    end

    # setup probability weights towards the sampling of rho_jt

```

```

ph .= 0.0
resize!(ph, nclus_iter[t]+1)
copy!(rho_tmp, @view Si_iter[:,t])

# compute nh_tmp (numerocities for each cluster label)
copy!(nh_tmp, @view nh[:,t])
# unit j contribute is already absent from the change we did above
nclus_temp = 0

# we now simulate the unit j to be assigned to one of the existing
↳ clusters...
for k in 1:nclus_iter[t]
    rho_tmp[j] = k
    indexes = findall(gamma_iter[:,t+1] .== 1)
    # we check the compatibility between rho_t^{h=k, R_(t+1)} ...
    Si_comp1 = @view rho_tmp[indexes]
    Si_comp2 = @view Si_iter[indexes,t+1] # and rho_(t+1)^{R_(t+1)}
    rho_comp = compatibility(Si_comp1, Si_comp2)

    if rho_comp != 1
        ph[k] = log(0) # assignment to cluster k is not compatible
    else
        # update params for "rho_jt = k" simulation
        nh_tmp[k] += 1
        nclus_temp = count(a->(a>0), nh_tmp)

    lPP .= 0.
    for kk in 1:nclus_temp
        aux_idx = findall(rho_tmp .== kk)
        if sPPM
            copy!(s1n, @view sp1[aux_idx])
            copy!(s2n, @view sp2[aux_idx])
            spatial_cohesion!(spatial_cohesion_idx, s1n, s2n,
                ↳ sp_params_struct, true, M_dp, S, 1, true, lPP)
        end
        if cl_xPPM
            for p in 1:p_cl
                Xn_view = @view Xcl_covariates[aux_idx,p,t]
                covariate_similarity!(covariate_similarity_idx, Xn_view,
                    ↳ cv_params, true, 1, true, lPP)
            end
        end
        lPP[1] += log_Mdp + lgamma(nh_tmp[kk])
    end

    if t==1
        ph[k] = loglikelihood(Normal(
            muh_iter[k,t] + (lk_xPPM ? dot(view(Xlk_covariates,j,:,t),
                ↳ beta_iter[t]) : 0),
            sqrt(sig2h_iter[k,t])),
            Y[j,t]) + lPP[1]
    else
        ph[k] = loglikelihood(Normal(
            muh_iter[k,t] + eta1_iter[j]*Y[j,t-1] + (lk_xPPM ?
                ↳ dot(view(Xlk_covariates,j,:,t), beta_iter[t]) : 0),
            sqrt(sig2h_iter[k,t]*(1-eta1_iter[j]^2))),
            Y[j,t]) + lPP[1]
    end

    # restore params after "rho_jt = k" simulation
    nh_tmp[k] -= 1
end

```



```

end
# ... plus the case of being assigned to a new (singleton for now)
↪ cluster
k = nclus_iter[t]+1
rho_tmp[j] = k
# declare (for later scope accessibility) the new params here
muh_draw = 0.0; sig2h_draw = 0.0

indexes = findall(gamma_iter[:,t+1] .== 1)
Si_comp1 = @view rho_tmp[indexes]
Si_comp2 = @view Si_iter[indexes,t+1]
rho_comp = compatibility(Si_comp1, Si_comp2)

if rho_comp != 1
    ph[k] = log(0) # assignment to a new cluster is not compatible
else
    # sample new params for this new cluster
    muh_draw = rand(Normal(theta_iter[t], sqrt(tau2_iter[t])))
    sig2h_draw = rand(InverseGamma(sig2h_priors[1], sig2h_priors[2]))

    # update params for "rho_jt = k" simulation
    nh_tmp[k] += 1
    nclus_temp = count(a->(a>0), nh_tmp)

    lPP .= 0.
    for kk in 1:nclus_temp
        aux_idx = findall(rho_tmp .== kk)
        if sPPM
            copy!(s1n, @view sp1[aux_idx])
            copy!(s2n, @view sp2[aux_idx])
            spatial_cohesion!(spatial_cohesion_idx, s1n, s2n,
                ↪ sp_params_struct, true, M_dp, S, 1, true, lPP)
        end
        if cl_xPPM
            for p in 1:p_cl
                Xn_view = @view Xcl_covariates[aux_idx,p,t]
                covariate_similarity!(covariate_similarity_idx, Xn_view,
                    ↪ cv_params, true, 1, true, lPP)
            end
        end
        lPP[1] += log_Mdp + lgamma(nh_tmp[kk])
    end

    if t==1
        ph[k] = loglikelihood(Normal(
            muh_draw + (lk_xPPM ? dot(view(Xlk_covariates,j,:),t),
                ↪ beta_iter[t]) : 0),
            sqrt(sig2h_draw)),
            Y[j,t]) + lPP[1]
    else
        ph[k] = loglikelihood(Normal(
            muh_draw + eta1_iter[j]*Y[j,t-1] + (lk_xPPM ?
                ↪ dot(view(Xlk_covariates,j,:),t), beta_iter[t]) : 0),
            sqrt(sig2h_draw*(1-eta1_iter[j]^2))),
            Y[j,t]) + lPP[1]
    end

    # restore params after "rho_jt = k" simulation
    nh_tmp[k] -= 1
end

# now exponentiate the weights...

```

```

max_ph = maximum(ph)
sum_ph = 0.0
for k in eachindex(ph)
    # for numerical purposes we subtract max_ph
    ph[k] = exp(ph[k] - max_ph)
    sum_ph += ph[k]
end
# ... and normalize them
ph ./= sum_ph

# now sample the new label Si_iter[j,t]
u = rand(Uniform(0,1))
cph = cumsum(ph)
cph[end] = 1 # fix numerical problems of having sums like 0.999999etc
new_label = 0
for k in eachindex(ph)
    if u <= cph[k]
        new_label = k
        break
    end
end

if new_label <= nclus_iter[t]
    # we enter an existing cluster
    Si_iter[j, t] = new_label
    nh[new_label, t] += 1
else
    # we create a new singleton cluster
    nclus_iter[t] += 1
    cl_new = nclus_iter[t]
    Si_iter[j, t] = cl_new
    nh[cl_new, t] = 1
    muh_iter[cl_new, t] = muh_draw
    sig2h_iter[cl_new, t] = sig2h_draw
end

# now we need to relabel after the possible mess created by the
#   ↪ sampling
# eg: (before sampling)    (after sampling)
#   units j 2 3 4 5 ->   units j 2 3 4 5
#   labels 1 1 1 2 2     labels 3 1 1 2 2
# the after case has to be relabelled
Si_tmp = @view Si_iter[:,t]

relabel_full!(Si_tmp, n, Si_relab, nh_reorder, old_lab)
# - Si_relab gives the relabelled partition
# - nh_reorder gives the numerosities of the relabelled partition, ie
#   ↪ "nh_reorder[k] = #(units of new cluster k)"
# - old_lab tells "the index in position i (which before was cluster i)"
#   ↪ "is now called cluster old_lab[i]"
# eg:
#           Original labels (Si): 4 2 1 1 1 3 1 4 5
#           Relabeled groups (Si_relab): 1 2 3 3 3 4 3 1 5
#           Reordered cluster sizes (nh_reorder): 2 1 4 1 1 0 0 0 0
#           Old labels (old_lab): 4 2 1 3 5 0 0 0 0

# now fix everything (morally permute params)
Si_iter[:,t] = Si_relab
copy!(muh_iter_copy, muh_iter)
copy!(sig2h_iter_copy, sig2h_iter)
len = findlast(x -> x != 0, nh_reorder)
for k in 1:nclus_iter[t]
    muh_iter[k,t] = muh_iter_copy[old_lab[k],t]

```

```

        sig2h_iter[k,t] = sig2h_iter_copy[old_lab[k],t]
        nh[k,t] = nh_reorder[k]
    end

end # for j in movable_units

##### update muh #####
if t==1
    for k in 1:nclus_iter[t]
        sum_Y = 0.0
        for j in 1:n
            if Si_iter[j,t]==k
                sum_Y += Y[j,t] - (lk_xPPM ? dot(view(Xlk_covariates,j,:,t),
                    ↪ beta_iter[t]) : 0.0)
            end
        end
        sig2_star = 1 / (1/tau2_iter[t] + nh[k,t]/sig2h_iter[k,t])
        mu_star = sig2_star * (theta_iter[t]/tau2_iter[t] +
            ↪ sum_Y/sig2h_iter[k,t])

        muh_iter[k,t] = rand(Normal(mu_star,sqrt(sig2_star)))
    end
else # t>1
    for k in 1:nclus_iter[t]
        sum_Y = 0.0
        sum_e2 = 0.0
        for j in 1:n
            if Si_iter[j,t]==k
                aux1 = 1 / (1-eta1_iter[j]^2)
                sum_e2 += aux1
                sum_Y += (Y[j,t] - eta1_iter[j]*Y[j,t-1] - (lk_xPPM ?
                    ↪ dot(view(Xlk_covariates,j,:,t), beta_iter[t]) : 0.0)) *
                    ↪ aux1
            end
        end
        sig2_star = 1 / (1/tau2_iter[t] + sum_e2/sig2h_iter[k,t])
        mu_star = sig2_star * (theta_iter[t]/tau2_iter[t] +
            ↪ sum_Y/sig2h_iter[k,t])

        muh_iter[k,t] = rand(Normal(mu_star,sqrt(sig2_star)))
    end
end

##### update sigma2h #####
if t==1
    for k in 1:nclus_iter[t]
        a_star = sig2h_priors[1] + nh[k,t]/2
        sum_Y = 0.0
        S_kt = findall(Si_iter[:,t] .== k)
        for j in S_kt
            sum_Y += (Y[j,t] - muh_iter[k,t] - (lk_xPPM ?
                ↪ dot(view(Xlk_covariates,j,:,t), beta_iter[t]) : 0.0))^2
        end

        b_star = sig2h_priors[2] + sum_Y/2
        sig2h_iter[k,t] = rand(InverseGamma(a_star, b_star))
    end
else # t>1

```

```

for k in 1:nclus_iter[t]
    a_star = sig2h_priors[1] + nh[k,t]/2
    sum_Y = 0.0
    S_kt = findall(Si_iter[:,t] .== k)
    for j in S_kt
        sum_Y += (Y[j,t] - muh_iter[k,t] - eta1_iter[j]*Y[j,t-1] -
        ↪ (lk_xPPM ? dot(view(Xlk_covariates,j,:,t), beta_iter[t]) :
        ↪ 0.0))^2
    end

    b_star = sig2h_priors[2] + sum_Y/2
    sig2h_iter[k,t] = rand(InverseGamma(a_star, b_star))
end
end

##### update beta #####
# if lk_xPPM && i>=beta_update_threshold # conditional update version
if lk_xPPM
    if t==1
        sum_Y = zeros(p_lk)
        A_star = I(p_lk)/s2_beta
        for j in 1:n
            X_jt = @view Xlk_covariates[j,:,t]
            sum_Y += (Y[j,t] - muh_iter[Si_iter[j,t],t]) * X_jt /
            ↪ sig2h_iter[Si_iter[j,t],t]
            A_star += (X_jt * X_jt') / sig2h_iter[Si_iter[j,t],t]
        end
        b_star = beta0/s2_beta + sum_Y
        A_star = Symmetric(A_star)
        # Symmetric is needed for numerical problems
        # but A_star is indeed symm and pos def (by construction) so there
        ↪ is no problem
        beta_iter[t] = rand(MvNormalCanon(b_star, A_star))
        # quicker and more accurate method
        # old method with the MvNormal and the inversion required was
        # beta_iter[t] = rand(MvNormal(inv(Symmetric(A_star))*b_star,
        ↪ inv(Symmetric(A_star))))
    else
        sum_Y = zeros(p_lk)
        A_star = I(p_lk)/s2_beta
        for j in 1:n
            X_jt = @view Xlk_covariates[j,:,t]
            sum_Y += (Y[j,t] - muh_iter[Si_iter[j,t],t] -
            ↪ eta1_iter[j]*Y[j,t-1]) * X_jt / sig2h_iter[Si_iter[j,t],t]
            A_star += (X_jt * X_jt') / sig2h_iter[Si_iter[j,t],t]
        end
        b_star = beta0/s2_beta + sum_Y
        A_star = Symmetric(A_star)
        beta_iter[t] = rand(MvNormalCanon(b_star, A_star))
    end
end

##### update theta #####
aux1 = 1 / (lambda2_iter*(1-phi1_iter^2))
kt = nclus_iter[t]
sum_mu = 0.0
for k in 1:kt
    sum_mu += muh_iter[k,t]
end

```

```

if t==1
  sig2_post = 1 / (1/lambda2_iter + phi1_iter^2*aux1 + kt/tau2_iter[t])
  mu_post = sig2_post * (phi0_iter/lambda2_iter + sum_mu/tau2_iter[t] +
    ↪ (phi1_iter*(theta_iter[t+1] - (1-phi1_iter)*phi0_iter))*aux1)

  theta_iter[t] = rand(Normal(mu_post, sqrt(sig2_post)))

elseif t==T
  sig2_post = 1 / (aux1 + kt/tau2_iter[t])
  mu_post = sig2_post * (sum_mu/tau2_iter[t] + ((1- phi1_iter)*phi0_iter
    ↪ + phi1_iter*theta_iter[t-1])*aux1)

  theta_iter[t] = rand(Normal(mu_post, sqrt(sig2_post)))

else # 1<t<T
  sig2_post = 1 / ((1+phi1_iter^2)*aux1 + kt/tau2_iter[t])
  mu_post = sig2_post * (sum_mu/tau2_iter[t] +
    ↪ (phi1_iter*(theta_iter[t-1]+theta_iter[t+1]) +
    ↪ phi0_iter*(1-phi1_iter)^2)*aux1)

  theta_iter[t] = rand(Normal(mu_post, sqrt(sig2_post)))
end

##### update tau2 #####
kt = nclus_iter[t]
aux1 = 0.0
for k in 1:kt
  aux1 += (muh_iter[k,t] - theta_iter[t])^2
end
a_star = tau2_priors[1] + kt/2
b_star = tau2_priors[2] + aux1/2
tau2_iter[t] = rand(InverseGamma(a_star, b_star))

end # for t in 1:T

##### update eta1 #####
# the input argument eta1_priors[2] is already the std dev
if update_eta1
  for j in 1:n
    eta1_old = eta1_iter[j]
    eta1_new = rand(Normal(eta1_old, eta1_priors[2])) # proposal value

    if (-1 <= eta1_new <= 1)
      ll_old = 0.0
      ll_new = 0.0
      for t in 2:T
        # likelihood contribution
        ll_old += loglikelihood(Normal(
          muh_iter[Si_iter[j,t],t] + eta1_old*Y[j,t-1] + (lk_xPPM ?
            ↪ dot(view(Xlk_covariates,j,:,t), beta_iter[t]) : 0),
          sqrt(sig2h_iter[Si_iter[j,t],t]*(1-eta1_old^2))
        ), Y[j,t])
        ll_new += loglikelihood(Normal(
          muh_iter[Si_iter[j,t],t] + eta1_new*Y[j,t-1] + (lk_xPPM ?
            ↪ dot(view(Xlk_covariates,j,:,t), beta_iter[t]) : 0),
          sqrt(sig2h_iter[Si_iter[j,t],t]*(1-eta1_new^2))
        ), Y[j,t])
      end
      logit_old = aux_logit(eta1_old)
      logit_new = aux_logit(eta1_new)
    end
  end
end

```

```

    # prior contribution
    ll_old += -log(2*eta1_priors[1]) -1/eta1_priors[1]*abs(logit_old)
    ll_new += -log(2*eta1_priors[1]) -1/eta1_priors[1]*abs(logit_new)

    ll_ratio = ll_new-ll_old
    u = rand(Uniform(0,1))
    if (ll_ratio > log(u))
        eta1_iter[j] = eta1_new # accept the candidate
        acceptance_ratio_eta1 += 1
    end
end
end
end

##### update alpha #####
if update_alpha
    if time_specific_alpha==false && unit_specific_alpha==false
        # a scalar
        sumg = sum(@view gamma_iter[:,1:T])
        a_star = alpha_priors[1] + sumg
        b_star = alpha_priors[2] + n*T - sumg
        alpha_iter = rand(Beta(a_star, b_star))

    elseif time_specific_alpha==true && unit_specific_alpha==false
        # a vector in time
        for t in 1:T
            sumg = sum(@view gamma_iter[:,t])
            a_star = alpha_priors[1] + sumg
            b_star = alpha_priors[2] + n - sumg
            alpha_iter[t] = rand(Beta(a_star, b_star))
        end

    elseif time_specific_alpha==false && unit_specific_alpha==true
        # a vector in units
        for j in 1:n
            sumg = sum(@view gamma_iter[j,1:T])
            a_star = alpha_priors[1,j] + sumg
            b_star = alpha_priors[2,j] + T - sumg
            alpha_iter[j] = rand(Beta(a_star, b_star))
        end

    elseif time_specific_alpha==true && unit_specific_alpha==true
        # a matrix
        for j in 1:n
            for t in 1:T
                sumg = gamma_iter[j,t] # nothing to sum in this case
                a_star = alpha_priors[1,j] + sumg
                b_star = alpha_priors[2,j] + 1 - sumg
                alpha_iter[j,t] = rand(Beta(a_star, b_star))
            end
        end
    end
end
end

##### update phi0 #####
aux1 = 1/lambda2_iter
aux2 = 0.0
for t in 2:T
    aux2 += theta_iter[t] - phi1_iter*theta_iter[t-1]
end

```

```

sig2_post = 1 / ( 1/phi0_priors[2] + aux1 * (1 +
  ↪ (T-1)*(1-phi1_iter)/(1+phi1_iter)) )
mu_post = sig2_post * ( phi0_priors[1]/phi0_priors[2] + theta_iter[1]*aux1 +
  ↪ aux1/(1+phi1_iter)*aux2 )
phi0_iter = rand(Normal(mu_post, sqrt(sig2_post)))

##### update phi1 #####
# the input argument phi_priors is already the std dev
if update_phi1
  phi1_old = phi1_iter
  phi1_new = rand(Normal(phi1_old, phi1_priors)) # proposal value

  if (-1 <= phi1_new <= 1)
    ll_old = 0.0; ll_new = 0.0
    for t in 2:T
      # likelihood contribution
      ll_old += loglikelihood(Normal(
        (1-phi1_old)*phi0_iter + phi1_old*theta_iter[t-1],
        sqrt(lambda2_iter*(1-phi1_old^2))
      ), theta_iter[t])
      ll_new += loglikelihood(Normal(
        (1-phi1_new)*phi0_iter + phi1_new*theta_iter[t-1],
        sqrt(lambda2_iter*(1-phi1_new^2))
      ), theta_iter[t])
    end

    # prior contribution
    ll_old += loglikelihood(Uniform(-1,1), phi1_old)
    ll_new += loglikelihood(Uniform(-1,1), phi1_new)

    ll_ratio = ll_new-ll_old
    u = rand(Uniform(0,1))
    if (ll_ratio > log(u))
      phi1_iter = phi1_new # accept the candidate
      acceptance_ratio_phi1 += 1
    end
  end
end

##### update lambda2 #####
aux1 = 0.0
for t in 2:T
  aux1 += (theta_iter[t] - (1-phi1_iter)*phi0_iter -
  ↪ phi1_iter*theta_iter[t-1])^2
end
a_star = lambda2_priors[1] + T/2
b_star = lambda2_priors[2] + ((theta_iter[1] - phi0_iter)^2 + aux1) / 2
lambda2_iter = rand(InverseGamma(a_star,b_star))

##### save MCMC iterates #####
if i>burnin && i%thin==0
  Si_out[:,i_out] = Si_iter[:,1:T]
  gamma_out[:,i_out] = gamma_iter[:,1:T]
  if time_specific_alpha==false && unit_specific_alpha==false
    # for each iterate, a scalar
    alpha_out[i_out] = alpha_iter
  elseif time_specific_alpha==true && unit_specific_alpha==false
    # for each iterate, a vector in time
    alpha_out[:,i_out] = alpha_iter[1:T]
  end
end

```

```

elseif time_specific_alpha==false && unit_specific_alpha==true
  # for each iterate, a vector in units
  alpha_out[:,i_out] = alpha_iter
elseif time_specific_alpha==true && unit_specific_alpha==true
  # for each iterate, a matrix
  alpha_out[:,i_out] = alpha_iter[:,1:T]
end
for t in 1:T
  for j in 1:n
    sigma2h_out[j,t,i_out] = sig2h_iter[Si_iter[j,t],t]
    muh_out[j,t,i_out] = muh_iter[Si_iter[j,t],t]
  end
end
eta1_out[:,i_out] = eta1_iter
if lk_xPPM
  for t in 1:T
    beta_out[t,:,i_out] = beta_iter[t]
  end
end
theta_out[:,i_out] = theta_iter[1:T]
tau2_out[:,i_out] = tau2_iter[1:T]
phi0_out[i_out] = phi0_iter
phi1_out[i_out] = phi1_iter
lambda2_out[i_out] = lambda2_iter

##### save fitted values and metrics #####
for j in 1:n
  for t in 1:T
    muh_jt = muh_iter[Si_iter[j,t],t]
    sig2h_jt = sig2h_iter[Si_iter[j,t],t]
    X_lk_term = lk_xPPM ? dot(view(Xlk_covariates,j,:,t), beta_iter[t])
    ↪ : 0.0

    if t==1
      llike[j,t,i_out] = logpdf(Normal(
        muh_jt + X_lk_term,
        sqrt(sig2h_jt)
      ), Y[j,t])
      fitted[j,t,i_out] = muh_jt + X_lk_term
    else # t>1
      llike[j,t,i_out] = logpdf(Normal(
        muh_jt + eta1_iter[j]*Y[j,t-1] + X_lk_term,
        sqrt(sig2h_jt*(1-eta1_iter[j]^2))
      ), Y[j,t])
      fitted[j,t,i_out] = muh_jt + eta1_iter[j]*Y[j,t-1] + X_lk_term
    end

    mean_likelhd[j,t] += exp(llike[j,t,i_out])
    mean_loglikelhd[j,t] += llike[j,t,i_out]
    CPO[j,t] += exp(-llike[j,t,i_out])
  end
end

i_out += 1
end

next!(progresso)

end # for i in 1:draws

println("\ndone!")

```



```

t_end = now()
println("Elapsed time: ",
  ↪ Dates.canonicalize(Dates.CompoundPeriod(t_end-t_start)))

##### compute LPML and WAIC #####
for j in 1:n
  for t in 1:T
    LPML += log(CPO[j,t])
  end
end
LPML -= n*T*log(nout) # scaling factor
LPML = -LPML # fix sign
println("LPML: ", LPML, " (the higher the better)")

# adjust mean variables
mean_likelhd ./= nout
mean_loglikelhd ./= nout
for j in 1:n
  for t in 1:T
    WAIC += 2*mean_loglikelhd[j,t] - log(mean_likelhd[j,t])
  end
end
WAIC *= -2
println("WAIC: ", WAIC, " (the lower the better)")

if update_eta1 @printf "acceptance ratio eta1: %.2f%%\n"
  ↪ acceptance_ratio_eta1/(n*draws)*100 end
if update_phi1 @printf "acceptance ratio phi1: %.2f%%"
  ↪ acceptance_ratio_phi1/draws*100 end
println()

if perform_diagnostics
  chn = Chains(
    hcat(lambda2_out,phi0_out,tau2_out',theta_out',eta1_out',alpha_out'),
    ["lambda2","phi0",
     [string("tau2_t", i) for i in 1:T]...,
     [string("theta_t", i) for i in 1:T]...,
     [string("eta1_j", i) for i in 1:n]...,
     [string("alpha_t", i) for i in 1:T]...,
    ]
  )
  ss = DataFrame(summarystats(chn))
  println("\nDiagnostics:")
  @show ss[!, [1,4,5,6,7]];
  if logging CSV.write(log_file,ss[!, [1,4,5,6,7]]) end
end

close(log_file)

if simple_return
  return Si_out, LPML, WAIC
else
  return Si_out, Int.(gamma_out), alpha_out, sigma2h_out, muh_out, include_eta1
  ↪ ? eta1_out : NaN, lk_xPPM ? beta_out : NaN, theta_out, tau2_out,
  ↪ phi0_out, include_phi1 ? phi1_out : NaN, lambda2_out, fitted, llike,
  ↪ LPML, WAIC
end

```

## B.2 Interface

Now some more technical details about the whole implementation design. The fitting code was written in Julia, but its main intended use is from R. This choice was made because R is currently the best language for statistical purposes, or at least the most spread; in fact all other models “competitors” to the DRPM are available through some R package. Therefore we thought that letting our work be also accessible from R, and not only from Julia, would have eased the possibilities of testing and comparisons with other models or datasets.

To do so, we relied on the `JuliaConnector` library [LHB22] on R, which allows the interaction between the two languages. In this sense, we can load in R the Julia package `JDRPM`, which stores the Julia project (i.e. all codes and packages dependencies) about the improved version of the DRPM model, and call it using data and arguments from R. The output produced by the Julia functions has then to be converted back into R structures, which is done automatically through a dedicated function of the package. The structure of this workflow is summarized in Listing 4.

**Listing 4:** Instructions on how to use the `JDRPM` model from R.

```
##### Requirements #####
# install the required package
install.packages("JuliaConnector")

##### Setup #####
# load the package
library(JuliaConnector)
# check it returns TRUE
juliaSetupOk()

# load the Package manager on Julia
juliaEval("using Pkg")
# enter into the JDRPM project
juliaEval("Pkg.activate("<path/to/where/you/stored/JDRPM>\\")")

# downloads and install, only once, all the dependencies
juliaEval("Pkg.instantiate()")
# now, as a check, this should print the list of packages that JDRPM uses,
# such as Distributions, Statistics, LinearAlgebra, SpecialFunctions, etc.
juliaEval("Pkg.status()")

# locate the "main" file
module = normalizePath("<path/to/where/you/stored/JDRPM>/src/JDRPM.jl")
# load the "main" file into a callable R object
module_JDRPM = juliaImport(juliaCall("include", module))

# trigger the compilation of the function, otherwise all first runs
# will be slow since the function still would have to be compiled
module_JDRPM$trigger_compilation()

##### Fit #####
# perform the fit
out = module_JDRPM$MCMC_fit(...)
```

```

# convert the output to R structures
rout = juliaGet(out)
names(rout) = c("Si", "gamma", "alpha", "sigma2h", "muh", "eta1", "beta", "theta",
  ↪ "tau2", "phi0", "phi1", "lambda2", "fitted", "llike", "lpml", "waic")

# and reshape it to uniform to the DRPM output form
rout$Si = aperm(rout$Si, c(2, 1, 3))
rout$gamma = aperm(rout$gamma, c(2, 1, 3))
rout$sigma2h = aperm(rout$sigma2h, c(2, 1, 3))
rout$muh = aperm(rout$muh, c(2, 1, 3))
rout$fitted = aperm(rout$fitted, c(2, 1, 3))
rout$llike = aperm(rout$llike, c(2, 1, 3))
rout$alpha = aperm(rout$alpha, c(2, 1))
rout$theta = aperm(rout$theta, c(2, 1))
rout$tau2 = aperm(rout$tau2, c(2, 1))
rout$eta1 = aperm(rout$eta1, c(2, 1))
rout$phi0 = matrix(rout$phi0, ncol = 1)
rout$phi1 = matrix(rout$phi1, ncol = 1)
rout$lambda2 = matrix(rout$lambda2, ncol = 1)
# this reshape works in the case of full model fit, but in the case of special
# fitting options (e.g. unit_specific_alpha=true) it needs to be adjusted

```

The `trigger_compilation` function runs the fitting function on a small test case to simply give Julia a friendly nudge to compile the function, making all the subsequent and more serious fits faster. In fact, especially for more complex projects, there are packages such as `PrecompileTools` and `PackageCompiler` which helps to solve this “time to first execution” problem of Julia.

Regarding instead the visual interface, in the sense of the feedback provided by the function, we decided to make it more user-friendly and possibly informative than the original C implementation. The most relevant add-ons are the possibility to perform diagnostics on a subset of the sampled parameters, and the real-time progress monitoring, which updates itself every second to show the estimated remaining time to complete the fit. As a further proof of the ease of this language, these features were just a simple insertion of few lines of code, thanks to the Julia packages `MCMCChains` and `ProgressMeter`.

**Listing 5:** Feedback from the JDRPM implementation.

```

# if verbose=true this initial parameter section is also printed
Parameters:
sig2h ~ invGamma(0.01, 0.01)
Logit(1/2(eta1+1)) ~ Laplace(0, 0.9)
tau2 ~ invGamma(1.9, 0.4)
phi0 ~ Normal(μ=0.0, σ=10.0)
lambda2 ~ invGamma(1.9, 0.4)
alpha ~ Beta(2.0, 2.0)

- using seed 113.0 -
fitting 100000 total iterates (with burnin=80000, thinning=5)
thus producing 4000 valid iterates in the end

on n=105 subjects
for T=12 time instants

```

```
[✓] with space? true (cohesion 3.0)
[X] with covariates in the likelihood? false
[X] with covariates in the clustering process? false
[X] are there missing data in Y? false
```

2024-10-14 09:33:11

Starting MCMC algorithm

Progress: 100% Time: 0:25:39 (15.40 ms/it)

done!

Elapsed time: 25 minutes, 39 seconds, 569 milliseconds

LPML: 517.182456879369 (the higher the better)

WAIC: -1283.8930457498177 (the lower the better)

acceptance ratio etal: 74.66%

# if perform\_diagnostics=true this final diagnostics section is also printed

Diagnostics:

ss[!, [1, 4, 5, 6, 7]] = 143×5 DataFrame

Row	parameters	mcse	ess_bulk	ess_tail	rhat
	Symbol	Float64	Float64	Float64	Float64
1	lambda2	0.000817173	4243.04	3970.25	0.999769
2	phi0	0.00218706	3533.95	3675.99	1.00018
3	tau2_t1	0.00540064	3716.56	3645.99	0.999968
	⋮				
14	tau2_t12	0.00259168	3965.77	3655.55	0.999951
15	theta_t1	0.00404988	3603.34	3765.78	0.999834
	⋮				
26	theta_t12	0.00337843	3588.83	3907.13	0.999866
27	etal_j1	0.0112187	451.588	1107.96	1.00163
	⋮				
131	etal_j105	0.00328424	1539.36	2194.83	1.00002
132	alpha_t1	0.000213087	3774.24	3920.48	1.00044
	⋮				
143	alpha_t12	0.00266005	541.427	1867.54	1.0084

# Appendix C

## Further plots



# Bibliography

- [Bar+12] Luis E Nieto Barajas et al. “A Time-Series DDP for Functional Proteomics Profiles”. In: *Biometrics* 68.3 (Jan. 2012), pp. 859–868. DOI: 10.1111/j.1541-0420.2011.01724.x. URL: <https://doi.org/10.1111/j.1541-0420.2011.01724.x> (cit. on p. 3).
- [AW15] Isadora Antoniano Villalobos and Stephen Walker. “A Nonparametric Model for Stationary Time Series”. In: *Journal of Time Series Analysis* 63 (Aug. 2015). DOI: 10.1111/jtsa.12146 (cit. on p. 3).
- [GMR16] Luis Gutiérrez, Ramsés H. Mena, and Matteo Ruggiero. “A time dependent Bayesian nonparametric model for air quality analysis”. In: *Computational Statistics & Data Analysis* 95.C (2016), pp. 161–175. DOI: 10.1016/j.csda.2015.10.00. URL: <https://ideas.repec.org/a/eee/csda/v95y2016icp161-175.html> (cit. on p. 3).
- [Jo+16] Seongil Jo et al. “Dependent Species Sampling Models for Spatial Density Estimation”. In: *Bayesian Analysis* 12 (May 2016). DOI: 10.1214/16-BA1006 (cit. on p. 3).
- [KG18] Maria Kalli and Jim Griffin. “Bayesian nonparametric vector autoregressive models”. In: *Journal of Econometrics* 203 (Jan. 2018). DOI: 10.1016/j.jeconom.2017.11.009 (cit. on p. 3).
- [DK18] Maria De Iorio and Athanasios Kottas. “Modeling for Dynamic Ordinal Regression Relationships: An Application to Estimating Maturity of Rockfish in California”. In: *Journal of the American Statistical Association* 113.521 (2018), pp. 68–80. DOI: 10.1080/01621459.2017.1328357. eprint: <https://doi.org/10.1080/01621459.2017.1328357>. URL: <https://doi.org/10.1080/01621459.2017.1328357> (cit. on p. 3).
- [De +19] Maria De Iorio et al. *Bayesian nonparametric temporal dynamic clustering via autoregressive Dirichlet priors*. Oct. 2019. DOI: 10.48550/arXiv.1910.10443 (cit. on p. 3).
- [Car+17] François Caron et al. “Generalized póya urn for time-varying pitman-yor processes”. In: *J. Mach. Learn. Res.* 18.1 (Jan. 2017), pp. 836–867. ISSN: 1532-4435 (cit. on p. 3).
- [PQD22] Garrit L. Page, Fernando A. Quintana, and David B. Dahl. “Dependent Modeling of Temporal Sequences of Random Partitions”. In: *Journal of Computational and Graphical Statistics* 31.2 (2022), pp. 614–627. DOI: 10.1080/10618600.2021.1987255. eprint: <https://doi.org/>

- 10.1080/10618600.2021.1987255. URL: <https://doi.org/10.1080/10618600.2021.1987255> (cit. on pp. 3, 27, 28).
- [PQ15] Garritt Page and Fernando Quintana. “Spatial Product Partition Models”. In: *Bayesian Analysis* 11 (Apr. 2015). DOI: 10.1214/15-BA971 (cit. on p. 10).
- [DH01] D. Denison and C Holmes. “Bayesian Partitioning for Estimating Disease Risk”. In: *Biometrics* 57 (Apr. 2001), pp. 143–9. DOI: 10.1111/j.0006-341X.2001.00143.x (cit. on p. 10).
- [De +15] Pierpaolo De Blasi et al. “Are Gibbs-Type Priors the Most Natural Generalization of the Dirichlet Process?” In: *IEEE Trans. Pattern Anal. Mach. Intell.* 37.2 (Feb. 2015), pp. 212–229. ISSN: 0162-8828. DOI: 10.1109/TPAMI.2013.217. URL: <https://doi.org/10.1109/TPAMI.2013.217> (cit. on p. 11).
- [MQR11] Peter Müller, Fernando Quintana, and Gary Rosner. “A Product Partition Model With Regression on Covariates”. In: *Journal of computational and graphical statistics: a joint publication of American Statistical Association, Institute of Mathematical Statistics, Interface Foundation of North America* 20 (Mar. 2011), pp. 260–278. DOI: 10.1198/jcgs.2011.09066 (cit. on p. 11).
- [QMP15] Fernando Quintana, Peter Müller, and Ana Luisa Papoila. “Cluster-Specific Variable Selection for Product Partition Models”. In: *Scandinavian Journal of Statistics* 42 (Mar. 2015). DOI: 10.1111/sjos.12151 (cit. on p. 11).
- [PQ18] Garritt Page and Fernando Quintana. “Calibrating covariate informed product partition models”. In: *Statistics and Computing* 28 (Sept. 2018), pp. 1–23. DOI: 10.1007/s11222-017-9777-z (cit. on p. 14).
- [Gow71] J. C. Gower. “A General Coefficient of Similarity and Some of Its Properties”. In: *Biometrics* 27.4 (1971), pp. 857–871. ISSN: 0006341X, 15410420. URL: <http://www.jstor.org/stable/2528823> (visited on 10/16/2024) (cit. on p. 15).
- [Bez+17] Jeff Bezanson et al. “Julia: A fresh approach to numerical computing”. In: *SIAM Review* 59.1 (2017), pp. 65–98. DOI: 10.1137/141000671. URL: <https://epubs.siam.org/doi/10.1137/141000671> (cit. on p. 19).
- [Law+79] C. L. Lawson et al. “Basic Linear Algebra Subprograms for Fortran Usage”. In: *ACM Trans. Math. Softw.* 5.3 (Sept. 1979), pp. 308–323. ISSN: 0098-3500. DOI: 10.1145/355841.355847. URL: <https://doi.org/10.1145/355841.355847> (cit. on p. 19).
- [Bes+21] Mathieu Besançon et al. “Distributions.jl: Definition and Modeling of Probability Distributions in the JuliaStats Ecosystem”. In: *Journal of Statistical Software* 98.16 (2021), pp. 1–30. ISSN: 1548-7660. DOI: 10.18637/jss.v098.i16. URL: <https://www.jstatsoft.org/v098/i16> (cit. on p. 19).



- [Lin+19] Dahua Lin et al. *JuliaStats/Distributions.jl: a Julia package for probability distributions and associated functions*. July 2019. DOI: 10.5281/zenodo.2647458. URL: <https://doi.org/10.5281/zenodo.2647458> (cit. on p. 19).
- [CR16] Jiahao Chen and Jarrett Revels. “Robust benchmarking in noisy environments”. In: *arXiv e-prints*, arXiv:1608.04295 (Aug. 2016). arXiv: 1608.04295 [cs.PF] (cit. on p. 20).
- [HA85] Lawrence J. Hubert and Phipps Arabie. “Comparing partitions”. In: *Journal of Classification* 2 (1985), pp. 193–218. URL: <https://api.semanticscholar.org/CorpusID:189915041> (cit. on p. 27).
- [Fas+23] A. Fassò et al. *AgrImOnIA: Open Access dataset correlating livestock and air quality in the Lombardy region, Italy (3.0.0)*. 2023. DOI: <https://doi.org/10.5281/zenodo.7956006> (cit. on pp. 29, 36).
- [Gel04] Andrew Gelman. “Prior Distributions for Variance Parameters in Hierarchical Models”. In: *Economics and Econometrics Research Institute (EERI), EERI Research Paper Series* 1 (Jan. 2004) (cit. on p. 50).
- [LHB22] Stefan Lenz, Maren Hackenberg, and Harald Binder. “The JuliaConnectoR: A Functionally-Oriented Interface for Integrating Julia in R”. In: *Journal of Statistical Software* 101.6 (2022), pp. 1–24. DOI: 10.18637/jss.v101.i06 (cit. on p. 76).



# Acknowledgements

*“This is to be my haven for many long years, my niche which I enter with such a mistrustful, such a painful sensation... And who knows? Maybe when I come to leave it many years hence I may regret it!”*

— Fëdor Dostoevskij, *The House of the Dead*



# Ringraziamenti

*“Ecco il mio ponte d’approdo per molti lunghi anni, il mio angoletto, nel quale faccio il mio ingresso con una sensazione così diffidente, così morbosa... Ma chi lo sa? Forse, quando tra molti anni mi toccherà abbandonarlo, magari potrei anche rimpiangerlo!”*

— Fëdor Dostoevskij, *Memorie da una casa di morti*